

OFFICE OF CIVILIAN RADIOACTIVE WASTE MANAGEMENT
SPECIAL INSTRUCTION SHEET

1. QA: QA
Page: 1 of: 1

Complete Only Applicable Items

This is a placeholder page for records that cannot be scanned or microfilmed

2. Record Date
03/08/2001

3. Accession Number

MOL. 20010309.0019

4. Author Name(s)
MICHAEL L. WILSON

5. Author Organization
N/A

6. Title
ABSTRACTION OF DRIFT SEEPAGE

7. Document Number(s)
ANL-NBS-MD-000005

8. Version
REV 01

9. Document Type
REPORT

10. Medium
OPTIC/PAPER

11. Access Control Code
PUB

12. Traceability Designator
DC # 26824

13. Comments
THIS IS A ONE-OF-A-KIND DOCUMENT DUE TO THE COLORED GRAPHS ENCLOSED AND CAN BE LOCATED THROUGH THE RPC

*Read #7410
NMS507
WM-11*

**OFFICE OF CIVILIAN RADIOACTIVE WASTE MANAGEMENT
ANALYSIS/MODEL COVER SHEET
Complete Only Applicable Items**

1. QA: QA
Page: 1 of 49

2. Analysis Check all that apply

Type of Analysis	<input type="checkbox"/> Engineering
	<input checked="" type="checkbox"/> Performance Assessment
	<input type="checkbox"/> Scientific
Intended Use of Analysis	<input type="checkbox"/> Input to Calculation
	<input checked="" type="checkbox"/> Input to another Analysis or Model
	<input checked="" type="checkbox"/> Input to Technical Document
	<input type="checkbox"/> Input to other Technical Products
Describe use: Input to TSPA for Site Recommendation and to UZ Flow and Transport PMR	

3. Model Check all that apply

Type of Model	<input type="checkbox"/> Conceptual Model	<input checked="" type="checkbox"/> Abstraction Model
	<input type="checkbox"/> Mathematical Model	<input type="checkbox"/> System Model
	<input type="checkbox"/> Process Model	
Intended Use of Model	<input type="checkbox"/> Input to Calculation	
	<input checked="" type="checkbox"/> Input to another Model or Analysis	
	<input checked="" type="checkbox"/> Input to Technical Document	
	<input type="checkbox"/> Input to other Technical Products	
Describe use: Input to TSPA for Site Recommendation and to UZ Flow and Transport PMR		

4. Title:
Abstraction of Drift Seepage

5. Document Identifier (including Rev. No. and Change No., if applicable):
ANL-NBS-MD-000005 REV 01

6. Total Attachments: 4	7. Attachment Numbers - No. of Pages in Each: I - 14 pp., II - 14 pp., III - 8 pp., IV - 2 pp.
----------------------------	---

	Printed Name	Signature	Date
8. Originator	Michael L. Wilson	<i>Michael Wilson</i>	2/7/01
9. Checker	Ron D. McCurley (technical check)	<i>Ron D. McCurley</i>	2/8/01
	Leigh Lechel (compliance check)	<i>Leigh Lechel</i>	2/7/01
10. Lead/Supervisor	Michael L. Wilson	<i>Michael Wilson</i>	2/8/01
11. Responsible Manager	Clifford K. Ho	<i>Clifford K. Ho</i>	2/8/01

12. Remarks:
Clifford Ho provided the "weep" analysis of the UZ flow fields that is documented in Section 6.4.3 of this report.

OFFICE OF CIVILIAN RADIOACTIVE WASTE MANAGEMENT
ANALYSIS/MODEL REVISION RECORD
Complete Only Applicable Items

1. Page: 2 of 49

2. Analysis or Model Title:

Abstraction of Drift Seepage

3. Document Identifier (including Rev. No. and Change No., if applicable):

ANL-NBS-MD-000005 REV 01

4. Revision/Change No.

5. Description of Revision/Change

00

Initial issue

01

Update to incorporate new seepage data and revisions to upstream reports. This revision also addresses deficiency report LVMO-00-D-118 by including more documentation of underlying assumptions, alternative conceptual models, and NRC IRSR issues. Changes are not indicated with change bars because the changes are extensive throughout the report.

CONTENTS

	Page
1. PURPOSE.....	6
2. QUALITY ASSURANCE.....	6
3. COMPUTER SOFTWARE AND MODEL USAGE.....	7
4. INPUTS.....	8
4.1 DATA AND PARAMETERS.....	8
4.2 CRITERIA.....	9
4.3 CODES AND STANDARDS.....	10
5. ASSUMPTIONS.....	11
6. ANALYSIS/MODEL.....	13
6.1 OVERVIEW.....	13
6.2 CONCEPTUAL MODELS.....	14
6.3 INITIAL ABSTRACTION OF SEEPAGE RESULTS.....	15
6.3.1 Seepage Statistics.....	15
6.3.2 Spatial Variability of k and $1/\alpha$	21
6.3.3 Uncertainty in k and $1/\alpha$	23
6.3.4 Discrete Probability Distributions for k and $1/\alpha$	25
6.3.5 Variability and Uncertainty of Seepage.....	28
6.4 ADJUSTMENTS FOR OTHER EFFECTS.....	29
6.4.1 Drift Degradation and Rock Bolts.....	29
6.4.2 Possible Correlation of k and $1/\alpha$	30
6.4.3 Focusing of Flow above the Drifts.....	31
6.4.4 Episodic Flow.....	36
6.4.5 Coupled Processes.....	36
6.5 SUMMARY OF ABSTRACTION OF SEEPAGE INTO DRIFTS.....	37
6.6 VALIDITY OF ABSTRACTION OF SEEPAGE INTO DRIFTS.....	42
7. CONCLUSIONS.....	44
8. INPUTS AND REFERENCES.....	45
8.1 DOCUMENTS CITED.....	45
8.2 CODES, STANDARDS, REGULATIONS, AND PROCEDURES CITED.....	47
8.3 SOURCE DATA, LISTED BY DATA TRACKING NUMBER.....	48
8.4 OUTPUT DATA, LISTED BY DATA TRACKING NUMBER.....	49
9. ATTACHMENTS.....	49
ATTACHMENT I – ASSUMPTIONS RELATING TO INPUT DATA.....	I-1
ATTACHMENT II – SOFTWARE ROUTINE T2WEEP V. 1.0.....	II-1

ATTACHMENT III – REPOSITORY ELEMENTS	III-1
ATTACHMENT IV – DIRECTORY OF FILES SUBMITTED TO TDMS.....	IV-1

FIGURES

	Page
Figure 1. Histograms of Log Weep Spacing for Glacial-Transition Climate and Base Infiltration.....	34
Figure 2. Seepage Fraction vs. Percolation Flux	39
Figure 3. Mean Seep Flow Rate vs. Percolation Flux.....	40
Figure 4. Standard Deviation of Seep Flow Rate vs. Percolation Flux	41
Figure 5. Effect of Flow Focusing on Seepage Fraction	42
Figure 6. Effect of Flow Focusing on Mean Seep Flow Rate.....	42

TABLES

	Page
Table 1. Software Routine Used in this Analysis/Model.....	7
Table 2. Input Data and Parameters Used in this Analysis/Model	9
Table 3. Summary Statistical Information for Computed Seepage Percentage.....	17
Table 4. Summary Statistical Information for Seep Flow Rate (in m ³ /yr)	19
Table 5. Disturbed-Zone Air-Permeability Data	21
Table 6. Calibrated Values of the 1/ α Parameter.....	22
Table 7. Uncertainty Cases for Seepage Abstraction.....	25
Table 8. Example Three-Point Discrete Distribution	26
Table 9. Example Two-Point Discrete Distribution	26
Table 10. Two-Variable Discrete Distribution	27

Table 11. Fraction of Repository in Host Units..... 27

Table 12. Final Discrete Distribution for Low-Seepage Case 28

Table 13. Weighted Seepage Statistics for the Basic Seepage Results..... 28

Table 14. Hydrologic Parameters Used in Calculation of Weep Spacings..... 33

Table 15. Statistics for Weep Spacings, Glacial-Transition Climate..... 34

Table 16. Triangular Distributions of Seepage vs. Percolation Flux 38

1. PURPOSE

Drift seepage refers to flow of liquid water into repository emplacement drifts, where it can potentially contribute to degradation of the engineered systems and release and transport of radionuclides within the drifts. Because of these important effects, seepage into emplacement drifts is listed as a "principal factor for the postclosure safety case" in the screening criteria for grading of data in Attachment 1 of AP-3.15Q, Rev. 2, *Managing Technical Product Inputs*. Abstraction refers to distillation of the essential components of a process model into a form suitable for use in total-system performance assessment (TSPA). Thus, the purpose of this analysis/model is to put the information generated by the seepage process modeling in a form appropriate for use in the TSPA for the Site Recommendation. This report also supports the Unsaturated-Zone Flow and Transport Process Model Report. The scope of the work is discussed below.

This analysis/model is governed by the *Technical Work Plan for Unsaturated Zone Flow and Transport Process Model Report* (CRWMS M&O 2000a). Details of this activity are in Addendum A of the technical work plan. The original Work Direction and Planning Document is included as Attachment 7 of Addendum A. Note that the Work Direction and Planning Document contains tasks identified for both Performance Assessment Operations (PAO) and Natural Environment Program Operations (NEPO). Only the PAO tasks are documented here. The planning for the NEPO activities is now in Addendum D of the same technical work plan and the work is documented in a separate report (CRWMS M&O 2000b). (The Project has been reorganized since the document was written. The responsible organizations in the new structure are the Performance Assessment Department and the Unsaturated Zone Department, respectively.) The work plan for the seepage abstraction calls for determining an appropriate abstraction methodology, determining uncertainties in seepage, and providing probability distributions of seepage. These are all discussed in detail in this report. In addition, the work plan calls for evaluation of effects of episodic flow and thermal-hydrologic-chemical alteration of hydrologic properties. As discussed in Section 5, these effects are not addressed in detail in this report because they can be argued to be insignificant. Effects of thermal-mechanical alteration of hydrologic properties are also not addressed in detail in this report because suitable process-model results are not available at this time. If these effects are found to be important, they should be included in the seepage abstraction in a future revision.

2. QUALITY ASSURANCE

The Quality Assurance program applies to the development of this analysis/model. The responsible manager has evaluated this activity (CRWMS M&O 2000a, Addendum A, Attachment 9) and has determined that the development of this analysis/model is subject to the requirements in the *Quality Assurance Requirements and Description* (DOE 2000). The control of electronic management of data was evaluated in accordance with AP-SV.1Q, *Control of the Electronic Management of Data*. The evaluation determined that work processes and procedures are adequate for the control of electronic management of data for this activity (CRWMS M&O 2000a, Addendum A, Attachment 8). The analysis/model and documentation were developed in accordance with AP-3.10Q, *Analyses and Models*.

This analysis/model does not contain field activities, and the classification of permanent items is not applicable.

3. COMPUTER SOFTWARE AND MODEL USAGE

A software routine was developed to calculate the spacing between actively flowing fractures in the site-scale unsaturated-zone (UZ) flow model (Section 6.4.3). This routine was checked as part of this analysis/model to ensure that it provides correct results for the input files used. The use and documentation of this software routine complies with Section 5.1.1 of AP-SI.1Q Rev. 2 ICN 4, *Software Management*.

Table 1. Software Routine Used in this Analysis/Model

Software Routine	Computer Platform/ Operating System	Comments
T2WEEP v. 1.0	Sun UltraSPARC SunOS 5.7	This software routine extracts percolation fluxes and weep spacings from TOUGH2 flow fields. It was compiled using FORTRAN 77 on the Sun OS 5.7 server (worf) at Sandia National Laboratories. As part of this analysis/model, the results from the software routine T2WEEP v. 1.0 were visually inspected to ensure that the routine provided correct results for the input files and formulation that were used (see Section 6.4.3.1 and Attachment II). A listing of this routine is in Attachment II. All files associated with this software routine have been submitted to the Technical Data Management System under DTN: SN9912T0511599.002.

The steps that T2WEEP performs are summarized as follows:

- 1) Read in user-prescribed files and data.
- 2) Read in repository elements from user-prescribed file.
- 3) Read in element information (name, material, coordinates) from ELEM card and assign parameter values to repository elements.
- 4) Read in connection information from CONNE card for connections between repository element and element directly above it. Record connection area.
- 5) Read TOUGH2 output file. First read in liquid saturations for prescribed repository elements. Then read in mass flow rates for repository connections.
- 6) Calculate percolation flux (not used in weep-spacing calculation) from mass flow using connection area and liquid density.
- 7) Calculate weep spacing using Eqs. 5–7 in Section 6.4.3.1.
- 8) Print results to output file.

In addition to the input values listed in Section 6.4.3.1 (Table 14), inputs are site-scale UZ flow fields and mesh file. Attachment II provides sample input and output files for T2WEEP, as well as a listing of the source file. The sample files in Attachment II constitute a test case for the routine. Values for the calculated percolation flux and weep spacings were spot-checked in the sample output file to ensure that the software routine was performing correctly. Results were

verified in this manner for the input and output files used in this analysis. Thus, the range of input parameter values for which results were verified are those discussed in Section 6.4.3.1.

In accordance with AP-SIII.3Q (*Submittal and Incorporation of Data to the Technical Data Management System*), all input and output files used in the T2WEEP calculations have been submitted to the TDMS under DTN: SN9912T0511599.002. Note that in Attachment II and in the files submitted to the TDMS the mesh file is referred to as mpa_pchl.v1. This is the name as it was originally received in an input transmittal. In the final submission to the TDMS (see Table 2, item 11 in Section 4.1) the name of the file was changed to 3d2kpa_pcl.mesh. It was confirmed through a UNIX "diff" command that the two are, indeed, the same.

Aside from the above software routine, only off-the-shelf commercially available software was used for this analysis/model. Calculations and plots were made using Microsoft Excel 97 SR-2 (i). The results were spot-checked by hand to ensure that the results were correct. The computer used was a Dell Precision 410 with Pentium II processor, running Microsoft Windows NT 4.00.1381.

This report documents the Seepage Abstraction Model. No other models are used directly, though results from the following models are used: Seepage Model for PA, Seepage Calibration Model, Calibrated Properties Model, and Unsaturated Zone Flow Model. The results that are used as inputs to the seepage abstraction are listed in Section 4.1.

4. INPUTS

4.1 DATA AND PARAMETERS

Table 2 summarizes the input data and parameters used in this analysis/model. Some of the data were originally obtained via input transmittal (per AP-3.14Q, *Transmittal of Input*), but they are now in the Technical Data Management System (TDMS) and it has been confirmed that the TDMS data are the same as the data obtained by input transmittal. A few numbers were corrected by the originators between the input transmittal and the TDMS submittal; in such cases the corrected values from the TDMS have been used. Input status of all data can be determined by checking the Document Input Reference System (DIRS) and Automated Technical Data Tracking (ATDT) system. This document may be affected by technical product input information that requires confirmation. Any changes to the document that may occur as a result of completing the confirmation activities will be reflected in subsequent revisions.

Table 2. Input Data and Parameters Used in this Analysis/Model

Item	Description	Input Source	Comments	Documentation
1	Seepage Results	LB0011SMDCREV1.002 LB0101SMDCREV1.001	Seepage percentage for suite of cases	MDL-NBS-HS-000002 (CRWMS M&O 2000b)
2	Drift and Waste-Package Geometry	SN9908T0872799.004	Drift diameter, average waste-package length, waste-package spacing	CAL-EBS-HS-000002 (CRWMS M&O 2000c)
3	Seepage Calibration Results	LB0010SCMREV01.002	Post-construction permeability and calibrated fracture alpha parameter	MDL-NBS-HS-000004 (CRWMS M&O 2000d)
4	Subsurface Layout	ANL-SFS-MG-000001 (CRWMS M&O 2000e, Table 18)	Fraction of repository in each host unit	ANL-SFS-MG-000001 (CRWMS M&O 2000e)
5	Site-Scale Calibrated Properties	LB997141233129.001	Base-infiltration case: gamma parameter, residual liquid fracture saturation	MDL-NBS-HS-000003 (CRWMS M&O 2000f)
6		LB997141233129.002	High-infiltration case: gamma parameter, residual liquid fracture saturation	
7		LB997141233129.003	Low-infiltration case: gamma parameter, residual liquid fracture saturation	
8	Flow Field Simulations for Infiltration Scenarios	LB990801233129.007	Glacial-transition low-infiltration flow field, plus gamma parameter and residual liquid fracture saturation for fault zones	MDL-NBS-HS-000006 (CRWMS M&O 2000g)
9		LB990801233129.009	Glacial-transition base-infiltration flow field, plus gamma parameter and residual liquid fracture saturation for fault zones	
10		LB990801233129.011	Glacial-transition high-infiltration flow field, plus gamma parameter and residual liquid fracture saturation for fault zones	
11	Mesh	LB990701233129.001	Mesh file used with flow fields (3d2kpa_pc1.mesh)	ANL-NBS-HS-000015 (CRWMS M&O 2000h)
12	Hydrologic Properties	LB990501233129.001	Uncalibrated constant properties for all units: fracture frequency, fracture/matrix area	ANL-NBS-HS-000002 (CRWMS M&O 2000i)
13	Repository Outline	SN9907T0872799.001	Coordinates for repository outline	CAL-MGR-HS-000001 (CRWMS M&O 2000j)

4.2 CRITERIA

The relevant criteria for this activity are the U.S. Nuclear Regulatory Commission (NRC) acceptance criteria related to model abstraction for the quantity and chemistry of water

contacting waste packages and waste forms from the total system performance assessment and integration (TSPA) issue resolution status report (IRSR) (NRC 2000, Section 4.3.1.1.3). (A later revision of that IRSR was released recently, but it does not include the acceptance criteria. It is expected that the acceptance criteria for this integrated subissue in the Yucca Mountain Review Plan, when available, will be substantially the same as those listed below.) The acceptance criteria are as follows:

- T1 Sufficient data (field, laboratory, or natural analog data) are available to adequately define relevant parameters and conceptual models necessary for developing the quantity and chemistry of water contacting waste packages and waste forms abstraction in a TSPA. Where adequate data do not exist, other information sources such as expert elicitation have been appropriately incorporated into the TSPA.
- T2 Parameter values, assumed ranges, probability distributions, and bounding assumptions used in the quantity and chemistry of water contacting waste packages and waste forms abstraction, such as the pH, carbonate concentration, chloride concentration, and amount of water flowing in and out of the breached waste package, are technically defensible and reasonably account for uncertainties and variability.
- T3 Alternative modeling approaches consistent with available data and current scientific understanding are investigated and results and limitations appropriately factored into the quantity and chemistry of water contacting waste packages and waste forms abstraction.
- T4 Output of quantity and chemistry of water contacting waste packages and waste forms abstraction are supported by comparison to output of detailed process models or empirical observations (laboratory testing, natural analogs, or both).
- T5 Important design features, physical phenomena and couplings, and consistent and appropriate assumptions are incorporated into the quantity and chemistry of water contacting waste packages and waste forms abstraction.

The application of these acceptance criteria to this analysis/model is limited in two ways. First, this analysis/model is concerned only with quantity of water, not chemistry. And second, this analysis/model is concerned only with the amount of water entering the emplacement drifts. Water chemistry and the further interactions of water with waste packages and waste forms inside the drifts are the subjects of other analysis/model reports.

4.3 CODES AND STANDARDS

The seepage-abstraction analysis/model supports the definition of hydrologic parameters for performance assessment as required by the interim guidance from the U.S. Department of Energy pending issuance of new regulations by the NRC (Dyer 1999). Relevant requirements for performance assessment from Section 114 of that document are: "Any performance assessment used to demonstrate compliance with Sec. 113(b) shall: (a) Include data related to the geology, hydrology, and geochemistry ... used to define parameters and conceptual models used in the assessment. (b) Account for uncertainties and variabilities in parameter values and provide the technical basis for parameter ranges, probability distributions, or bounding values used in the performance assessment. ... (g) Provide the technical basis for models used in the

performance assessment such as comparisons made with outputs of detailed process-level models”

5. ASSUMPTIONS

Assumptions that pertain to this abstraction analysis/model are as follows.

1. *Seepage can be treated as a random process.* The locations and amount of seepage into drifts are sensitive to the heterogeneity in fracture properties around the drifts (CRWMS M&O 2000d, Section 6.1.6). The heterogeneity is not knowable in detail, but rather is typically described using geostatistics (CRWMS M&O 2000d, Sections 6.1.6, 6.3.2.1, and 6.4.2.1). Thus, it is appropriate to treat seepage probabilistically in TSPA simulations. This is a basic assumption that applies throughout the report.
2. *The extent of flow focusing can be estimated using the active-fracture model.* The “active fracture” conceptual flow model (Liu et al. 1998) that is being used for site-scale UZ flow calculations is based on the concept that flow is channeled in fractures, so that only some fractures are actively flowing. There are no data on the spacing of active flow channels or the extent of flow focusing, but the conceptual model can provide an estimate of the degree of channeling in fractures and thus the degree of intermediate-scale focusing of flow. Spacing between active flow channels is calculated assuming discrete flow in vertical fractures that are either saturated or unsaturated, yielding two bounding conditions for “weep” spacings. Explanation and justification for the active-fracture model are given in the paper (Liu et al. 1998); use of the active-fracture model to estimate focusing of flow above drifts is discussed in Section 6.4.3 of this report.
3. *Effects of episodic flow on seepage can be neglected.* While seepage under conditions of episodic flow can be evaluated (CRWMS M&O 2000b, Section 6.6.6), there are no data to indicate that significant amounts of episodic flow exist at the repository depth in Yucca Mountain. Bomb-pulse ^{36}Cl found in the exploratory studies facility (ESF) is widely regarded as indirect evidence for the existence of some episodic flow, but it is generally believed that only a small fraction of the water is involved (Bodvarsson et al. 1997, Chapter 16). No data are available to quantify the fraction of water that might be involved in episodic flow at the repository. Theoretical studies have shown that the Paintbrush nonwelded hydrogeologic unit above the repository damps out flow transients (CRWMS M&O 1998, Section 2.4.2.8). In the screening of features, events, and processes (FEPs) for UZ flow and transport, episodic flow effects resulting from episodic infiltration have been excluded (CRWMS M&O 2000k, Section 6.3.5). There is some additional discussion in Section 6.4.4 of this report.
4. *Thermal-mechanical and thermal-chemical effects on seepage can be neglected.* Changes in hydrologic properties around the emplacement drifts caused by thermal-mechanical stresses and by thermal-chemical dissolution and precipitation processes are of potential concern. A fully coupled drift-scale thermal-hydrologic-chemical model has recently been developed (CRWMS M&O 2000l). Simulations with that model show only very small changes in

hydrologic properties (at most 0.5% change in fracture porosity: CRWMS M&O 2000l, Section 6.3.5). These results justify neglecting thermal-chemical effects on seepage. A similar evaluation of thermal-mechanical effects on seepage is not yet available. Because results are not available, thermal-mechanical effects are not included in the seepage abstraction at this time; however, this assumption requires confirmation. The assumption of neglecting thermal-mechanical effects applies throughout the report.

5. *Seepage for non-convergent simulations can be bounded by 100% of the flow above a drift segment.* As discussed in Section 6.3.1, there were convergence problems with some of the seepage process-model simulations. In those cases, it is assumed that 100% of the flow above the footprint of the drift seeps into the drift. This assumption is intended to be conservative. In principle, it could be possible for seepage percentage to be somewhat higher than 100%, but such a result is not expected, and seepage even as high as 100% of the flow above the drift was not observed in any of the simulations (CRWMS M&O 2000b, Tables 4–8; Table 2 of this report, item 1).
6. *Seepage is increased by 50% to account for the effects of drift degradation and rock bolts.* This assumption is discussed in detail in Section 6.4.1, where it is argued that this adjustment is conservative.
7. *Evaporation effects do not significantly affect the seepage calibration.* As discussed in the Seepage Calibration Model report, there is some concern that the seepage-test results were unduly influenced by evaporation, especially the tests in the Cross Drift (CRWMS M&O 2000d, Section 5.6; Table I-1 of this report, assumption C.6). Steps were taken in the seepage calibration to minimize the effects (e.g., using seepage data during unventilated periods for the calibration), but it is felt that further verification is needed for the assumption that the tests are not significantly affected by evaporation. This assumption is used implicitly in Section 6.3.2, where the seepage-calibration results are used, and is discussed again in Section 7.
8. *Full seepage of all percolating water at a percolation flux of 3000 mm/yr can be used as an upper interpolation point to calculate seepage for high fluxes.* Extrapolation to high percolation fluxes is a potential problem because the results from the Seepage Model for PA only go up to 500 mm/yr. This flux is much higher than most fluxes under present-day conditions or even under expected future wetter conditions; for example, estimates of average infiltration (averaged over the repository area) range from a low of 0.4 mm/yr for the present-day low-infiltration case to 37 mm/yr for the glacial-transition high-infiltration case to a high of 110 mm/yr for the wettest full-glacial case (CRWMS M&O 2000m, Tables 3.2-2 and 3.2-6). However, when heterogeneity of flow is considered, and in particular when flow focusing is included in the seepage calculation as described in Section 6.4.3, some locations can be above 500 mm/yr for some climate/infiltration cases. In all cases, though, the average behavior is below 500 mm/yr. For example, if the wettest average infiltration of 110 mm/yr is multiplied by the average flow-focusing factor for the high-infiltration case of 3.8, the result is approximately 420 mm/yr. While some fraction of the focused percolation fluxes will be above 500 mm/yr in that case, the average seepage behavior should be determined by the parts of the seepage curves below 500 mm/yr. Thus, while a method for dealing with high percolation fluxes is needed, those high fluxes are not expected to have a large effect on

TSPA results. Accordingly, seepage percentage is assumed to be 100% (that is, all percolating water above a drift seeps into the drift) for all cases at 3000 mm/yr, and seepage for other large flux values is obtained by linear interpolation or extrapolation. This choice is expected to be conservative (i.e., overestimate seepage) given that computed seepage is still at or near zero at 3000 mm/yr for parameter values representative of the Topopah Spring lower lithophysal hydrogeologic unit (CRWMS M&O 2000b, Table 11 and Attachment III), in which most of the repository is to be located. This assumption is used in Section 6.5.

Of these assumptions, only number 7 and part of number 4 (the neglect of thermal-mechanical effects) are considered to need further confirmation. The confirmation status of these two assumptions may be determined by review of the DIRS database. As discussed above, the others are considered to be justified as either reasonable or conservative, such that additional confirmation with respect to this analysis/model is not necessary.

In addition to the above assumptions, which were made in the development of this analysis/model, assumptions were made in the upstream analyses that provided the input data listed in Table 2. Those upstream assumptions are summarized in Attachment I.

6. ANALYSIS/MODEL

6.1 OVERVIEW

This analysis/model supports the "principal factor for the postclosure safety case" of seepage into emplacement drifts (AP-3.15Q, Rev. 2, Attachment 1). Therefore, this analysis/model is classified as being of primary (Level 1) importance.

The approach of this analysis/model is to generate probability distributions that represent the uncertainty and spatial variability of seepage. Seepage can then be treated as a stochastic quantity in TSPA simulations by sampling values from the probability distributions. In defining the probability distributions, the dependence of seepage on key input parameters (including percolation flux, fracture permeability, and fracture capillary strength) is taken into account, and the influence of perturbing physical processes (including drift degradation, thermal processes, and flow focusing) is considered.

The abstraction method is an extension of the method used for the TSPA for the Viability Assessment (DOE 1998, Sections 3.1.1.4, 3.1.2.4, and 3.1.3.3; CRWMS M&O 1998, Sections 2.2.4, 2.4.4, and 2.5.2). The objective is to provide the amount of seepage of liquid water into repository emplacement drifts for TSPA simulations. This analysis/model provides the amount of seepage as a function of percolation flux; the actual calculation of seepage is performed within the TSPA, where distributions for percolation flux are combined with the seepage abstraction to obtain the estimated amount of seepage at representative waste-package locations. The emplacement drifts are located in the unsaturated zone at Yucca Mountain, cutting across three hydrogeologic units: the Topopah Spring middle nonlithophysal, lower lithophysal, and lower nonlithophysal units. In the UZ Flow Model these units are named tsw34, tsw35, and tsw36, respectively. These units are all densely welded, highly fractured tuff. In Section 6.2 conceptual models are discussed, including possible alternative conceptual models. In Section 6.3 the basic results from the Seepage Model for PA are summarized and probability distributions that

represent the uncertainty and spatial variability of seepage are derived. The basic seepage model is idealized in several respects, including assumptions of no degradation of the drift and no repository thermal effects. In Section 6.4 adjustments to the basic results to take into account several perturbing physical processes are discussed. The adjustments are based on basic physical arguments and on perturbed seepage simulations (CRWMS M&O 2000b, Sections 6.6.4 and 6.6.6). Section 6.5 then presents the final abstraction of seepage that is to be used for TSPA simulations for the Site Recommendation and Section 6.6 discusses the validity of the seepage abstraction for TSPA simulations.

6.2 CONCEPTUAL MODELS

Several conceptual models enter into the abstraction of drift seepage.

At the highest level is the seepage abstraction itself. The basic conceptual model for the abstraction is that seepage is treated as a random process, with seepage amounts sampled from uncertainty distributions in TSPA simulations. This treatment is listed as assumption 1 in Section 5. For reasons discussed there, this treatment is considered to be appropriate and no alternatives (e.g., deterministic treatment of seepage) are considered.

Underlying the abstraction of seepage are the Seepage Calibration Model (CRWMS M&O 2000d) and the Seepage Model for PA (CRWMS M&O 2000b). These are drift-scale UZ flow models, which simulate flow through a fracture continuum with geostatistically-defined hydrologic properties. The most important potential alternative conceptual model for seepage is a model that simulates flow through discrete features rather than through a continuum. This alternative, referred to as the discrete fracture-network model is discussed in great detail by Finsterle (2000), and in lesser detail in the Seepage Calibration Model report (CRWMS M&O 2000d, Section 6.5.1) and the Seepage Model for PA report (CRWMS M&O 2000b, Section 6.7). It has been concluded that the fracture-continuum model is acceptable for seepage modeling and the discrete fracture-network model is unnecessary to carry further (see assumptions A.1 and C.1 in Table I-1).

Other potential alternatives for seepage modeling are continuum models that include flow in the rock matrix in addition to flow in the fractures. The most common models of this sort are the equivalent-continuum model and the dual-permeability model. Since seepage into drifts is expected to be dominated by fracture processes, it is considered unnecessary to include matrix flow in the model (see assumptions A.5 and C.5 in Table I-1). The Seepage Calibration Model report (CRWMS M&O 2000d, Sections 6.5.2 and 6.5.3) also discusses two possible alternative methods of estimating seepage into drifts: estimating seepage from the local ponding probability (derived from the spatial variability of the permeability field) and estimating seepage from deposition rates of calcite and opal in lithophysal cavities. These methods are not alternative models in the same sense, as they are not alternative process models of seepage.

In addition to the seepage models, the estimation of “weep” spacing discussed in Section 6.4.3 uses results of the UZ Flow Model (CRWMS M&O 2000g) and other models and analyses underlying it. The UZ Flow Model uses a dual-permeability formulation modified by the active-fracture concept, which takes into account that only some of the fractures are actively flowing under unsaturated conditions. Important potential alternative conceptual models are similar to

those for seepage: the discrete-fracture model and the equivalent-continuum model. These alternatives are discussed briefly in the UZ Flow Model report (CRWMS M&O 2000g, Section 6.1.2). Discrete-fracture models are considered to have too much uncertainty in the fracture distribution data within the mountain and to require too much computational burden. The equivalent-continuum approach may not capture important rapid transient interactions in flow and transport between fractures and matrix. A fracture-only continuum such as used for seepage modeling was not even considered for the UZ Flow Model because it would not be appropriate for that model to neglect the effects of flow in the rock matrix. It is therefore concluded that the dual-permeability/active-fracture model is the most appropriate choice (see assumption F.9 in Table I-1). The UZ Flow Model was used to evaluate two conceptual models of the perched water below the repository (CRWMS M&O 2000g, Section 6.2.2). However, flow at the repository is the same in those two conceptual models, so their differences have no impact on seepage.

6.3 INITIAL ABSTRACTION OF SEEPAGE RESULTS

6.3.1 Seepage Statistics

The Seepage Model for PA report presents seepage results for a large number of cases (CRWMS M&O 2000b, Tables 4–8). The tables of results from the report are in the TDMS (see Table 2, item 1). The basic results are for the *seepage percentage* (percentage of percolating water above the footprint of a drift segment that seeps into the drift) for a matrix of values of key input parameters. Note that the computed seepage percentage conservatively includes water that seeps into the drift from anywhere on the drift wall; it is not limited to water that seeps in above the footprint of a waste package or drip shield, or even to the top half of the drift (though the amount of water that seeps into the lower half of the drift is small, so including water only from above the springlines would not change the results very much).

The key parameters varied in the simulations are percolation flux above the drift q (denoted Q_p in CRWMS M&O 2000b), the geometric mean of fracture permeability \bar{k} (denoted k_{FC} in CRWMS M&O 2000b), the standard deviation of the natural log of permeability σ , and the fracture capillary-strength parameter $1/\alpha$ (the capillary-strength parameter is the inverse of the van Genuchten α parameter). Additional information on the parameters and why they are important to seepage can be found in the model report (CRWMS M&O 2000b, Section 6.3). Note that only fracture permeability is heterogeneous in the simulations; $1/\alpha$ and other parameters have fixed values for each simulation. Computed seepage percentage is available for the following parameter values:

- $q = 5, 14.6, 73.2, 213, \text{ and } 500 \text{ mm/yr}$
- $\bar{k} = 0.9 \times 10^{-14}, 0.9 \times 10^{-13}, 0.9 \times 10^{-12}, 0.9 \times 10^{-11}, \text{ and } 0.9 \times 10^{-10} \text{ m}^2$
- $\sigma = 1.66, 1.93, \text{ and } 2.5 \text{ (dimensionless)}$
- $1/\alpha = 200, 400, 800, \text{ and } 1600 \text{ Pa}$

Seepage percentage was calculated three times for each combination of the above parameters, with three different geostatistical realizations of the heterogeneity. This is a total of 900 three-dimensional drift-scale flow simulations. (Some of the simulations were not actually run. If

seepage is zero for a given \bar{k} and $1/\alpha$, it can be inferred that it is also zero for any larger \bar{k} or $1/\alpha$ with the same values of the other parameters; those larger \bar{k} and $1/\alpha$ cases do not have to be run.) Each simulation is for a drift segment slightly longer than a waste package, so the statistics represent the variability and uncertainty of seepage for a single waste-package location. Convergence problems were encountered in a few of the seepage simulations. Some simulations are marked in the tables with asterisks and the note "Seepage large, solution not convergent." For this analysis/model, the seepage percentage is taken to be 100 for those cases (see Section 5, assumption 5).

Examination of the results reveals that seepage percentage is not strongly dependent on σ within the range considered. Thus, for the abstraction analysis/model, simulations with all values of σ are lumped together and treated as having nine simulations for each combination of the other parameters. Seepage is treated as a function of three variables rather than four.

Summary statistical data on seepage percentage for the simulated values of q , \bar{k} , and $1/\alpha$ are given in Table 3. The symbol f_s is used to denote the *seepage fraction*, which is the fraction of waste-package locations (model simulations) that have seepage (i.e., that have nonzero seepage percentage). Note that seepage percentage and seepage fraction are quite different quantities and are not just related by a factor of 100. In calculating the mean values of seepage fraction, seepage percentage, and square of seepage percentage, the mean is a simple average over the nine simulations (three values of σ times three geostatistical realizations) with the given values of q , \bar{k} , and $1/\alpha$.

Table 4 gives the same statistical information for *seep flow rate*, which will be denoted Q_s^* . Seep flow rate is defined as the volumetric flow rate of the seepage in a drift segment. The mean seep flow rate is obtained from the mean seepage percentage by multiplying by percolation flux and area; the mean square seep flow rate is obtained from the mean square seepage percentage by multiplying by the square of percolation flux times the square of the area. The area to multiply by is the width of a drift (5.5 m) and the length of an average waste package plus waste-package spacing (5.13 m + 0.1 m), or 28.8 m². (Drift diameter, average waste-package length, and waste-package spacing are taken from the TDMS; see Table 2, item 2.) The asterisk is present to indicate that the average is over all seepage simulations. Later, Q_s , without an asterisk will be used to indicate the average seep flow rate, averaged over only the simulations that have some seepage (that is, the mean seep flow rate for the locations with seepage).

Table 3. Summary Statistical Information for Computed Seepage Percentage

\bar{k} (m ²) 1/α (Pa)	q = 5 mm/yr			q = 14.6 mm/yr			q = 73.2 mm/yr			q = 213 mm/yr			q = 500 mm/yr		
	Mean f _s	Mean of Seep %	Mean Square of Seep %												
0.9×10 ⁻¹⁴ 200	1	92.00	8466.00	1	92.67	8589.33	1	93.00	8651.22	1	94.33	8902.78	1	97.33	9477.33
0.9×10 ⁻¹⁴ 400	1	66.44	4430.00	1	82.00	6731.78	1	91.11	8304.67	1	93.44	8735.22	1	95.89	9198.33
0.9×10 ⁻¹⁴ 800	0.67	1.14	5.42	1	22.67	523.33	1	69.44	4839.67	1	84.89	7217.78	1	92.00	8474.89
0.9×10 ⁻¹⁴ 1600	0	0	0	0.11	0.28	0.69	1	28.33	821.22	1	62.44	3926.44	1	80.89	6572.00
0.9×10 ⁻¹³ 200	1	85.11	7249.78	1	90.11	8123.44	1	92.11	8486.78	1	92.67	8589.33	1	92.67	8588.67
0.9×10 ⁻¹³ 400	1	4.68	29.74	1	33.89	1157.44	1	72.67	5292.22	1	85.67	7346.11	1	90.11	8123.44
0.9×10 ⁻¹³ 800	0	0	0	0	0	0	1	5.64	40.58	1	36.89	1370.44	1	61.00	3734.78
0.9×10 ⁻¹³ 1600	0	0	0	0	0	0	0	0	0	0.56	0.98	4.40	1	14.33	213.22
0.9×10 ⁻¹² 200	1	46.67	2184.89	1	70.00	4911.33	1	87.56	7671.11	1	91.22	8324.33	1	92.00	8466.00
0.9×10 ⁻¹² 400	0	0	0	0	0	0	1	11.56	139.94	1	46.11	2131.44	1	66.11	4385.00
0.9×10 ⁻¹² 800	0	0	0	0	0	0	0	0	0	0	0	0	0.67	1.12	5.42
0.9×10 ⁻¹² 1600	0	0	0	0	0	0	0	0	0	0	0	0	0	0	0

Table 3. Summary Statistical Information for Computed Seepage Percentage (continued)

\bar{k} (m ²) 1/ α (Pa)	$q = 5$ mm/yr			$q = 14.6$ mm/yr			$q = 73.2$ mm/yr			$q = 213$ mm/yr			$q = 500$ mm/yr		
	Mean f_s	Mean of Seep %	Mean Square of Seep %	Mean f_s	Mean of Seep %	Mean Square of Seep %	Mean f_s	Mean of Seep %	Mean Square of Seep %	Mean f_s	Mean of Seep %	Mean Square of Seep %	Mean f_s	Mean of Seep %	Mean Square of Seep %
0.9×10^{-11} 200	0	0	0	0	0	0	0.56	0.75	3.31	1	18.56	350.11	1	46.67	2184.89
0.9×10^{-11} 400	0	0	0	0	0	0	0	0	0	0	0	0	0	0	0
0.9×10^{-11} 800	0	0	0	0	0	0	0	0	0	0	0	0	0	0	0
0.9×10^{-11} 1600	0	0	0	0	0	0	0	0	0	0	0	0	0	0	0
0.9×10^{-10} 200	0	0	0	0	0	0	0	0	0	0	0	0	0.11	0.20	0.36
0.9×10^{-10} 400	0	0	0	0	0	0	0	0	0	0	0	0	0	0	0
0.9×10^{-10} 800	0	0	0	0	0	0	0	0	0	0	0	0	0	0	0
0.9×10^{-10} 1600	0	0	0	0	0	0	0	0	0	0	0	0	0	0	0

Input data: see Table 2, item 1. Averages computed in Excel spreadsheet Seep-sr1.xls, submitted with this report under DTN: SN0012T0511599.003.

Table 4. Summary Statistical Information for Seep Flow Rate (in m³/yr)

\bar{k} (m ²) 1/α (Pa)	q = 5 mm/yr		q = 14.6 mm/yr		q = 73.2 mm/yr		q = 213 mm/yr		q = 500 mm/yr	
	Mean Q _s	Mean Square Q _s								
0.9×10 ⁻¹⁴ 200	0.132	1.75×10 ⁻²	0.389	0.151	1.96	3.84	5.78	33.4	14.0	196
0.9×10 ⁻¹⁴ 400	9.56×10 ⁻²	9.16×10 ⁻³	0.344	0.119	1.92	3.68	5.73	32.8	13.8	190
0.9×10 ⁻¹⁴ 800	1.63×10 ⁻³	1.12×10 ⁻⁵	9.52×10 ⁻²	9.23×10 ⁻³	1.46	2.15	5.20	27.1	13.2	175
0.9×10 ⁻¹⁴ 1600	0	0	1.17×10 ⁻³	1.22×10 ⁻⁵	0.597	0.364	3.83	14.7	11.6	136
0.9×10 ⁻¹³ 200	0.122	1.50×10 ⁻²	0.378	0.143	1.94	3.76	5.68	32.2	13.3	178
0.9×10 ⁻¹³ 400	6.73×10 ⁻³	6.15×10 ⁻⁵	0.142	2.04×10 ⁻²	1.53	2.35	5.25	27.6	13.0	168
0.9×10 ⁻¹³ 800	0	0	0	0	0.119	1.80×10 ⁻²	2.26	5.14	8.77	77.3
0.9×10 ⁻¹³ 1600	0	0	0	0	0	0	5.99×10 ⁻²	1.65×10 ⁻²	2.06	4.41
0.9×10 ⁻¹² 200	6.71×10 ⁻²	4.52×10 ⁻³	0.294	8.66×10 ⁻²	1.84	3.40	5.59	31.2	13.2	175
0.9×10 ⁻¹² 400	0	0	0	0	0.243	6.20×10 ⁻²	2.83	8.00	9.51	90.7
0.9×10 ⁻¹² 800	0	0	0	0	0	0	0	0	0.161	0.112
0.9×10 ⁻¹² 1600	0	0	0	0	0	0	0	0	0	0

Table 4. Summary Statistical Information for Seep Flow Rate (in m3/yr) (continued)

\bar{k} (m ²) 1/ α (Pa)	$q = 5$ mm/yr		$q = 14.6$ mm/yr		$q = 73.2$ mm/yr		$q = 213$ mm/yr		$q = 500$ mm/yr	
	Mean Q_s	Mean Square Q_s	Mean Q_s	Mean Square Q_s	Mean Q_s	Mean Square Q_s	Mean Q_s	Mean Square Q_s	Mean Q_s	Mean Square Q_s
0.9×10^{-11} 200	0	0	0	0	1.59×10^{-2}	1.47×10^{-3}	1.14	1.31	6.71	45.2
0.9×10^{-11} 400	0	0	0	0	0	0	0	0	0	0
0.9×10^{-11} 800	0	0	0	0	0	0	0	0	0	0
0.9×10^{-11} 1600	0	0	0	0	0	0	0	0	0	0
0.9×10^{-10} 200	0	0	0	0	0	0	0	0	2.88×10^{-2}	7.45×10^{-3}
0.9×10^{-10} 400	0	0	0	0	0	0	0	0	0	0
0.9×10^{-10} 800	0	0	0	0	0	0	0	0	0	0
0.9×10^{-10} 1600	0	0	0	0	0	0	0	0	0	0

Numbers from Table 3 converted in Excel spreadsheet Seep-sr1.xls, submitted with this report under DTN: SN0012T0511599.003.

6.3.2 Spatial Variability of k and $1/\alpha$

The next step in the analysis is to assign probabilities, or weights, to the various cases in Table 3 and Table 4.

There is quite a bit of permeability data available from air-injection tests. However, only a small subset of the data relates to characterization of the disturbed zone around the emplacement drifts, where the fracture properties are altered by the excavation. The properties of this disturbed zone are more relevant to calculations of seepage than properties of undisturbed rock, since the zone immediately surrounding the drifts is where the processes that determine seepage take place. Note that the disturbed-zone fracture properties are applied to the entire model domain, including the region beyond the disturbed zone, in the seepage simulations. This approach is discussed in the seepage model reports (CRWMS M&O 2000d, Section 6.2.2; CRWMS M&O 2000b, Section 6.3.2). Disturbed-zone air-permeability data from four locations are discussed in the Seepage Calibration Model report (CRWMS M&O 2000d, Section 6.2.2); see also Table 2 of this report, item 3. These post-excavation data are the best data available for determining the permeability field in the disturbed zone around an emplacement drift. Three of the locations are niches in the ESF in the Topopah Spring middle nonlithophysal hydrogeologic unit; the fourth is in the Cross Drift in the Topopah Spring lower lithophysal unit. The Cross Drift is the same shape as the potential emplacement drifts (circular), with a slightly smaller diameter (5 m, whereas the emplacement drifts are to be 5.5 m in diameter). The shape of the niches is not the same, but the width and height of the niches are comparable to emplacement drifts (approximately 4 m \times 3 m). In both cases the size and shape are reasonably close to those of the emplacement drifts, so the geometric-average measured post-excavation permeability should be a reasonable analog for \bar{k} , which is the geometric average of the permeability field in the seepage model. The data and averages are given in Table 5. Note that log denotes the base-10 logarithm everywhere in this report.

Table 5. Disturbed-Zone Air-Permeability Data

Topopah Spring Middle Nonlithophysal Unit		Topopah Spring Lower Lithophysal Unit	
Location	Mean log(k) (k in m^2)	Location	Mean log(k) (k in m^2)
Niche 3107	-12.14	SYBT-ECRB-LA#2	-10.73
Niche 3650	-11.66		
Niche 4788	-11.79		
Average	-11.86		-10.73
Std.Dev.	0.25		0.25 ^a

^aMiddle-nonlithophysal standard deviation used as analog.

Input data: see Table 2, item 3. Average and standard deviation computed in Excel spreadsheet Seep-sr1.xls, submitted with this report under DTN: SN0012T0511599.003.

It is significant that permeability is higher in the lower lithophysal unit since higher permeability corresponds to less seepage (see Table 3 and Table 4). Permeability in the lower lithophysal unit is not as well determined as for the middle nonlithophysal unit since it is based on only one measurement location. Furthermore, there are not enough data to calculate a standard deviation of log permeability for the lower lithophysal unit. There is other evidence to corroborate that the lower-lithophysal permeability should be higher: The drift-scale properties generated as part of the Calibrated Properties Model have the same trend—the lower-lithophysal (tsw35) permeability is one-half to one order of magnitude higher than the middle-nonlithophysal (tsw34) permeability, depending on the case (CRWMS M&O 2000f, Table 17). It is necessary to estimate a representative value of log standard deviation of permeability for the lower lithophysal unit since there are insufficient data from that unit. It is likely that the standard deviation is similar in the two units; for example, the standard deviation for smaller-scale variability is comparable for the two units (CRWMS M&O 2000d, Section 6.2.2). Thus, the middle-nonlithophysal standard deviation is used for the lower lithophysal unit as well. The greater uncertainty regarding the lower lithophysal unit is taken into account by means of uncertainty distributions, as discussed in Section 6.3.3.

Next we need information on the capillary-strength parameter for fractures, $1/\alpha$. This information comes from analysis of seepage tests. The capillary-strength parameter is used as a calibration variable, leading to calibrated $1/\alpha$ values that are consistent with seepage processes and with the conceptual and numerical model used for calculating seepage. The resultant calibrated $1/\alpha$ values are given in the Seepage Calibration Model report (CRWMS M&O 2000d, Section 7.1; see also Table 2 of this report, item 3). Calibration studies were performed for three of the locations discussed above for permeability; Niche 3650 was not calibrated, but was only used for validation studies. The data and averages are given in Table 6.

Table 6. Calibrated Values of the $1/\alpha$ Parameter

Topopah Spring Middle Nonlithophysal Unit		Topopah Spring Lower Lithophysal Unit	
Location	Log($1/\alpha$) ($1/\alpha$ in Pa)	Location	Log($1/\alpha$) ($1/\alpha$ in Pa)
Niche 3107	2.87	SYBT-ECRB-LA#2	2.94
Niche 4788	2.74 ^a		
Average	2.81		2.73 ^b
Std.Dev.	0.092		0.092 ^c

^aAverage of calibrations for three boreholes.

^bReduced by 0.21 to account for lithophysae; see text.

^cMiddle-nonlithophysal standard deviation used as analog.

Input data: see Table 2, item 3. Average and standard deviation computed in Excel spreadsheet Seep-sr1.xls, submitted with this report under DTN: SN0012T0511599.003.

The value listed in the table for Niche 4788 is the average of three values that were developed for that niche, using different boreholes for water injection. The Seepage Calibration Model report

treated those three measurements as independent, and combined them with the one measurement for Niche 3107 to estimate mean and standard deviation for the middle nonlithophysal unit as 2.77 and 0.10 (CRWMS M&O 2000d, Table 11). For the purposes of the seepage abstraction, it is more consistent to treat each niche as a distinct location and calculate the average and standard deviation as indicated in Table 6. There is little difference in the two estimates, however.

As noted in Table 6, the calibrated $1/\alpha$ value for the lower lithophysal unit was reduced to account for effects of lithophysal cavities on seepage. As discussed in the Seepage Calibration Model report (CRWMS M&O 2000d, Section 6.3.3.3), lithophysal cavities tend to increase seepage. Since lithophysal cavities are not included explicitly in the Seepage Model for PA, it is necessary to include them implicitly by reducing the estimated $1/\alpha$ (the estimate of 2.94 for $\log[1/\alpha]$ is for a model with lithophysae included). One calibration case was run with and without lithophysal cavities in the model, and the calibrated $\log(1/\alpha)$ without lithophysal cavities was lower than the value with lithophysal cavities by 0.21 (CRWMS M&O 2000d, Section 6.3.3.3). As with permeability, the standard deviation of $\log(1/\alpha)$ for the middle nonlithophysal unit is used for the lower lithophysal unit as well. An estimate of 0.08 for the lower-lithophysal standard deviation was developed by running multiple geostatistical realizations of the Seepage Calibration Model (CRWMS M&O 2000d, Section 6.3.3.3 and Table 11). Using the slightly larger middle-nonlithophysal standard deviation is expected to be conservative. (As discussed further in the following section, larger standard deviations tend to increase the estimated seepage.)

To close out this section, note that there is another potential host unit for the repository, the Topopah Spring lower nonlithophysal hydrogeologic unit. No seepage data from that unit are available, but the information that is available generally indicates that the properties of that unit are in-between those of the middle nonlithophysal and lower lithophysal units. For example, the Calibrated Properties Model drift-scale fracture permeability for tsw36 is between those for tsw34 and tsw35 for each case (CRWMS M&O 2000f, Table 17), and the fracture α for tsw36 is between tsw34 and tsw35 for two out of three cases and slightly larger than the tsw35 value for the third case (CRWMS M&O 2000f, Tables 13–15). Thus, the seepage behavior of the lower nonlithophysal unit should be encompassed within the range of behaviors of the other two host units.

6.3.3 Uncertainty in k and $1/\alpha$

The distinction between spatial variability and uncertainty in \bar{k} and $1/\alpha$ (or any other parameter) can be understood in terms of the way a TSPA calculation works. A TSPA calculation is a Monte Carlo simulation, in which a number of realizations of the total system are generated and repository performance computed for each one. The Monte Carlo simulation is basically an uncertainty analysis: Any one of the realizations could be the “correct” one. The differences between one realization and another are within the range of our uncertainty, with each parameter being sampled from its uncertainty distribution for each realization. Some parameters, like fracture permeability or $1/\alpha$ parameter, are uncertain, so they vary from one TSPA realization to another, but they are also spatially variable, so they vary from location to location within each TSPA realization.

The spatial variability of \bar{k} and $1/\alpha$ was discussed in Section 6.3.2. There are only a few measurements of \bar{k} and $1/\alpha$, including only one measurement for the lower lithophysal unit and none for the lower nonlithophysal unit. Thus, in addition to spatial variability within each TSPA realization, it is important to treat \bar{k} and $1/\alpha$ as uncertain and vary them across realizations.

With few data available, the treatment of uncertainty is necessarily somewhat arbitrary. The method chosen is to define "bounding" high- and low-seepage cases in addition to the "best-estimate" case that uses the parameter values described in Section 6.3.2. Following are the considerations used in defining the high and low cases:

- For the middle nonlithophysal unit, the high-seepage case uses mean \bar{k} and $1/\alpha$ one standard deviation lower than the base-case values, and the low-seepage case uses mean \bar{k} and $1/\alpha$ one standard deviation higher than the base-case values.
- For the lower lithophysal unit, because there is much less data than for the middle nonlithophysal unit, the uncertainty range is increased and the high and low cases use mean \bar{k} and $1/\alpha$ two standard deviations lower or higher than the base-case values.
- In addition, the standard deviations of \bar{k} and $1/\alpha$ are doubled for the high-seepage case. Because the standard deviations are based on so few data points, they are uncertain also. In Section 6.3.4, the means and standard deviations are used to define weighting factors that are used to combine seepage results for multiple $(\bar{k}, 1/\alpha)$ cases into a single weighted estimate of seepage for a given percolation flux. Larger standard deviations lead to combining more values, while smaller standard deviations lead to combining fewer values. Because of the nonlinearity of the seepage dependence on \bar{k} and $1/\alpha$, especially at lower percolation fluxes, the effect of combining results for more $(\bar{k}, 1/\alpha)$ cases is generally to increase the seepage estimate, because more weight is given to lower values, where seepage can be much higher. Thus, a larger standard deviation tends to increase the estimated seepage.

The three seepage-abstraction cases are summarized in Table 7. These three cases are used to define uncertainty distributions for seepage by assigning a triangular shape to the distributions, with the minimum of the triangle at the low-seepage value; the peak of the triangle, or highest probability, at the base-case seepage value; and the maximum of the triangle at the high-seepage value. This distribution appropriately represents the key features desired, which are that seepage values for the base case are most likely and that \bar{k} and $1/\alpha$ could be within the ranges discussed above, but the high- and low-seepage cases are less likely to be representative of repository conditions.

Table 7. Uncertainty Cases for Seepage Abstraction

	Topopah Spring Middle Nonlithophysal Unit		Topopah Spring Lower Lithophysal Unit	
Base Case				
Mean $\log(\bar{k})$	μ_{kmn}	-11.86	μ_{kl}	-10.73
Std.dev. $\log(\bar{k})$	σ_k	0.25	σ_k	0.25
Mean $\log(1/\alpha)$	$\mu_{\alpha mn}$	2.81	$\mu_{\alpha ll}$	2.73
Std.dev. $\log(1/\alpha)$	σ_α	0.09	σ_α	0.09
High-Seepage Case				
Mean $\log(\bar{k})$	$\mu_{kmn} - \sigma_k$	-12.11	$\mu_{kl} - 2\sigma_k$	-11.23
Std.dev. $\log(\bar{k})$	$2\sigma_k$	0.50	$2\sigma_k$	0.50
Mean $\log(1/\alpha)$	$\mu_{\alpha mn} - \sigma_\alpha$	2.71	$\mu_{\alpha ll} - 2\sigma_\alpha$	2.55
Std.dev. $\log(1/\alpha)$	$2\sigma_\alpha$	0.18	$2\sigma_\alpha$	0.18
Low-Seepage Case				
Mean $\log(\bar{k})$	$\mu_{kmn} + \sigma_k$	-11.62	$\mu_{kl} + 2\sigma_k$	-10.23
Std.dev. $\log(\bar{k})$	σ_k	0.25	σ_k	0.25
Mean $\log(1/\alpha)$	$\mu_{\alpha mn} + \sigma_\alpha$	2.90	$\mu_{\alpha ll} + 2\sigma_\alpha$	2.91
Std.dev. $\log(1/\alpha)$	σ_α	0.09	σ_α	0.09

μ_{kmn} , μ_{kl} , $\mu_{\alpha mn}$, $\mu_{\alpha ll}$, σ_k , and σ_α are the averages and standard deviations from Table 5 and Table 6. Numbers are rounded from values calculated in Excel spreadsheet Seep-sr1.xls (DTN: SN0012T0511599.003). Units of \bar{k} are m^2 , units of $1/\alpha$ are Pa.

6.3.4 Discrete Probability Distributions for k and $1/\alpha$

Given distributions for \bar{k} and $1/\alpha$, a corresponding distribution can be developed for seepage using the information in Table 3 and Table 4. To do that, the \bar{k} and $1/\alpha$ distributions must first be discretized—that is, the continuous distributions (log-normal distributions with the given means and standard deviations) must be converted to discrete weighting factors for the \bar{k} and $1/\alpha$ values in Table 3 and Table 4.

The increments of the $\log(\bar{k})$ and $\log(1/\alpha)$ values in Table 3 and Table 4 (1 and 0.3, respectively, since \bar{k} values are a factor of 10 apart and $1/\alpha$ values are a factor of 2 apart) are much greater than the base-case standard deviations (0.25 and 0.09, respectively), which makes it difficult to represent the distributions accurately. The best that can be done is to match the mean and standard deviation with a three-point discrete distribution. In many cases, it is not even possible to fit a three-point distribution to the data (one of the weighting factors would have to be negative, which is not allowed), so a two-point distribution that matches the mean is used. In such cases, the actual standard deviation of the two-point discrete distribution is larger than the standard deviation of the continuous distribution that is being approximated. Having a higher standard deviation is acceptable since it just implies a little more variability than was called for.

Examples of three-point and two-point discrete distributions are given in Table 8 and Table 9. All of the discrete distributions can be found in the spreadsheet Seep-sr1.xls.

Table 8. Example Three-Point Discrete Distribution
(Middle Nonlithophysal Unit, Low-Seepage Case)

$1/\alpha$ (Pa)	200	400	800	1600
$\log(1/\alpha)$	2.30	2.60	2.90	3.20
Normalized Weight	0	0.057	0.906	0.037
Mean of the discrete distribution:				2.90
Standard deviation of the discrete distribution:				0.09

Taken from Excel spreadsheet Seep-sr1.xls, submitted with this report under DTN: SN0012T0511599.003. Numbers in this table are rounded, but the spreadsheet keeps additional significant figures.

Table 9. Example Two-Point Discrete Distribution
(Middle Nonlithophysal Unit, Low-Seepage Case)

\bar{k} (m^2)	0.9×10^{-14}	0.9×10^{-13}	0.9×10^{-12}	0.9×10^{-11}	0.9×10^{-10}
$\log(\bar{k})$	-14.05	-13.05	-12.05	-11.05	-10.05
Normalized Weight	0	0	0.569	0.431	0
Mean of the discrete distribution:					-11.62
Standard deviation of the discrete distribution:					0.50

Taken from Excel spreadsheet Seep-sr1.xls, submitted with this report under DTN: SN0012T0511599.003. Numbers in this table are rounded, but the spreadsheet keeps additional significant figures.

The next step in the calculation is to combine the \bar{k} and $1/\alpha$ distributions into a single two-dimensional distribution by multiplying them together. The combination of the distributions from Table 8 and Table 9 is shown in Table 10.

Table 10. Two-Variable Discrete Distribution
(Middle Nonlithophysal Unit, Low-Seepage Case)

		\bar{k} (m ²)					Sum
		0.9×10^{-14}	0.9×10^{-13}	0.9×10^{-12}	0.9×10^{-11}	0.9×10^{-10}	
$1/\alpha$ (Pa)	200	0	0	0	0	0	0
	400	0	0	0.032	0.025	0	0.057
	800	0	0	0.516	0.390	0	0.906
	1600	0	0	0.021	0.016	0	0.037
Sum		0	0	0.569	0.431	0	1.000

Taken from Excel spreadsheet Seep-sr1.xls, submitted with this report under DTN: SN0012T0511599.003. Numbers in this table are rounded, but the spreadsheet keeps additional significant figures.

The final step in generating discrete distributions for \bar{k} and $1/\alpha$ is to combine the distributions for the different repository host units. To do so, the distributions are weighted according to the fraction of the repository that is to be in each host unit. Those fractions are given in Table 11. The design report (CRWMS M&O 2000e, Table 18) lists fractions for the base design and for the base design plus contingency area. The host-unit fractions are very similar for the two cases, but the fraction of lower lithophysal is slightly smaller when the contingency area is included. Since the lower lithophysal unit is predicted to have less seepage than the other host units, the fractions that include the contingency area are conservatively used for the seepage abstraction. As discussed in Section 6.3.2, there are no seepage data for the lower nonlithophysal unit, but its seepage behavior is expected to be encompassed within the range of behaviors of the middle nonlithophysal and lower lithophysal units. For the seepage abstraction, the lower nonlithophysal unit is conservatively lumped together with the middle nonlithophysal unit. The fractions as obtained from the design report add up to 99.9% rather than 1 because of rounding errors, so the fractions are “renormalized” by dividing by 0.999.

Table 11. Fraction of Repository in Host Units

Unit	Fraction for Each Unit	Fraction for Nonlithophysal and Lithophysal Units	Fraction with Numbers Renormalized to Sum to 1
Topopah Spring middle nonlithophysal	8.0%	20.3%	20.3%
Topopah Spring lower nonlithophysal	12.3%		
Topopah Spring lower lithophysal	79.6%	79.6%	79.7%

Input data: see Table 2, item 4. Numbers in the last column are rounded, but Excel spreadsheet Seep-sr1.xls keeps additional significant figures.

The final discrete probability distribution for \bar{k} and $1/\alpha$ for the low-infiltration case is obtained by weighting the nonlithophysal (shown in Table 10) and lithophysal (not shown, but available

in Excel spreadsheet Seep-sr1.xls) distributions by their respective fractions from the last column of Table 11. The resulting combined distribution is shown in Table 12. The same process is followed for the base case and the high-infiltration case. Those results are not given here, but are available in Excel spreadsheet Seep-sr1.xls.

Table 12. Final Discrete Distribution for Low-Seepage Case

		\bar{k} (m ²)					Sum
		0.9×10^{-14}	0.9×10^{-13}	0.9×10^{-12}	0.9×10^{-11}	0.9×10^{-10}	
1/ α (Pa)	200	0	0	0	0	0	0
	400	0	0	0.007	0.009	0.019	0.035
	800	0	0	0.105	0.215	0.586	0.906
	1600	0	0	0.004	0.013	0.042	0.059
Sum		0	0	0.116	0.237	0.647	1.000

Taken from Excel spreadsheet Seep-sr1.xls, submitted with this report under DTN: SN0012T0511599.003. Numbers in this table are rounded, but the spreadsheet keeps additional significant figures.

6.3.5 Variability and Uncertainty of Seepage

If the seepage information in Table 3 and Table 4 is combined with the weighting factors in Table 12 (plus the weighting factors for the other two cases, which are not shown), weighted seepage statistics are obtained, representing the spatial variability of seepage within a TSPA realization. Those results are shown in Table 13 for the three uncertainty cases.

Table 13. Weighted Seepage Statistics for the Basic Seepage Results

q (mm/yr)	Low-Seepage Case			Base Case			High-Seepage Case		
	f_s	Mean of Q_s (m ³ /yr)	Std.Dev. of Q_s (m ³ /yr)	f_s	Mean of Q_s (m ³ /yr)	Std.Dev. of Q_s (m ³ /yr)	f_s	Mean of Q_s (m ³ /yr)	Std.Dev. of Q_s (m ³ /yr)
5	0	0	0	0	0	0	8.31×10^{-2}	5.71×10^{-2}	2.63×10^{-2}
14.6	0	0	0	0	0	0	8.31×10^{-2}	0.267	6.36×10^{-2}
73.2	6.60×10^{-3}	0.243	5.33×10^{-2}	5.41×10^{-2}	0.243	5.33×10^{-2}	0.376	0.525	0.682
213	6.60×10^{-3}	2.83	0.140	5.41×10^{-2}	2.83	0.140	0.452	2.66	1.56
500	7.65×10^{-2}	1.04	2.63	0.129	4.14	4.60	0.512	8.07	3.59

Taken from Excel spreadsheet Seep-sr1.xls, submitted with this report under DTN: SN0012T0511599.003.

Calculation of the weighted-mean seepage fraction f_s is straightforward. It is simply given by

$$\langle f_s(q) \rangle = \sum w_{ij} f_s(x_i, y_j, q) \tag{Eq. 1}$$

where the sum is over the discrete pairs of $x_i = \bar{k}$ and $y_j = 1/\alpha$, and w_{ij} are the weighting factors in Table 12 (for the low-seepage case). Calculation of the weighted mean and standard deviation of Q_s is slightly more complicated because the mean over locations with seepage is desired, rather than the overall mean. For the mean, it is just a matter of adjusting the average by the fraction of locations that have seepage:

$$\langle Q_s(q) \rangle = \frac{\sum w_{ij} Q_s^*(x_i, y_j, q)}{\langle f_s(q) \rangle} = \frac{\langle Q_s^*(q) \rangle}{\langle f_s(q) \rangle} \quad (\text{Eq. 2})$$

In this equation, $\langle Q_s^*(q) \rangle$ is the average seep flow rate over all locations, as listed in Table 4. The division by the seepage fraction makes it into an average over just the locations with seepage. The mean square seep flow rate, adjusted by seepage fraction, is calculated in the same way, and then the standard deviation of seep flow rate is obtained from

$$\sigma_{Q_s}^2 = \langle Q_s^2(q) \rangle - \langle Q_s(q) \rangle^2 \quad (\text{Eq. 3})$$

6.4 ADJUSTMENTS FOR OTHER EFFECTS

6.4.1 Drift Degradation and Rock Bolts

The basic seepage simulations that have been discussed so far were computed assuming the design drift configuration. Degradation of the drifts over time is expected and has been evaluated (CRWMS M&O 2000n). The effect that changes in drift shape might have on seepage is of concern. The Seepage Model for PA report (CRWMS M&O 2000b) includes some discussion of the impacts of drift degradation on seepage in Section 6.4 and results of some seepage simulations with degraded drift shapes in Section 6.6.4. A total of nine degraded-drift seepage simulations were performed (CRWMS M&O 2000b, Table 12). Degraded drift shapes lead to increases in computed seepage, with the increase ranging from negligible to 55% for the worst case modeled. (The three geostatistical realizations for that case had seepage increases of approximately 27%, 55%, and 15%, for an average increase of about 32%.) It is proposed (CRWMS M&O 2000o, Section 6.6.5) that the increase in seepage is approximately proportional to the increase in drift-wall area (including voids from which blocks have fallen in the area calculation). This approximation could be used to estimate seepage for cases that have not been computed with the seepage model.

The worst cases reported in the drift-degradation analysis (CRWMS M&O 2000n, Section 6.4.3 and Attachment XII) have worse drift degradation than the cases for which seepage is modeled (CRWMS M&O 2000b, Sections 6.4 and 6.6.4). However, the drift-degradation results indicate that the rock in the repository is strong enough that drift failures are infrequent: The fraction of drift length affected by rockfall ranges from only 0.4% up to 14.2% for the repository host units (CRWMS M&O 2000n, Attachment XII). Furthermore, the lowest numbers (0.4% to 1.0% for various cases) are for the host unit that contains most of the repository (Topopah Spring lower lithophysal). While we want to increase the seepage amounts to account for drift degradation, it would greatly overestimate the effects to assume the worst possible degradation at all locations.

An additional consideration is the possibility that the rock bolts used for ground support could become preferential paths for seepage as they degrade. This "surface needle" effect could be important (CRWMS M&O 2000b, Sections 6.7 and 7). According to a preliminary estimate, seepage could increase by as much as 70%, depending on how many of these preferential paths there are. Specifically, increases of 3%, 40%, and 70% are reported for cases with 3, 33, and 330 "needles" along a 16.5-m length of drift (CRWMS M&O 2000b, Section 6.7). According to a design input transmittal (CRWMS M&O 1999, item 1, attachment III, p. 1), rock bolts are not planned for the lower lithophysal unit, which will contain most of the repository, but in the nonlithophysal units there may be six rock bolts every 1.5 m along the drifts, which would be 66 along a 16.5-m length of drift. Thus, the preliminary estimate would be for an increase of somewhat more than 40% due to the rock bolts in the nonlithophysal units (linear interpolation between the results for 33 and 330 needles gives a 43% increase, while logarithmic interpolation gives a 49% increase).

To summarize, a potential for increased seepage is indicated in locations where rock bolts are used for ground support, which is expected to be principally in the nonlithophysal repository host units. In addition, after the ground support has degraded and the shape of the drifts starts to degrade, the seepage model predicts increased seepage. The potential for drift degradation is predicted to be higher in the nonlithophysal units than in lithophysal rock, and highest in the middle nonlithophysal unit. The effects of rock bolts and drift degradation on seepage are not necessarily additive, however. In locations where drift degradation is minor, the rock-bolt effect would dominate, and in locations with extensive drift degradation the damage can extend above the rock-bolt holes, so they no longer have an additional effect. As just discussed, the potential for both of these effects is lower in the lower lithophysal unit, where most of the emplacement drifts are to be located. However, because of the uncertainty associated with these effects, and because we wish to simplify the treatment of seepage in the TSPA, the lower lithophysal unit will conservatively not be differentiated from the others in the abstraction.

As an approximate treatment, seepage will be increased by 50% to account for these effects. That is, for TSPA the seep flow rates in Table 13 will be increased by 50% as an adjustment for drift degradation and rock bolts. The worst drift-degradation case for which seepage was modeled had a seepage increase averaging 32%, as discussed above, and according to the drift-degradation analysis, there is only a small probability of more extensive drift degradation (the most extreme cases in Attachment XII of CRWMS M&O 2000n). According to the preliminary evaluation of rock-bolt effects on seepage, they might increase seepage by approximately 50% in the nonlithophysal units, but there might be no rock bolts in the lower lithophysal unit. Finally, it is worth noting that analyses have shown that drift degradation tends to increase the seep flow rate but does not change the seepage threshold (CRWMS M&O 2000b, Section 6.6.4). This result implies that drift degradation does not affect the seepage fraction, confirming that the abstraction approach of increasing only the seep flow rate is reasonable.

6.4.2 Possible Correlation of k and $1/\alpha$

There are theoretical reasons to expect fracture permeability and the fracture $1/\alpha$ parameter to be correlated (e.g., they are both related to fracture aperture). For Rev. 00, the seepage calibration was performed with k and $1/\alpha$ correlated but then the Seepage Model for PA changed the conceptual model somewhat by assuming no correlation. A few cases were run with correlation

between k and $1/\alpha$ in the Seepage Model for PA (CRWMS M&O 2000o, Section 6.6.4); the seepage results were quite similar, but higher than the base-case results by up to 10%. Because of this result, seepage was increased in the seepage abstraction to account for the possible effects.

For Rev. 01, however, correlation between k and $1/\alpha$ is neglected in both the Seepage Calibration Model and the Seepage Model for PA. Thus, the calibrated $1/\alpha$ values are fully appropriate to the conceptual model used in the Seepage Model for PA, and there is no need to consider increasing seepage to account for possible correlation effects. To consider such correlation consistently, it would need to be introduced in both the Seepage Calibration Model and the Seepage Model for PA, and the calibrated $1/\alpha$ values might be a little different as a result. However, since the current conceptual model with no correlation reasonably reproduces the seepage test results, there is no real need to incorporate the correlation and if it were done it should not change the results significantly.

6.4.3 Focusing of Flow above the Drifts

Focusing of flow in the unsaturated zone is an issue for seepage into drifts, since it could result in higher fluxes in some locations, which would then increase the amount of seepage in those locations. Flow focusing on large scales (hundreds of meters) is taken into account by the site-scale UZ flow model (CRWMS M&O 2000g). Flow focusing on small scales (a few meters) is already included in the drift-scale UZ flow model that is used for seepage calculations (CRWMS M&O 2000b). What is missing is an explicit consideration of flow focusing on intermediate scales (tens of meters). Such focusing could potentially concentrate flow from an area of tens of meters square onto a particular drift segment, thereby increasing the local percolation flux and seepage at that location. It is important to realize, though, that if flow is concentrated in one location, conservation of water mass requires that flow be reduced in other areas so that the total amount of water flow is unchanged.

The “active fracture” conceptual flow model (Liu et al. 1998) that is being used for site-scale UZ flow calculations is based on the concept that flow is channeled in fractures, so that only some fractures are actively flowing. This conceptual model can provide an estimate of the degree of channeling in fractures and thus the degree of intermediate-scale focusing of flow.

6.4.3.1 Calculation of Weep Spacings

Discrete fracture flow paths, referred to as “weeps,” are believed to occur in the unsaturated zone at Yucca Mountain as a result of heterogeneities and instabilities in wetting-front propagation. While channeling and fingering of flow have been observed in laboratory settings (Glass and Tidwell 1991, p. 50), current models of flow through the UZ at Yucca Mountain are based on continuum approximations. In this analysis/model, the weep spacing is calculated as the distance that separates the active fractures, which is typically larger than the geometric spacing of fractures used in the development of the continuum model. The weep spacings can be derived from dual-continuum models as described in Ho and Wilson (1998) and Liu et al. (1998). A slightly modified version of the method used in Ho and Wilson (1998) is presented here to derive an upper bound for the weep spacings assuming that each active fracture is saturated (i.e., flow occupies the entire fracture). The method used in Liu et al. (1998, Section 2.4) assumes that the

active fractures are unsaturated, and Eq. 17 in that paper is used to provide a lower bound on the weep spacings.

Upper Bound on Weep Spacings. The upper bound on weep spacing is calculated using geometric arguments for the reduced wetted fracture area in a computational grid block of the site-scale UZ flow model. In Ho and Wilson (1998), the ratio of the available weep area, A_{weep} , to the total geometric fracture area, A_{DKM} , in a computational grid block was defined as a fracture/matrix reduction factor, X_{fm} :

$$X_{fm} = \frac{A_{weep}}{A_{DKM}} \quad (\text{Eq. 4})$$

In the site-scale flow fields, the geometric fracture area, A_{DKM} , per volume of grid block, V , is provided as a constant parameter ($A^* = A_{DKM}/V$) for each unit. The available weep area, A_{weep} , is derived in this analysis/model assuming that each fracture containing a weep is saturated. This is equivalent to assuming that the weep width w is equal to the weep spacing a in Eq. 3 of Ho and Wilson (1998), yielding $A_{weep} = 2V/a$. Substituting these relations into Eq. 4 and solving for the weep spacing yields:

$$a = \frac{2}{X_{fm} A^*} \quad (\text{Eq. 5})$$

To be consistent with the active-fracture model used in the site-scale flow fields, the reduction factor X_{fm} is calculated as the product of the first two terms on the right-hand side of Eq. 12 of Liu et al. (1998), which describes the ratio of the available weep area to the total fracture area per grid block. The resulting reduction factor X_{fm} is equal to the effective liquid saturation, S_e , of the fractures in the grid block (see Eq. 2 of Liu et al. 1998):

$$X_{fm} = S_e = \frac{S_f - S_r}{1 - S_r} \quad (\text{Eq. 6})$$

where S_f is the average liquid saturation of the fractures in the grid block and S_r is the residual liquid saturation of the fractures. Eqs. 5 and 6 yield an upper bound to the discrete weep spacings because the active fractures are assumed to be saturated, which maximizes the distances separating the active fractures.

Lower Bound on Weep Spacings. Eq. 17 from Liu et al. (1998) is used directly to calculate a lower bound for the weep spacing a (i.e., the separation distance between active fractures):

$$a = \frac{d}{S_e^\gamma} \quad (\text{Eq. 7})$$

where d is the geometric fracture spacing for each grid block (constant for each unit) and γ is a calibrated parameter (between 0 and 1) that is associated with the fraction of fractures that are active in the fracture network. The active fractures are assumed to be only partially saturated, so

the derived spacing in Eq. 7 will be less than if the active fractures are assumed to be saturated as given in Eqs. 5 and 6.

Inputs. The parameters used in Eqs. 5–7 that are relevant to this analysis/model are summarized in Table 14. Note that tswF4, tswF5, and tswF6 are the names given to the fracture materials in the UZ Flow Model for the Topopah Spring middle nonlithophysal, lower lithophysal, and lower nonlithophysal units, respectively; tswFf refers to the fracture material in fault zones.

Table 14. Hydrologic Parameters Used in Calculation of Weep Spacings

Unit	Material	A* (m ² /m ³)	d (m)	S _r	γ		
					Low Infiltration	Base Infiltration	High Infiltration
tsw34	tswF4	13.54	0.23	0.01	0.23	0.41	0.38
tsw35	tswF5	9.68	0.32	0.01	0.23	0.41	0.38
tsw36	tswF6	12.31	0.25	0.01	0.23	0.41	0.38
All 3	tswFf	8.6	0.59	0.01	0.5	0.5	0.5

A*, d inputs: see Table 2, item 12. S_r, γ inputs: see Table 2, items 8–10 for tswFf; Table 2, items 5–7 for others.

Results. The software routine T2WEEP v. 1.0 was used to calculate the weep spacings derived above. In order to calculate the weep spacings, elements must be prescribed so that relevant hydrologic parameters and variables are appropriately assigned. Attachment III contains a description and listing of the elements that are used to derive the weep spacing of flow entering the repository region. The repository outline is taken from the TDMS (see Table 2, item 13).

A number of flow fields have been generated for the TSPA for Site Recommendation, including flow for three climate states (present-day, monsoon, and glacial transition), three infiltration levels (low, “base,” and high), and two alternative models for flow beneath the repository (perched-water models #1 and #2). The percolation fluxes and liquid saturations at the repository horizon are not affected by the differences in the perched-water models, so only model #1 is used. The glacial-transition climate is chosen to obtain the weep-spacing distributions because that climate is in effect most of the time; the present-day and monsoon climates are only in effect at relatively early times. Thus, T2WEEP is run for three flow fields: (1) glacial-transition climate, low infiltration, perched-water model #1; (2) glacial-transition climate, base infiltration, perched-water model #1; and (3) glacial-transition climate, high infiltration, perched-water model #1 (see Table 2, items 8–10).

Results for the base-infiltration case are shown in Figure 1. (Results for the other two cases are qualitatively similar.) Shown are histograms for the log of weep spacing assuming saturated active fractures (Eqs. 5–6) and unsaturated active fractures (Eq. 7). Note that the repository elements that were assigned fault properties (as denoted by an ‘f’ in the fifth character of the material name) have been excluded from the histograms. The elements with fault properties used parameters significantly different from the other repository units (see Table 14) and yielded extremely large weep spacings that could exceed the size of the grid block. It makes sense to exclude the fault elements from this analysis because we are concerned with seepage at waste-package locations, and waste packages are not expected to be emplaced directly in fault zones. It can be seen in the figure that both methods produce weep spacings that are approximately log-

normally distributed and that, as expected, the assumption of saturated active fractures leads to larger weep-spacing estimates. The means and standard deviations of log spacings are listed in Table 15.

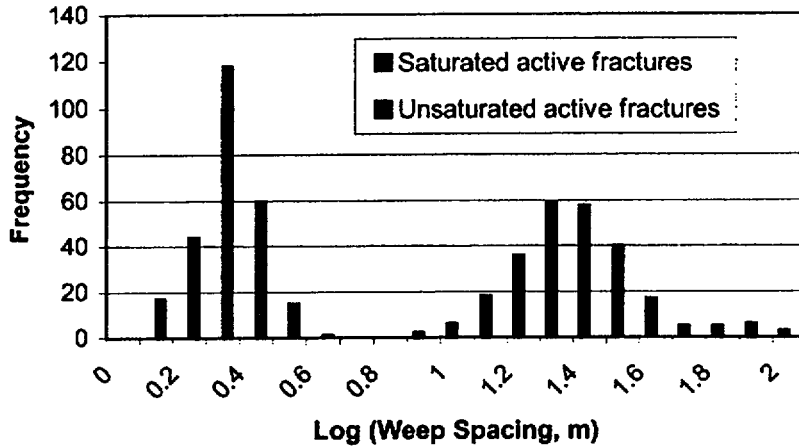


Figure 1. Histograms of Log Weep Spacing for Glacial-Transition Climate and Base Infiltration

Taken from Excel spreadsheet Seep-sr1.xls, submitted with this report under DTN: SN0012T0511599.003.

Table 15. Statistics for Weep Spacings, Glacial-Transition Climate

		Low Infiltration	Base Infiltration	High Infiltration
Log(a) (saturated active fractures; a in m)	Mean	1.43	1.43	1.23
	Std.Dev.	0.35	0.19	0.21
Log(a) (unsaturated active fractures; a in m)	Mean	-0.03	0.36	0.22
	Std.Dev.	0.11	0.10	0.10

Taken from Excel spreadsheet Seep-sr1.xls, submitted with this report under DTN: SN0012T0511599.003.

Note that the spacings tend to increase with lower infiltration. The reduced infiltration reduces the number of actively flowing fractures, which consequently increases the weep spacing. The weep spacings for low infiltration do not fit smoothly on the trend for the two higher-infiltration cases because the active-fracture γ parameter is significantly different for low infiltration (see Table 14).

6.4.3.2 Distribution of Flow-Focusing Factors

The mean log spacing of 1.43 for the base-infiltration case (see Table 15) corresponds to an actual spacing of about 27 m. A spacing of 27 m between flowing fractures would indicate a potential for the flow from a 27 m × 27 m area to be focused into a relatively small area. This is the estimate based on saturated flowing fractures in the active-fracture model (see Section 6.4.3.1 and Eqs. 5 and 6). The estimate based on unsaturated flowing fractures is much smaller—only 2.3 m (see Table 15).

The upper-boundary area in the drift seepage model is 15 m × 5.23 m = 78.5 m² (CRWMS M&O 2000b, Section 6.3.1). The area corresponding to 27 m × 27 m is 729 m². If all the flow from 729 m² were focused into the area above one of these model domains, that would lead to a local percolation flux a factor of about 9.3 times as high as the average (729/78.5). On the other hand, spacings of up to several meters are contained within the size of the model, and focusing over that distance would not be expected to change the seepage model significantly. (Note that water flow within a seepage simulation would take place primarily within the high-permeability channels of the heterogeneous model regardless of how flux is introduced at the boundary.) Thus, a range of focusing factors is supported by the information available. The shape of the distribution is speculative, but a log-uniform distribution will be used, as it is appropriate for an uncertain multiplicative factor, in that high and low multipliers are weighted equally. The lower bound of the log-uniform distribution should be 1, or no significant focusing. The upper bound will be taken from one standard deviation above the mean of the log weep-spacing distribution. Because of the normal shape of the log weep-spacing distributions (see Figure 1) the likelihood of values higher than one standard deviation above the mean is small, and they would not be appropriate for use with a log-uniform distribution of focusing factors. An example of the derivation of the upper bound is as follows. For the base-infiltration case, the mean and standard deviation of log spacing from Table 15 are 1.43 and 0.19, respectively, so one standard deviation above the mean is at $\log(a) = 1.62$, or $a \cong 42$ m. An area of 42 m × 42 m is about 1800 m², and this area divided by 78.5 m² (the area of the seepage model domain) gives a focusing factor of approximately 22, which is used for the upper bound of the log-uniform distribution of focusing factors for base infiltration. In a similar manner, the upper bounds for low and high infiltration are found to be approximately 47 m and 9.7 m, respectively. As noted above, the estimated weep spacings, and thus the estimated focusing factors, are higher when infiltration is lower.

This distribution of flow-focusing factors is an uncertainty distribution, which means that one value of it is sampled for each TSPA realization. That value is then applied to modify the spatial variability of seepage within the realization. The way it would be applied is as follows. Say the initial estimate of percolation flux at a location is q_i and the focusing factor is F . The percolation flux is modified to $q = Fq_i$ and the seepage fraction f_s and seep flow rate Q_s are calculated (or sampled from distributions) based on that flux. They will be higher than if they had been calculated using q_i because q is a higher flux. But further modification is necessary, because a higher flux q over an area implies lower fluxes over a larger area in order to preserve the correct average percolation flux (in other words, in order to conserve water mass). Percolation increased by a factor of F over an area A would have to be balanced by zero flux over an area $(F-1)A$ (or a nonzero flux over an even larger area) in order to leave the average flux unchanged. A simple abstraction for this effect is to reduce the seepage fraction by F to f_s/F , consistent with a conceptual picture that percolation increased by a factor F at one location is balanced by $(F-1)$

other locations with zero percolation and zero seepage. The seep flow rate Q_s is not reduced because it is supposed to represent the average seep flow rate for locations with seepage; thus, adding any number of non-seeping locations does not change it. The total effect is to reduce the seepage fraction and increase the seep flow rate relative to results that do not account for flow focusing.

6.4.4 Episodic Flow

As discussed in Section 5, we assume for the seepage abstraction analysis/model that episodic flow can be neglected, because there is no evidence for it at the repository depth and flow simulations have shown that the Paintbrush nonwelded unit above the repository damps out episodic flow. However, it would be relatively easy to approximate episodic effects in the seepage abstraction, and for completeness this subsection explains how it could be done.

Episodic flow can increase the amount of seepage for a given yearly flux because, if flow only occurs a portion of the year, the percolation flux must be higher during the periods when flow does occur. This effect was confirmed by a seepage simulation for an example episodic-flow scenario (CRWMS M&O 2000b, Section 6.6.6). As would be expected, the seepage rate cycles up and down with the percolation flux, and the peak value of the seepage percentage is approximately what would be expected based on the peak value of the percolation flux (CRWMS M&O 2000b, Section 6.6.6). The average seepage percentage (averaged over both wet and dry periods) is significantly lower than the peak values.

As with flow focusing, there is a simple approximation for this effect. If the initial estimate of percolation flux at a location is q_i and the fraction of the time that flow occurs is E , then during flowing periods the percolation flux is given by $q = q_i/E$. The seepage fraction f_s and seep flow rate Q_s for the wet period can be calculated (or sampled from distributions) based on that flux. Further modification is necessary in order to preserve the correct time-average flux. If the seep flow rate is Q_s during the wet period and approximately zero during the dry period, the average seep flow rate over both periods is EQ_s . The effective seepage fraction should remain at f_s because that is the fraction of locations that have seepage, but the seepage occurs for only a fraction of the time rather than being continuous.

6.4.5 Coupled Processes

Coupled processes include the various thermally driven processes that could affect seepage into emplacement drifts, including thermal-hydrologic, thermal-hydrologic-mechanical, and thermal-hydrologic-chemical processes. As discussed in Section 5, thermal-hydrologic-chemical processes have been found to have little effect on seepage. Thermal-hydrologic-mechanical processes are neglected because process-model results are not available at this time. Unlike effects of episodic flow, there is no simple abstraction for the possible effects of these processes, so they will not be discussed further.

Thermal-hydrologic effects on seepage, not counting the permanent changes in hydrologic properties that could possibly be caused by mechanical or chemical processes, are transient and consist of potential effects such as reduced seepage for a time because of thermal dryout or increased seepage during the heat-up and cool-down phases because of drainage of thermally

mobilized water. An approximate method for including thermal effects on seepage is to use percolation flux above the emplacement drifts from a thermal-hydrology model as input to the seepage abstraction, rather than percolation flux from the isothermal UZ flow model. That way, if the thermal-hydrology model indicates a period of increased liquid flow because of condensate drainage, it will automatically be translated to an increase in seepage during that period. However, in order to be conservative, if the thermal-hydrology model indicates a period of reduced liquid flow because of dryout of the rock around a drift, seepage should instead be continued at its ambient (pre-heating) level through that period, in recognition that it may be possible for rapid fracture flow in discrete flow paths to penetrate the hot rock and reach the drift. Only the fracture component of the liquid flux should be taken from the thermal-hydrology model, because capillarity in the rock matrix is high enough that matrix flow would not seep into the drifts.

6.5 SUMMARY OF ABSTRACTION OF SEEPAGE INTO DRIFTS

The abstraction of drift seepage, as described in the preceding sections, consists of three parts:

- 1) Distributions for the amount of seepage as a function of percolation flux, derived directly from seepage process-model results (CRWMS M&O 2000b) and constrained by measurements of permeability and calibration of seepage tests at two niches in the ESF and one location in the Cross Drift (CRWMS M&O 2000d)—see Table 13
- 2) Increase of the seep flow rates from (1) by 50% to adjust for effects of drift degradation and rock bolts—see Section 6.4.1
- 3) Distributions of the degree of flow focusing above the drifts, based on estimates of “weep” spacings implied by the active-fracture model of UZ flow. The flow-focusing factor is used to scale the percolation flux and the seepage fraction; it is log-uniformly distributed, with minimum of 1 and maximums of 47 for the low-infiltration case, 22 for the base-infiltration case, and 9.7 for the high-infiltration case—see Section 6.4.3.2

As discussed in Section 6.3.3, seepage is a function of the geometric-mean fracture permeability \bar{k} and the fracture capillary-strength parameter $1/\alpha$, and the effects of uncertainties in these parameters is evaluated by calculating seepage for three cases: a base case, a high-seepage case, and a low-seepage case (see Table 7). A triangular shape is chosen for the seepage uncertainty distributions, with the minimum of the triangle at the low-seepage value; the peak of the triangle, or highest probability, at the base-case seepage value; and the maximum of the triangle at the high-seepage value.

Table 16 summarizes the seepage distributions as they vary with percolation flux. The table was generated from Table 13 by multiplying all the seep flow rates (mean and standard deviation) by 1.5. (Note, however, that the seepage fractions remain unchanged.) Four additional rows are included as well:

- 1) If the mean seep flow rate for the high-seepage case is linearly extrapolated downward, it goes to zero at a percolation flux of approximately 2.7 mm/yr. A row is

included in the table to indicate that seepage is expected to be zero in all cases at a percolation of 2.7 mm/yr and lower.

- 2) If the mean seep flow rate for the base case or the low-seepage case is linearly extrapolated downward, it goes to zero at a percolation flux of approximately 60 mm/yr. A row is included in the table to indicate that seepage is expected to be zero in all except the high-seepage case at a percolation of 60 mm/yr and lower. Seepage parameters at 60 mm/yr for the high-seepage case were estimated by linear interpolation.
- 3) A row is added for 3000 mm/yr, as discussed in Section 5, assumption 8. Rather than setting the standard deviation of the seep flow rate to zero, as would be implied by 100% seepage for all cases, the standard deviation is set to one-half of the mean value in order to allow for some spatial variability. As discussed in Section 5, these choices are not expected to have very much effect on the TSPA results. Note that the seepage is set to 100% before application of the 50% increase for drift degradation, so the mean seep flow rate listed in the table for 3000 mm/yr is actually 50% more than the amount of water flow above the drift.
- 4) A row for $q = 1000$ mm/yr is included (generated by linear interpolation) simply to constrain the following plots better.

Table 16. Triangular Distributions of Seepage vs. Percolation Flux

q (mm/yr)	Minimum of Triangle			Peak of Triangle			Maximum of Triangle		
	f_s	Mean Q_s (m^3/yr)	Std.Dev. Q_s (m^3/yr)	f_s	Mean Q_s (m^3/yr)	Std.Dev. Q_s (m^3/yr)	f_s	Mean Q_s (m^3/yr)	Std.Dev. Q_s (m^3/yr)
2.4 ^a	0	0	0	0	0	0	0	0	0
5	0	0	0	0	0	0	8.31×10^{-2}	8.57×10^{-2}	3.95×10^{-2}
14.6	0	0	0	0	0	0	8.31×10^{-2}	0.401	9.55×10^{-2}
60.0 ^a	0	0	0	0	0	0	0.310	0.701	0.815
73.2	6.60×10^{-3}	0.365	7.99×10^{-2}	5.41×10^{-2}	0.365	7.99×10^{-2}	0.376	0.788	1.02
213	6.60×10^{-3}	3.99	0.210	5.41×10^{-2}	4.24	0.210	0.452	4.24	2.34
500	7.65×10^{-2}	1.56	3.94	0.129	6.20	5.39	0.512	12.1	6.89
1000 ^a	0.261	27.1	16.1	0.303	30.9	17.3	0.609	35.6	18.5
3000 ^b	1	129	64.7	1	129	64.7	1	129	64.7

^aThis row generated by linear interpolation or extrapolation.

^bSee text for explanation of the entries in this row.

Taken from Excel spreadsheet Seep-sr1.xls, submitted with this report under DTN: SN0012T0511599.003.

Linear interpolation or extrapolation can be used to obtain values of the seepage parameters for percolation fluxes not in the table. Note that an adjustment has been made in the standard deviations at 500 mm/yr and in the means at 213 mm/yr. The standard deviation of the seep flow rate is higher in the base case than in the high-seepage case at 500 mm/yr, and the mean seep flow rate in the high-seepage case is lower than in the base case and the low-seepage case at

213 mm/yr (see Table 13). For a triangular probability distribution, the minimum, peak, and maximum must be in order, so the values were switched for the purposes of defining the distribution.

Table 16 plus the distributions for the flow-focusing factor are the final products of the seepage abstraction, which are used in TSPA simulations to estimate seepage.

Figure 2 shows the seepage fraction as a function of percolation flux. Curves are shown for the three seepage cases that define the triangular distribution. The step-like shape of the curves is probably an artifact of the limited number of seepage cases available to develop the statistics from. These results indicate that there is no seepage throughout much of the repository even at 1000 mm/yr. At such high fluxes, seepage occurs in the model throughout most of the nonlithophysal units, but is still relatively rare in the lower lithophysal unit, which contains most of the repository.

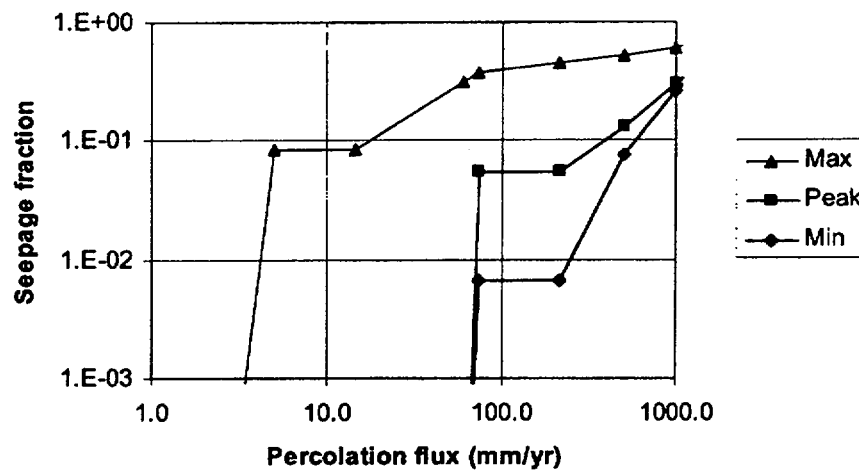


Figure 2. Seepage Fraction vs. Percolation Flux

Taken from Excel spreadsheet Seep-sr1.xls, submitted with this report under DTN: SN0012T0511599.003.

Figure 3 shows the mean seep flow rate as a function of percolation flux. Once again, curves are shown for the three seepage cases that define the triangular distribution, but in addition there is a curve (labeled "Perc") to show the total flow rate of water above a drift segment (i.e., the percolation flux times the area of the drift segment). If the seep flow rate were at that level, it would mean that all percolating water above the drift is seeping into the drift. It can be seen that most water is seeping into the drift in locations with seepage for the high-seepage case ("Max") above about 5 mm/yr, and for the base case ("Peak") above about 70 mm/yr. There is an anomalous dip in the curve for the low-seepage case ("Min"), which is lower at 500 mm/yr than it is at 213 mm/yr. This behavior occurs because the seepage fraction f_s increases more than the flow rate Q_s does in going from 213 mm/yr to 500 mm/yr. Because of that, the flow rate

averaged over seepage locations decreases. In other words, the overall seep flow rate increases, but the number of locations with seepage increases even faster, with the result that the average seep flow rate per location goes down. It is possible that this result is an artifact of the limited number of seepage cases available to develop the statistics from.

The mean seep flow rates for the three seepage cases are rather close together, indicating relatively little uncertainty in the seep flow rate *for locations that have seepage*. The major uncertainty is apparently in whether seepage occurs at all (i.e., how high the seepage threshold is) and not in how much flow there is when seepage occurs. Since all three curves are near the limiting percolation line, it can be concluded that the seepage model is acting almost like a switch, with either no seepage or almost all water seeping at a given location.

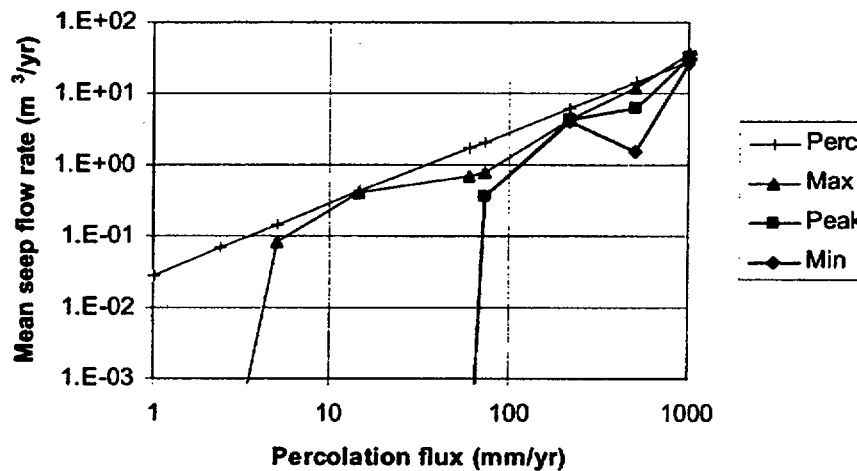


Figure 3. Mean Seep Flow Rate vs. Percolation Flux

Taken from Excel spreadsheet Seep-sr1.xls, submitted with this report under DTN: SN0012T0511599.003.

Figure 4 shows the standard deviation of seep flow rate as a function of percolation flux. The standard deviation determines the amount of spatial variability of seepage over the locations that have seepage.

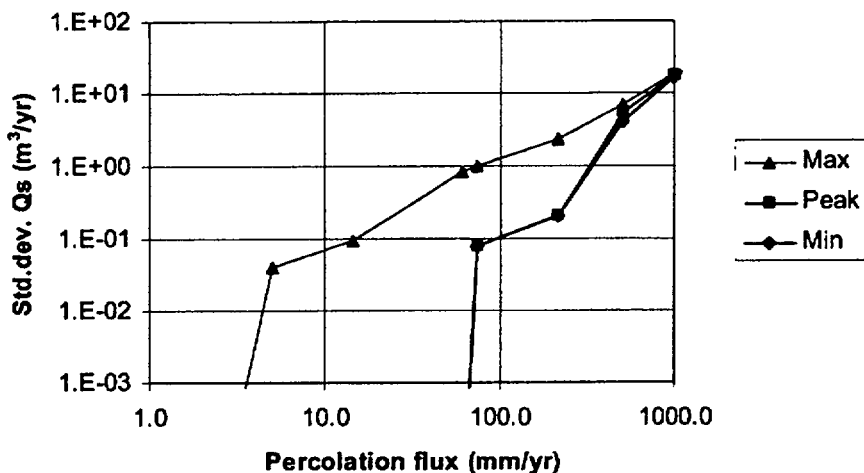


Figure 4. Standard Deviation of Seep Flow Rate vs. Percolation Flux

Taken from Excel spreadsheet Seep-sr1.xls, submitted with this report under DTN: SN0012T0511599.003.

The effect of flow focusing is illustrated in Figure 5 and Figure 6, for seepage fraction and mean seep flow rate, respectively. Each plot has four curves, for the focusing factor F equal to 1 (no flow focusing), 5, 15, and 45. The $F = 1$ curves are based on the mean of the respective uncertainty distributions (for a triangular distribution, the mean is $[\text{min} + \text{peak} + \text{max}]/3$, with min, peak, and max as listed in Table 16 and plotted in Figure 2 and Figure 3). The curves with higher values of F are generated from the $F = 1$ curves as described in Section 6.4.3.2. The result is as expected: more focusing of flow results in lower seepage fractions and higher seep flow rates. Note, however, that at very low percolation fluxes the seepage fraction is higher for higher focusing factors, because a percolation flux below the threshold for seepage can be boosted above the threshold by the focusing multiplier.

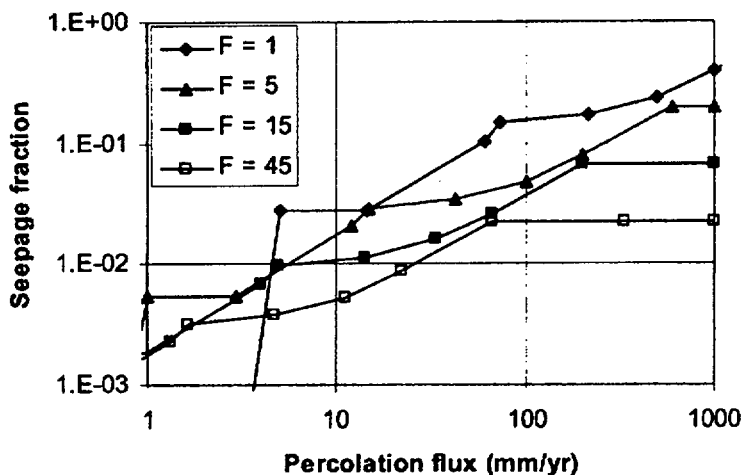


Figure 5. Effect of Flow Focusing on Seepage Fraction

Taken from Excel spreadsheet Seep-sr1.xls, submitted with this report under DTN: SN0012T0511599.003.

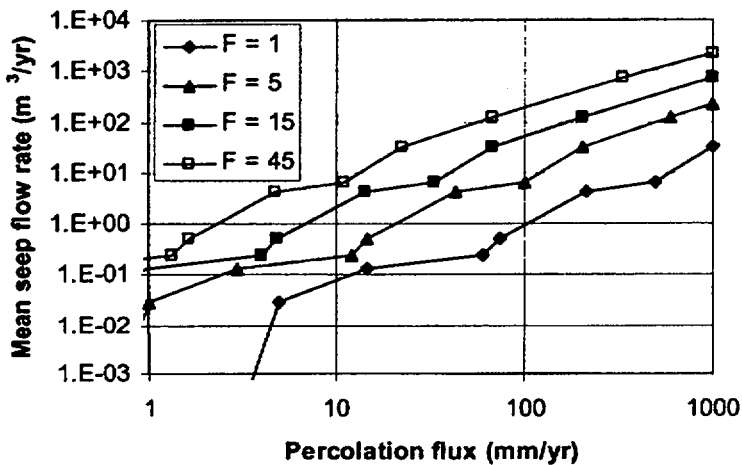


Figure 6. Effect of Flow Focusing on Mean Seep Flow Rate

Taken from Excel spreadsheet Seep-sr1.xls, submitted with this report under DTN: SN0012T0511599.003.

6.6 VALIDITY OF ABSTRACTION OF SEEPAGE INTO DRIFTS

AP-3.10Q, *Analyses and Models*, requires a discussion of validation for models, with model validation defined as the process of establishing confidence that the model adequately represents the phenomena in question. The procedure points out that what is adequate depends on the intended use of the model. The purpose of the seepage abstraction is to provide estimates of the

amount of seepage into emplacement drifts for use in TSPA simulations. As such, the estimates are not expected to be accurate predictions of the future (which would be impossible), but rather they are expected to reasonably represent the range of possibilities, consistent with our uncertainties regarding the relevant processes. As has been discussed, there is considerable uncertainty about the spatial locations and quantity of seepage that will enter the emplacement drifts, but this uncertainty has been represented by means of probability distributions and conservative approximations.

The seepage probability distributions that constitute the seepage abstraction are based directly on the results of the Seepage Calibration Model and the Seepage Model for PA, so the validity of the seepage abstraction derives from the validity of those models, which in turn comes from the use of accepted approaches and site-specific seepage data (CRWMS M&O 2000d, Sections 6.3.4 and 6.4.4; CRWMS M&O 2000b, Section 6.2). The parameters used in developing the abstraction (e.g., fracture permeability and $1/\alpha$ parameter) are reasonable and consistent with available data. Where few data are available, as for the Topopah Spring lower lithophysal and lower nonlithophysal units, estimates of the resulting uncertainty have been included.

The appropriate issue here is whether the seepage abstraction faithfully represents the results of the seepage process models. The primary output of the Seepage Calibration Model is values of the fracture $1/\alpha$ parameter that are appropriate for modeling seepage into drifts. Those values are used directly in the seepage abstraction to develop variability and uncertainty distributions of $1/\alpha$. The statistical descriptions of Table 6 are consistent with those given in the Seepage Calibration Model report (CRWMS M&O 2000d, Table 11). Thus, the seepage abstraction does faithfully represent the results of the Seepage Calibration Model. The output of the Seepage Model for PA is the percent of percolating water seeping into a drift segment for a wide range of cases. Once again, those outputs are used directly in the seepage abstraction to develop variability and uncertainty distributions of seepage. The method used to develop the seepage distributions is complicated enough to obscure the direct connection, so a simpler example will be presented to help make it clearer.

The Seepage Model for PA report presents a parameter Set A representative of the Topopah Spring middle nonlithophysal unit and a parameter Set B representative of the lower lithophysal unit (CRWMS M&O 2000b, Section 6.3.5). Tables 8a and 8b in that report give seepage percentages calculated for a percolation flux of 500 mm/yr. Set A and Set B do not exactly match any of the cases listed in the tables, but as an example consider the four cases closest to each one. For example, Set A has mean permeability of 1.38×10^{-12} and $1/\alpha$ of 589 Pa. The closest cases have permeabilities of 0.9×10^{-12} and 0.9×10^{-11} , $1/\alpha$ of 400 and 800. There are six occurrences of each combination of those parameters, for three geostatistical realizations and two local standard deviations. In all of those cases, the nonzero seepage percentages range from 0.003% to 70%; only 10 out of 24 of them are nonzero. Seep flow rates are obtained using the conversion factor $500 \text{ mm/yr} \times 28.8 \text{ m}^2 = 14.4 \text{ m}^3/\text{yr}$ (see Section 6.3.1 for explanation of the area of 28.8 m^2). Applying the conversion factor gives seep flow rates ranging from 4×10^{-4} to $10 \text{ m}^3/\text{yr}$. These flow rates are all less than the maximum mean seep flow rate for 500 mm/yr in Table 16 ($12.1 \text{ m}^3/\text{yr}$), and some are even lower than the abstracted minimum seep flow rate ($1.56 \text{ m}^3/\text{yr}$). Because of the intended use (for TSPA simulations), it is acceptable for the abstracted seepage estimates to be high, since higher seepage would correspond to higher

calculated doses in a TSPA. Ten out of 24 nonzero seepages leads to an estimate of 0.42 for the seepage fraction, but that is for properties representative of the middle nonlithophysal unit. The properties representative of the lower lithophysal unit all give zero seepage at 500 mm/yr percolation flux. Thus, the overall seepage fraction would be approximately $0.2 \times 0.42 \sim 0.08$ (from Table 11, the fraction of the repository in the nonlithophysal units is approximately 0.2). This estimate of 0.08 for the seepage fraction is within the bounds of the minimum and maximum for 500 mm/yr in Table 16 (0.008 to 0.51). This simple example shows that the seepage-abstraction results are consistent with the Seepage Model for PA results, as they should be.

7. CONCLUSIONS

For this analysis/model, results of seepage process-model simulations for a large number of cases were synthesized, and distributions representing the uncertainty and spatial variability of seepage into drifts as a function of percolation flux were derived. The final abstraction, summarized in Section 6.5, accounts for several potentially important perturbing effects, including changes in drift shape caused by rockfall, preferential pathways resulting from degraded rock bolts, and focusing of flow above drifts. For TSPA calculations, it is recommended that fracture flux above the drifts from a thermal-hydrology model be used as the flux to feed into the seepage abstraction, in order to account for thermal effects on seepage as discussed in Section 6.4.5. There are no known restrictions for subsequent use.

Many of the input data are unqualified, but no significant impact from them is expected, because significant changes to the inputs are not expected. One possible exception is the seepage-calibration results, because of concerns that they could be adversely affected by evaporation during the seepage tests. In the Seepage Calibration Model report, it was assumed that evaporation did not significantly affect the calibration (CRWMS M&O 2000d, Section 5.6; assumption 7 in Section 5 and assumption C.6 in Table I-1 of this report), but the assumption requires confirmation. The impact if this assumption is not confirmed could be a change in the calibrated values of the fracture $1/\alpha$ parameter, especially for the Topopah Spring lower lithophysal hydrogeologic unit. Another potentially important uncertainty is whether thermal-mechanical processes might affect seepage significantly. It was assumed for this seepage abstraction that thermal-mechanical effects can be neglected (see assumption 4 in Section 5), but this assumption needs to be confirmed. The impact of this assumption is unknown, but if it is determined that thermal-mechanical effects on seepage cannot be neglected then they should be included in the seepage abstraction in a future revision.

Bearing in mind that this analysis/model only addresses part of the issue of abstraction of the quantity and chemistry of water contacting waste packages and waste forms, the criteria listed in Section 4.2 have been addressed as follows:

- T1 Sufficient data are available to define the parameters for the seepage abstraction. There is significant uncertainty in the parameters, but that uncertainty is represented in the TSPA by means of sampling from distributions. See Sections 6.3.2 and 6.3.3.

- T2 The parameter values and their ranges and distributions are technically defensible because they are based on data from air-permeability tests and seepage tests that test the appropriate processes at the appropriate scale. The uncertainties and spatial variability are explicitly accounted for by distributions. See Sections 6.3.2 and 6.3.3.
- T3 Alternative modeling approaches were investigated by the seepage process modelers, but were not considered necessary to incorporate into the models. See Section 6.2.
- T4 The seepage abstraction is based directly on process-model outputs, so it is consistent with them. See Section 6.6.
- T5 Important design features, physical phenomena, and assumptions are incorporated into the seepage abstraction. For example, the appropriate drift geometry is used, the seepage process models include the appropriate physical phenomena, and the assumptions used in the seepage abstraction are consistent with assumptions in other models and in the TSPA.

The files generated for Rev. 00 of this analysis/model were submitted to the TDMS under DTN: SN9912T0511599.002. Additional files generated for Rev. 01 are being submitted to the TDMS under DTN: SN0012T0511599.003. Results of this analysis/model are considered unqualified pending qualification of upstream source data and confirmation of the assumptions that thermal-mechanical effects can be neglected and that the seepage calibration is not significantly affected by evaporation.

This document may be affected by technical product input information that requires confirmation. Any changes to the document that may occur as a result of completing the confirmation activities will be reflected in subsequent revisions. The status of the technical product input information quality may be confirmed by review of the DIRS database.

8. INPUTS AND REFERENCES

8.1 DOCUMENTS CITED

Bodvarsson, G.S.; Bandurraga, T.M.; and Wu, Y.S., eds. 1997. *The Site-Scale Unsaturated Zone Model of Yucca Mountain, Nevada, for the Viability Assessment*. LBNL-40376. Berkeley, California: Lawrence Berkeley National Laboratory. ACC: MOL.19971014.0232.

CRWMS M&O (Civilian Radioactive Waste Management System Management & Operating Contractor) 1998. "Unsaturated Zone Hydrology Model." Chapter 2 of *Total System Performance Assessment—Viability Assessment (TSPA-VA) Analyses Technical Basis Document*. B00000000-01717-4301-00002 REV 01. Las Vegas, Nevada: CRWMS M&O. ACC: MOL.19981008.0002.

CRWMS M&O 1999. *Request for Repository Subsurface Design Information to Support TSPA-SR*. Input transmittal PA-SSR-99218.Ta. Las Vegas, Nevada: CRWMS M&O. ACC: MOL.19990901.0312.

CRWMS M&O 2000a. *Technical Work Plan for Unsaturated Zone (UZ) Flow and Transport Process Model Report*. TWP-NBS-HS-000001 REV 00. Las Vegas, Nevada: CRWMS M&O. ACC: MOL.20001025.0152.

CRWMS M&O 2000b. *Seepage Model for PA Including Drift Collapse*. MDL-NBS-HS-000002 REV 01. Las Vegas, Nevada: CRWMS M&O. Submit to RPC

CRWMS M&O 2000c. *Tabulated In-Drift Geometric and Thermal Properties Used in Drift-Scale Models for TSPA-SR*. CAL-EBS-HS-000002 REV 00. Las Vegas, Nevada: CRWMS M&O. ACC: MOL.20000718.0219.

CRWMS M&O 2000d. *Seepage Calibration Model and Seepage Testing Data*. MDL-NBS-HS-000004 REV 01. Las Vegas, Nevada: CRWMS M&O. ACC: MOL.20010122.0093.

CRWMS M&O 2000e. *Site Recommendation Subsurface Layout*. ANL-SFS-MG-000001 REV 00. Las Vegas, Nevada: CRWMS M&O. ACC: MOL.20000908.0276.

CRWMS M&O 2000f. *Calibrated Properties Model*. MDL-NBS-HS-000003 REV 00. Las Vegas, Nevada: CRWMS M&O. ACC: MOL.19990721.0520.

CRWMS M&O 2000g. *UZ Flow Models and Submodels*. MDL-NBS-HS-000006 REV 00. Las Vegas, Nevada: CRWMS M&O. ACC: MOL.19990721.0527.

CRWMS M&O 2000h. *Development of Numerical Grids for UZ Flow and Transport Modeling*. ANL-NBS-HS-000015 REV 00. Las Vegas, Nevada: CRWMS M&O. ACC: MOL.19990721.0517.

CRWMS M&O 2000i. *Analysis of Hydrologic Properties Data*. ANL-NBS-HS-000002 REV 00. Las Vegas, Nevada: CRWMS M&O. ACC: MOL.19990721.0519.

CRWMS M&O 2000j. *Heat Decay Data and Repository Footprint for Thermal-Hydrologic and Conduction-Only Models for TSPA-SR*. CAL-MGR-HS-000001 REV 00. Las Vegas, Nevada: CRWMS M&O. ACC: MOL.20000516.0007.

CRWMS M&O 2000k. *Features, Events, and Processes in UZ Flow and Transport*. ANL-NBS-MD-000001 REV 00. Las Vegas, Nevada: CRWMS M&O. ACC: MOL.20000502.0240.

CRWMS M&O 2000l. *Drift-Scale Coupled Processes (DST and THC Seepage) Models*. MDL-NBS-HS-000001 REV 00. Las Vegas, Nevada: CRWMS M&O. ACC: MOL.19990721.0523.

CRWMS M&O 2000m. *Total System Performance Assessment for the Site Recommendation*. TDR-WIS-PA-000001 REV 00 ICN 01. Las Vegas, Nevada: CRWMS M&O. ACC: MOL.20001220.0045.

CRWMS M&O 2000n. *Drift Degradation Analysis*. ANL-EBS-MD-000027 REV 01. Las Vegas, Nevada: CRWMS M&O. ACC: MOL.20001206.0006.

CRWMS M&O 2000o. *Seepage Model for PA Including Drift Collapse*. MDL-NBS-HS-000002 REV 00. Las Vegas, Nevada: CRWMS M&O. ACC: MOL.19990721.0525.

DOE (U.S. Department of Energy) 1998. *Total System Performance Assessment*. Volume 3 of *Viability Assessment of a Repository at Yucca Mountain*. DOE/RW-0508. Washington, D.C.: U.S. Department of Energy, Office of Civilian Radioactive Waste Management. ACC: MOL.19981007.0030.

Finsterle, S. 2000. "Using the Continuum Approach to Model Unsaturated Flow in Fractured Rock." *Water Resources Research*, 36, (8), 2055–2066. [Washington, D.C.]: American Geophysical Union. TIC: 248769.

Glass, R.J. and Tidwell, V.C. 1991. *Research Program to Develop and Validate Conceptual Models for Flow and Transport Through Unsaturated, Fractured Rock*. SAND90-2261. Albuquerque, New Mexico: Sandia National Laboratories. ACC: NNA.19910906.0001.

Ho, C.K. and Wilson, M.L. 1998. "Calculation of Discrete Fracture Flow Paths in Dual-Continuum Models." *High-Level Radioactive Waste Management, Proceedings of the Eighth International Conference, Las Vegas, Nevada, May 11–14, 1998*, Pages 375–377. La Grange Park, Illinois: American Nuclear Society. TIC: 237082.

Liu, H.H.; Doughty, C.; and Bodvarsson, G.S. 1998. "An Active Fracture Model for Unsaturated Flow and Transport in Fractured Rocks." *Water Resources Research*, 34, (10), 2633–2646. Washington, D.C.: American Geophysical Union. TIC: 243012.

8.2 CODES, STANDARDS, REGULATIONS, AND PROCEDURES CITED

AP-3.10Q, Rev. 2, ICN 3. *Analyses and Models*. Washington, D.C.: U.S. Department of Energy, Office of Civilian Radioactive Waste Management. ACC: MOL.20000918.0282.

AP-3.14Q, Rev. 0, ICN 2. *Transmittal of Input*. Washington, D.C.: U.S. Department of Energy, Office of Civilian Radioactive Waste Management. ACC: MOL.20001122.0001.

AP-3.15Q, Rev. 2, ICN 0. *Managing Technical Product Inputs*. Washington, D.C.: U.S. Department of Energy, Office of Civilian Radioactive Waste Management. ACC: MOL.20001109.0051.

AP-SI.1Q, Rev. 2, ICN 4, ECN 1. *Software Management*. Washington, D.C.: U.S. Department of Energy, Office of Civilian Radioactive Waste Management. ACC: MOL.20001019.0023.

AP-SIII.3Q, Rev. 0, ICN 4. *Submittal And Incorporation Of Data To The Technical Data Management System*. Washington, D.C.: U.S. Department of Energy, Office of Civilian Radioactive Waste Management. ACC: MOL.20010117.0329.

AP-SV.1Q, Rev. 0, ICN 2. *Control of the Electronic Management of Information*. Washington, D.C.: U.S. Department of Energy, Office of Civilian Radioactive Waste Management. ACC: MOL.20000831.0065.

DOE 2000. *Quality Assurance Requirements and Description*. DOE/RW-0333P, Rev. 10. Washington, D.C.: U.S. Department of Energy, Office of Civilian Radioactive Waste Management. ACC: MOL.20000427.0422.

Dyer, J.R. 1999. "Revised Interim Guidance Pending Issuance of New U.S. Nuclear Regulatory Commission (NRC) Regulations (Revision 01, July 22, 1999), for Yucca Mountain, Nevada." Letter from J.R. Dyer (DOE/YMSCO) to D.R. Wilkins (CRWMS M&O), September 3, 1999, OL&RC:SB-1714, with enclosure, "Interim Guidance Pending Issuance of New NRC Regulations for Yucca Mountain (Revision 01)." ACC: MOL.19990910.0079.

NRC (U.S. Nuclear Regulatory Commission) 2000. *Issue Resolution Status Report Key Technical Issue: Total System Performance Assessment and Integration*. Rev. 2. Washington, D.C.: U.S. Nuclear Regulatory Commission. TIC: 247614.

8.3 SOURCE DATA, LISTED BY DATA TRACKING NUMBER

LB990501233129.001. Fracture Properties for the UZ Model Grids and Uncalibrated Fracture and Matrix Properties for the UZ Model Layers for AMR U0090, "Analysis of Hydrologic Properties Data". Submittal date: 08/25/1999.

LB990701233129.001. 3-D UZ Model Grids for Calculation of Flow Fields for PA for AMR U0000, "Development of Numerical Grids for UZ Flow and Transport Modeling". Submittal date: 09/24/1999.

LB990801233129.007. TSPA Grid Flow Simulations for AMR U0050, "UZ Flow Models and Submodels" (Flow Field #7). Submittal date: 11/29/1999.

LB990801233129.009. TSPA Grid Flow Simulations for AMR U0050, "UZ Flow Models and Submodels" (Flow Field #9). Submittal date: 11/29/1999.

LB990801233129.011. TSPA Grid Flow Simulations for AMR U0050, "UZ Flow Models and Submodels" (Flow Field #11). Submittal date: 11/29/1999.

LB997141233129.001. Calibrated Basecase Infiltration 1-D Parameter Set for the UZ Flow and Transport Model, FY99. Submittal date: 07/21/1999.

LB997141233129.002. Calibrated Upper-Bound Infiltration 1-D Parameter Set For the UZ Flow and Transport Model, FY99. Submittal date: 07/21/1999.

LB997141233129.003. Calibrated Lower-Bound Infiltration 1-D Parameter Set for the UZ Flow and Transport Model, FY99. Submittal date: 07/21/1999.

LB0010SCMREV01.002. Developed Data from Seepage Calibration Modeling AMR U0080. Submittal date: 11/29/2000.

LB0011SMDCREV1.002. Seepage Model for PA Including Drift Collapse: 2. Tables of Seepage Percentages AMR U0075 (MDL-NBS-HS-000002 REV01). Submittal date: 12/07/2000. Submit to RPC

LB0101SMDCREV1.001. Tables of Seepage Percentages for Stdev of $\ln k = 2.5$; Addendum to AMR U0075 (REV01). Submittal date: 01/10/2001.

SN9907T0872799.001. Heat Decay Data and Repository Footprint for Thermal-Hydrologic and Conduction-Only Models for TSPA-SR (Total System Performance Assessment–Site Recommendation). Submittal date: 07/27/1999.

SN9908T0872799.004. Tabulated In-Drift Geometric and Thermal Properties Used in Drift-Scale Models for TSPA-SR (Total System Performance Assessment–Site Recommendation). Submittal date: 08/30/1999.

8.4 OUTPUT DATA, LISTED BY DATA TRACKING NUMBER

SN9912T0511599.002. Revised Seepage Abstraction Results for TSPA-SR (Total System Performance Assessment–Site Recommendation). Submittal date: 12/15/1999.

SN0012T0511599.003. Results from Abstraction of Drift Seepage Rev. 01. Submittal date: 12/20/2000.

9. ATTACHMENTS

Attachment	Title
I	Assumptions Relating to Input Data
II	Software Routine T2WEEP v. 1.0
III	Repository Elements
IV	Directory of Files Submitted to TDMS

ATTACHMENT I

Assumptions Relating to Input Data

Table I-1 summarizes the assumptions and their rationales from the analyses and calculations that produced the input data used in this analysis/model. More details can be found in the source reports. The data used in this report from each one are listed in Table 2.

Table I-1. Assumptions from Source Analyses and Calculations

Assumption		Rationale from Source Report	Application to the Seepage Abstraction
<i>Seepage Model for PA Including Drift Collapse (CRWMS M&O 2000b, Section 5)</i>			
A.1	The continuum approach is valid	See assumption C.1 below.	See assumption C.1 below.
A.2	Unsaturated water flow can be described by Richards' equation	See assumption C.2 below.	See assumption C.2 below.
A.3	Permeabilities from air-injection tests are representative of the hydraulic conductivity of the excavation-disturbed zone around the opening	See assumption C.3 below.	See assumption C.3 below.
A.4	Relative permeability and capillary pressure can be described by the van Genuchten and Mualem model; capillary strength and permeability are not correlated	See assumption C.4 below.	See assumption C.4 below.
A.5	Transient effects from matrix imbibition are small and do not need to be modeled explicitly	See assumption C.5 below. In the Seepage Model for PA, except for an episodic percolation flux case, calculations are for steady-state flow conditions over long time frames. At steady-state, the flow exchange between fracture and matrix continua will settle to a small amount with the matrix close to full saturation. The flow partitions between the fracture and matrix continua according to their effective permeabilities and porosities, and it follows that the matrix, with its five to six orders-of-magnitude lower permeability, would not have significant effects on seepage into drifts, which would be controlled by the flow in the fracture continuum. For the episodic percolation flux case, the matrix continuum would provide a damping effect on seepage in the fracture continuum, and neglecting it represents a conservative case.	Model results based on this assumption are appropriate for use in the seepage abstraction.

Assumption		Rationale from Source Report	Application to the Seepage Abstraction
A.6	The effect of evaporation on the observed seepage rates is insignificant	See assumption C.6 below. While this assumption needs further confirmation for the Seepage Calibration Model, neglecting evaporation effects by prescribing a 100% relative-humidity boundary condition in the Seepage Model for PA is conservative. This assumption causes the model to underestimate vapor flow, but it yields the maximum liquid-phase influx, which is defined as drift seepage. The underestimation of vapor flow is irrelevant, since the assumption of 100% relative humidity already implies that the moisture content in the drift environment is as high as possible, maximizing the amount of moisture that can condense within the waste-emplacment drift. In a ventilated drift, the development of a dry-out zone increases the capillary pressure and local storage volume and thus reduces the risk of reaching seepage conditions; the assumption of 100% relative humidity in the drift is again conservative. The assumption is also reasonable for the time when ventilation is stopped and the waste-emplacment drift is closed. A repository design that includes ventilation yields reduced seepage.	Use of this assumption in the Seepage Model for PA is appropriate. Use of the assumption in the Seepage Calibration Model requires further verification—see assumption C.6 below and assumption 7 in Section 5 of this report.
A.7	The appropriate range of percolation flux is considered	Five values for Q_p are used, ranging from 5 to 500 mm/yr; more specifically $Q_p = 5, 14.6, 73.2, 213$ and 500 mm/yr. The range is chosen to cover various estimates of percolation fluxes. There is an average fracture flow of 4 to 5 mm/yr at the repository level under present climate conditions, based on a 3D UZ model of Yucca Mountain. Under a climate scenario simulating the most recent glacial period, the percolation flux ranges from 0 to 120 mm/yr, with the peak of the probability distribution around 20 mm/yr. The upper limit of 500 mm/yr is chosen to accommodate potential flow focusing in the geologic layers above the drift and to safely bracket an uncertainty range more than four times the high flux value of 120 mm/yr. In cases where seepage is very low or zero, even larger Q_p values are also used to find when seepage might occur.	The seepage abstraction could be improved if the range of percolation flux used for seepage calculations were extended to higher values. The lack of higher values is addressed by a conservative assumption—see assumption 8 in Section 5 of this report.
<i>Tabulated In-Drift Geometric and Thermal Properties Used in Drift-Scale Models for TSPA-SR (CRWMS M&O 2000c, Section 3)</i>			
B.1	The placement of the waste package is concentric within the drip shield	This waste-package placement was specified for previous studies.	This assumption is irrelevant to the information used for the seepage abstraction, which is drift diameter, average waste-package length, and waste-package spacing.

Assumption		Rationale from Source Report	Application to the Seepage Abstraction
B.2	Design information found in superceded Design Input Transmittals is still valid if the superceding Design Input Transmittal does not specifically supercede the respective design information	If a newer design input transmittal intended to supercede specific information in an older transmittal, then this would have been included in the new transmittal.	This assumption is administrative in nature and does not influence the seepage abstraction.
B.3	Naval spent nuclear fuel waste packages are 5.57 meters long	This corresponds to the length of the "regular" naval spent nuclear fuel waste package.	Length of the naval packages is used in calculating the average waste-package length, but it has very little impact on the average and therefore no significant impact on the seepage abstraction.
B.4	The radius of the Department of Energy/Other waste packages is the same as that of naval spent nuclear fuel packages	Since the heat load curves as well as the length of the DOE/Other waste package and the "regular" naval SNF waste package are both 5.570 meters, it is reasonable to assume that their radius will be the same.	This assumption is irrelevant to the information used for the seepage abstraction, which is drift diameter, average waste-package length, and waste-package spacing.

Assumption	Rationale from Source Report	Application to the Seepage Abstraction
<i>Seepage Calibration Model and Seepage Testing Data (CRWMS M&O 2000d, Section 5)</i>		
C.1	<p>The continuum approach is valid</p> <p>The continuum approach can be considered appropriate for seepage studies if it is capable of predicting seepage threshold and seepage percentages for a drift in a fractured formation. An independent study concluded that heterogeneous continuum representations of fractured media are self-consistent, i.e., appropriately estimated effective continuum parameters are able to represent the underlying fracture-network characteristics. Furthermore, it has been demonstrated that simulating seepage into underground openings excavated from a highly fractured formation can be performed using a model based on the continuum assumption, provided that the model is calibrated against seepage-relevant data (such as data from liquid-release tests). Synthetically generated data from a model that exhibits discrete flow and seepage behavior were used to calibrate a simplified fracture continuum model. Seepage predictions for low percolation fluxes made with the calibrated fracture continuum model were consistent with the synthetically generated data from the discrete feature model.</p> <p>The continuum approach is considered applicable for seepage studies if applied within the proper framework. Inverse modeling should be used for the estimation of process-specific, model-related, and scale-dependent parameters, and the same or similar conceptual model should be used for the subsequent seepage predictions.</p>	<p>Model results based on this assumption are appropriate for use in the seepage abstraction.</p>
C.2	<p>Unsaturated water flow can be described by Richards' equation</p> <p>Richards' equation states that isothermal flow of water in a porous medium occurs under the combined effect of gravitational and capillary forces, that flow resistance is a function of saturation, and that movement of the nonwetting air phase can be neglected. This general concept is believed reasonable for unsaturated water flow through both porous matrix and fractures.</p>	<p>Model results based on this assumption are appropriate for use in the seepage abstraction.</p>
C.3	<p>Permeabilities from air-injection tests are representative of the hydraulic conductivity of the excavation-disturbed zone around the opening</p> <p>Air-permeability estimates are used to condition the generation of a spatially correlated, random permeability field. Potential inaccuracies in this assumption are compensated for by the estimation of the van Genuchten $1/\alpha$ parameter. Air-injection tests are a standard method to obtain drift-scale permeability values. The use of these values during calibration and prediction of seepage ensures consistency. Excavation effects increase the permeabilities around the niches and the Cross Drift. Since seepage is determined by the formation properties within the boundary layer in the immediate vicinity of the opening, it is reasonable to use post-excavation air-permeability data for seepage calculations.</p>	<p>Model results based on this assumption are appropriate for use in the seepage abstraction.</p>

Assumption		Rationale from Source Report	Application to the Seepage Abstraction
C.4	Relative permeability and capillary pressure can be described by the van Genuchten and Mualem model; capillary strength and permeability are not correlated	The van Genuchten and Mualem model is the standard model used in the suite of UZ flow and transport models; it was chosen for consistency. Furthermore, the applicability of relative permeability and capillary pressure functions is consistent with the continuum assumption (C.1) and is appropriate to represent fractures that are rough and/or partially filled with porous material. The functional relationship describing the potential correlation between permeability and capillary strength is unknown. An increase in permeability may be attributed to larger fracture apertures (which would reduce capillary strength) or to an increase in fracture density (which would not affect capillary strength). The capillary strength parameter $1/\alpha$ is taken to be constant and is subjected to estimation by inverse modeling. The calibration process and the consistent conceptualization in the downstream models make this assumption a valid approach.	Model results based on this assumption are appropriate for use in the seepage abstraction.
C.5	Transient effects from matrix imbibition are small and do not need to be modeled explicitly	Matrix permeability is low, and the potential for matrix imbibition is limited because of relatively low porosity and relatively high liquid saturation. In a fracture-matrix system, the transient effects from matrix imbibition are restricted to intermediate times, i.e., they are insignificant (1) for a short-term liquid-release test with insufficient time for matrix imbibition, and (2) for a long-term seepage experiment, when near-steady late-time data are no longer affected by matrix imbibition. To match intermediate times during a long-term test, an effective porosity is estimated by inverse modeling to account for the storage capacity of both the fracture system and the matrix. Porosity estimates are irrelevant in the subsequent simulations of seepage under natural flow conditions, which are near steady state.	Model results based on this assumption are appropriate for use in the seepage abstraction.

Assumption		Rationale from Source Report	Application to the Seepage Abstraction
C.6	Evaporation and vapor diffusion can be neglected	<p>Under isothermal conditions, potential evaporation at the drift wall or in the capture system is small compared to the amount of water being released. Seepage experiments in the middle nonlithophysal zone of the Topopah Spring welded unit were conducted in niches that were closed off with a bulkhead, which leads to comparatively high relative humidity and low air circulation. Moreover, a humidifier was used in some of the experiments to ensure high relative humidity. Calculated evapo-infiltration thresholds for individual water droplets within fractures or emerging from fractured formations are significantly lower than the applied injection rates, suggesting a very minor influence of evaporation on measured seepage rates in experiments conducted in the niches.</p> <p>Evaporation from a large surface of free or nearly free water, however, may be significant. As injected water reaches the opening, it spreads along the surface on account of capillarity within the rough surface. As a result, water potentially seeping into the opening may not only form droplets with a small surface area, but may be spread over a large area, providing a large surface for evaporation. Depending on the evaporation potential of the air in the opening, the water film covering the wall of the opening may evaporate at a rate comparable to the injection or seepage rates.</p> <p>Moreover, evaporation may be significant during periods of active ventilation with high air flows in the drift in combination with low injection rates. Under these specific conditions, the evaporation rate may exceed the potential seepage rate, preventing the development of liquid droplets that drip into the opening. Ventilation effects are evident from the seepage data collected in the Cross Drift. To reduce the impact from ventilation effects, calibration was restricted to seepage rate data collected during nighttime and weekends, when ventilation was turned off.</p> <p>Currently, no quantitative estimates of evaporation potential under the conditions of the seepage experiments are available. The simplified assumption that evaporation rates are small compared to the injection rates is non-conservative and is therefore an assumption that needs to be verified.</p>	As stated, this assumption requires further verification. See also assumption 7 in Section 5 of this report.
<i>Site Recommendation Subsurface Layout (CRWMS M&O 2000e, Section 5)</i>			
D.1	Waste packages provide shielding for waste-package materials, but not enough for personnel protection	Controlled project assumption.	This assumption is irrelevant to the seepage abstraction.
D.2	Doors are required at emplacement-drift entrances	Controlled project assumption.	This assumption is irrelevant to the seepage abstraction.

Assumption		Rationale from Source Report	Application to the Seepage Abstraction
D.3	The repository will be designed to permit modular design and/or construction in stages	Controlled project assumption.	This assumption is irrelevant to the seepage abstraction.
D.4	The subsurface layout will be configured for post-closure drainage	Controlled project assumption.	This assumption is irrelevant to the seepage abstraction.
D.5	Some special-use drifts will be excavated within the pillars and left empty	These drifts have several uses and their impact is not critical because they do not affect the total area required for waste emplacement.	This assumption is irrelevant to the seepage abstraction.
D.6	Contingency areas are included in the subsurface design	Contingency areas allow for unexpected circumstances and their impact is not critical to the total area required for waste emplacement.	Contingency areas affect the seepage abstraction only to the extent that they are different from the primary emplacement area in some way (e.g., higher infiltration or different host rock). The effects are not expected to be significant.
D.7	Detailed assumptions regarding emplacement-drift turnouts	Reason given for each assumption. These assumptions are not critical because they do not affect the total area required for waste emplacement.	This assumption is irrelevant to the seepage abstraction.
D.8	The maximum emplacement-drift split length is 600 m	This maximum is based on the thermal analysis of ventilation effects and is not critical to the total area required for waste emplacement.	This assumption is irrelevant to the seepage abstraction.
D.9	Minimum spacings between drifts is specified	These minimums do not apply to emplacement drifts, and they are not critical to the total area required for waste emplacement.	This assumption is irrelevant to the seepage abstraction.
D.10	Minimum standoff distance for ventilation raises is specified	This minimum is to reduce interference with ventilation airflow and/or radiological monitoring. It is not critical to the total area required for waste emplacement.	This assumption is irrelevant to the seepage abstraction.
D.11	Detailed assumptions related to the ventilation strategy	Reason given for each assumption. These assumptions are not critical because they do not affect the total area required for waste emplacement.	This assumption is irrelevant to the seepage abstraction.
<i>Calibrated Properties Model (CRWMS M&O 2000f, Section 5)</i>			
E.1	One-dimensional vertical flow is adequate for non-fault property calibration	The effect of using 1-D columnar models is that all flow is forced to be vertical; there is no lateral flow. From the surface to the repository, lateral flow is not expected to be significant because perched water has not been found there. Below the repository, in the Calico Hills nonwelded unit and the Crater Flat undifferentiated unit, areas of perched water exist where lateral flow may be significant.	The seepage abstraction only uses properties from the repository host units, which should not be affected by lateral flow in these lower units.

Assumption		Rationale from Source Report	Application to the Seepage Abstraction
E.2	Two-dimensional flow (vertical and east-west) is adequate fault property calibration	For flow in and around a fault zone, a 2-D model is necessary to capture the interaction of the hanging wall, fault zone, and foot wall. An east-west, vertical cross section through USW UZ-7a and the Ghost Dance fault should capture this interaction. The cross section is aligned approximately parallel to the dip of the beds and parallel to the dip of the fault (perpendicular to the strike). Any lateral flow in or around the fault zone should follow the dip of the beds and the fault.	Model results based on this assumption are appropriate for use in the seepage abstraction. Note that the seepage abstraction does not use fault properties; however, the fault properties affect the UZ flow fields, which are used.
E.3	Layers bf3 and bf2 can be used as analogs for layers tr3 and tr2, respectively	Because the Tram Tuff has a structure similar to the Bullfrog Tuff and the two Tuffs are divided into model layers similarly, the hydrologic properties should also be similar. Further, model layers tr3 and tr2 constitute only a small portion of the unsaturated zone in the northern part of the model area and along the foot wall of the Solitario Canyon fault, so the properties are not likely to have a large impact on simulations of flow and transport.	These layers should have no effect on the seepage modeling or abstraction because they are well below the repository.
E.4	Fault properties calibrated for the Ghost Dance fault can be applied to all faults	The data from borehole USW UZ-7a represent the most complete data set from within a fault zone. Saturation, water potential, and pneumatic data are available from the surface down into the TSw. Other data sets that are influenced by faults from boreholes USW NRG-6, UE-25 UZ#4, and UE-25 UZ#5 include only pneumatic pressure data and are only relevant to the TSw. Because of the limited amount of data, it is best to characterize one fault as completely as possible and apply these properties to all other faults.	Model results based on this assumption are appropriate for use in the seepage abstraction. Note that the seepage abstraction does not use fault properties; however, the fault properties affect the UZ flow fields, which are used.
E.5	Thirty days is a sufficient simulation time to establish pneumatic initial conditions	Previous work has shown that 30 days is sufficient for the mean pressure to equilibrate.	Model results based on this assumption are appropriate for use in the seepage abstraction. Note that this assumption is used in determining the mountain-scale fracture permeabilities, which are not used in the seepage abstraction. However, the fracture permeabilities affect the UZ flow fields, which are used.

Assumption		Rationale from Source Report	Application to the Seepage Abstraction
E.6	Common values of the active-fracture parameter γ can be estimated for common rock types	The fracturing characteristics of the rocks of Yucca Mountain are assumed to be primarily dependent on the degree of welding and alteration. Data show that this is true of fracture frequency. The welded rocks have higher fracture frequencies than the non-welded. Because of the general division between the fracture characteristics of welded and nonwelded rocks and because there are no data on an appropriate active-fracture parameter to use for these rocks, model layers are grouped together based on welding to estimate common values of the active-fracture parameter. Alteration is believed to possibly influence the active-fracture parameter, so it is also used as a criterion for grouping layers.	Model results based on this assumption are appropriate for use in the seepage abstraction.
E.7	Reported saturation values greater than 1.0 are set to 1.0	Measurement error causes calculated saturation values (based on measurements of initial, saturated, and dry weight) to be greater than 1.0, but this is unphysical; saturation is physically constrained to a maximum of 1.0.	Model results based on this assumption are appropriate for use in the seepage abstraction.
E.8	Data uncertainty for some parameters is estimated based on the uncertainties of similar data	These uncertainties are based on the judgment of the analysts and are discussed case-by-case in the source report (CRWMS M&O 2000f, Section 6.1.2). The uncertainty estimates do not directly determine the calibrated parameters, but only the range that is considered in the calibration.	Model results based on this assumption are appropriate for use in the seepage abstraction.
<i>UZ Flow Models and Submodels (CRWMS M&O 2000g, Section 5)</i>			
F.1	Water pressure is set to atmospheric pressure at the water table, which is the bottom model boundary	The water table is a surface where the water pressure is a fixed single value. Within the numerical models, only one single set of model primary variables for solving Richards' equations is specified for the bottom boundary and this is equivalent to specifying a constant saturation.	This assumption should have no effect on the seepage abstraction because the water table is well below the repository.
F.2	Gas pressure is set to a fixed value at the water table, which is the bottom model boundary	Due to limitations in the way boundaries may be specified in the numerical models used, a constant gas pressure must be specified when a constant water pressure (saturation) is specified. The impact of this assumption on all but simulations of barometric pumping is insignificant (see assumption F.4 below for an alternate assumption used for simulations of barometric pumping).	Model results based on this assumption are appropriate for use in the seepage abstraction. Note that this assumption is used in determining the mountain-scale fracture permeabilities, which are not used in the seepage abstraction. However, the fracture permeabilities affect the UZ flow fields, which are used.

Assumption		Rationale from Source Report	Application to the Seepage Abstraction
F.3	Temperature is fixed (but spatially varying) at the water table, which is the bottom model boundary	This assumption is corroborated by data for temperature distribution along the water table and further confirmed by matching qualified temperature profiles from a number of boreholes.	Model results based on this assumption are appropriate for use in the seepage abstraction. Note that this assumption is used in determining the mountain-scale fracture permeabilities, which are not used in the seepage abstraction. However, the fracture permeabilities affect the UZ flow fields, which are used.
F.4	For simulations of barometric pumping, the bottom model boundary representing the water table is assumed to be a no-flow boundary	At the water table, a connected gas phase does not exist, so gas-phase flow does not occur across this boundary. Due to the limitations of the code used for simulation, this boundary must also be no-flow for the liquid phase (heat flow is not considered in these simulations). Liquid flow across the boundary over the time span of the simulation (360 days) is not large enough to significantly change the gas flow in the Topopah Spring welded hydrogeologic unit and above, where data are available.	Model results based on this assumption are appropriate for use in the seepage abstraction. Note that this assumption is used in determining the mountain-scale fracture permeabilities, which are not used in the seepage abstraction. However, the fracture permeabilities affect the UZ flow fields, which are used.
F.5	No-flow boundary conditions are used at the lateral model boundaries	The boundaries of the northern and southern model domain are located so far away from the potential repository area that lateral flow effects along these boundaries on flow at the potential repository should be small. The eastern boundary is for most parts along the Bow Ridge fault, and no lateral flow crossing the fault is reasoned. The western boundary is separated from the potential repository by the Solitario Canyon fault; therefore the effects of this boundary condition are expected to be insignificant.	Model results based on this assumption are appropriate for use in the seepage abstraction.
F.6	Perched water results from a permeability barrier	Consistent with the conceptual model that ambient conditions reflect long-term, steady-state or transient flow through the unsaturated zone, perched water under steady-state flow conditions may only be due to a permeability barrier.	This assumption should have no effect on the seepage abstraction because the perched water is well below the repository.

Assumption		Rationale from Source Report	Application to the Seepage Abstraction
F.7	For steady-state flow conditions, moisture flow and tracer transport processes can be decoupled	Steady-state flow conditions result in an unchanging flow field, and as long as the concentrations of tracers and/or radionuclides are such that they do not significantly change the properties of the fluid then the flow field does not have to be coupled to transport.	Model results based on this assumption are appropriate for use in the seepage abstraction. Note that this assumption is used in comparisons of the UZ flow model against geochemical and isotopic data and so does not directly affect the seepage abstraction. However, the improved confidence in the UZ model is relevant since UZ flow fields are used.
F.8	Water flow through the UZ can be modeled as steady-state	Transient, "fast-pathway" flow, such as conveyed ^{36}Cl to the ESF horizon, is assumed not to contribute significantly to the total flow through the UZ.	Model results based on this assumption are appropriate for use in the seepage abstraction.
F.9	The dual-permeability formulation is appropriate for simulating flow and transport	None given, but dual-permeability is a standard formulation widely used in modeling fractured systems.	Model results based on this assumption are appropriate for use in the seepage abstraction.
F.10	Climate-induced transients can be neglected, so that conditions within the UZ reflect the infiltration rates imposed at the upper model boundary	None given.	Model results based on this assumption are appropriate for use in the seepage abstraction.
F.11	In modeling calcite deposition, the gas phase is set to atmospheric pressure, air flow is neglected, constant infiltration and water chemistry are applied at the top model boundary, and water flow is taken to be steady-state	None given.	Model results based on this assumption are appropriate for use in the seepage abstraction. Note that this assumption is used in comparisons of the UZ flow model against geochemical data and so does not directly affect the seepage abstraction. However, the improved confidence in the UZ model is relevant since UZ flow fields are used.

Assumption		Rationale from Source Report	Application to the Seepage Abstraction
<i>Development of Numerical Grids for UZ Flow and Transport Modeling (CRWMS M&O 2000h, Section 5)</i>			
G.1	The water table is taken to be at 730 meters above sea level (masl) east of the Solitario Canyon fault and at 776 masl west of the Solitario Canyon fault	The data indicate that water levels in 19 out of the 21 wells that lie east of the Solitario Canyon fault vary by only 2.74 m (from 728.46 masl to 731.20 masl). Wells H-6, WT-7, WT-10, and H-5, which are all west of the Solitario Canyon fault (except for H-5, which lies west of a splay of the Solitario Canyon fault), have water levels ranging from 775.55 masl to 776.08 masl, which is approximately 46 m higher than the water levels east of the Solitario Canyon fault (except in WT#6, see discussion below for assumption G.3). Thus, it appears that the Solitario Canyon fault creates an elevation discontinuity in an otherwise uniform water table.	This assumption should have no effect on the seepage abstraction because the water table is well below the repository.
G.2	The Solitario Canyon fault acts as a barrier to lateral flow at the water table	This assumption provides the mechanism to explain the observed 46-m difference in water table elevation discussed in assumption G.1 above. This large-displacement, normal fault may act as a barrier to lateral flow because of the formation of low-permeability fault gouge, or because it juxtaposes layers with contrasting hydrogeologic properties.	This assumption should have no effect on the seepage abstraction because the water table is well below the repository.
G.3	The observed water levels in boreholes WT#6, G-2, and WT-24 represent perched water	Observed water levels in these three boreholes from northern Yucca Mountain (located east of the Solitario Canyon fault) are much higher than 730 masl. In borehole WT#6, water levels measure about 1,034 masl. In boreholes USW G-2 and USW WT-24, not included in Table 4, water levels are approximately 1,020 masl and 986 masl, respectively. These data indicate that existing data are inadequate to define precisely the water table altitude beneath northern Yucca Mountain. The perched water assumption enables the UZ Model to simulate and calibrate to perched water data under northern Yucca Mountain.	This assumption should have no effect on the seepage abstraction because the perched water and water table are well below the repository.
G.4	Saturated hydraulic conductivity (Ksat) data can be used as a surrogate for assigning grid-blocks within certain layers of the Calico Hills nonwelded hydrogeologic unit either vitric or zeolitic material names (and thus, separate hydrogeologic properties)	There are two main reasons why Ksat data are used as a surrogate to assign grid-blocks either vitric or zeolitic material names. First, existing data show that the Ksat of vitric tuff is orders of magnitude greater than that of zeolitic tuff. Also, there are much more available data on Ksat values than on mineralogic alteration (i.e., % zeolite).	This assumption should have no effect on the seepage abstraction since the Calico Hills unit is well below the repository.
G.5	In UZ Model layers ch1, ch2, ch3, ch4, and ch5, tuff is vitric where Ksat is greater than 10^{-10} m/s and zeolitic where Ksat is less than 10^{-10} m/s	Vitric Ksat values are on the order of 10^{-7} m/s, while zeolitic Ksat values are on the order of 10^{-10} to 10^{-11} m/s. No definitive Ksat cutoff value exists by which to distinguish vitric material from zeolitic material, as this transition occurs over about three orders of magnitude. The Ksat-value cutoff of 10^{-10} m/s is somewhat arbitrarily chosen; however, the sensitivity of the 10^{-10} m/s cutoff is not expected to be significant compared to using a 10^{-9} m/s or 10^{-8} m/s cutoff, since these contours are closely spaced in the repository footprint.	This assumption should have no effect on the seepage abstraction since the Calico Hills unit is well below the repository.

Assumption		Rationale from Source Report	Application to the Seepage Abstraction
G.6	Steeply dipping faults can be represented as vertical	This assumption is supported by sensitivity studies that indicate that flow through faults is much more sensitive to the rock properties assigned to fault zones than to slight variations in fault dip.	Analysis results based on this assumption are appropriate for use in the seepage abstraction.
<i>Analysis of Hydrologic Properties Data (CRWMS M&O 2000i, Section 5)</i>			
H.1	Heterogeneity is adequately represented by model layers with uniform hydrologic properties	First, the overall behavior of flow and transport processes in the unsaturated zone of Yucca Mountain is mainly determined by relatively large-scale heterogeneities introduced by stratification of the tuffs. Second, the complexity of a heterogeneity model needs to be consistent with the data availability. More complicated models generally introduce larger degrees of uncertainty in rock property estimations when data are limited. This is because more complicated models correspond to larger numbers of variables. Third, this layered approach is supported by field observations, such as matrix water saturation distributions. For a given geologic unit, measured matrix saturation distributions are very similar from different boreholes, indicating that matrix flow behavior and effective hydraulic properties should be similar within the unit.	Analysis results based on this assumption are appropriate for use in the seepage abstraction.
H.2	The van Genuchten relationships can be used for the active fracture continuum	Not all connected fractures are active in conducting liquid water in the unsaturated zone of Yucca Mountain. The active fracture continuum consists of fractures that actively conduct liquid water. The use of van Genuchten relations is based on a conceptual model that flow in fractures can be described using porous-medium equivalence.	Analysis results based on this assumption are appropriate for use in the seepage abstraction.
H.3	Simple averaging schemes are appropriate for upscaling of most properties. The relation of Pateologos et al., originally developed for porous media, is appropriate for upscaling matrix permeability.	The rock properties to which this assumption applies are mainly used as initial estimates for use in the inversion process of the Calibrated Properties Model (CRWMS M&O 2000f). The upscaling issue is further considered in the inversion process, which obtains the large-scale properties by matching the large-scale simulation results with grid-block-scale observations averaged from small-scale data.	Analysis results based on this assumption are appropriate for use in the seepage abstraction.
H.4	The van Genuchten fracture m value estimated for the Topopah Spring middle nonlithophysal hydrogeologic unit can be used to represent all UZ model layers	First, for other model layers, there are limited data for determining the m values. Second, the m value determined in this way is only used as an initial guess for use in the inversion process of the Calibrated Properties Model (CRWMS M&O 2000f). The inversion process results in more accurate m values for the model layers because it adjusts rock properties to make model simulation results match the relevant observations.	Analysis results based on this assumption are appropriate for use in the seepage abstraction.

Assumption	Rationale from Source Report	Application to the Seepage Abstraction
<i>Heat Decay Data and Repository Footprint for Thermal-Hydrologic and Conduction-Only Models for TSPA-SR (CRWMS M&O 2000j, Section 3)</i>		
I.1	The heating data used for noncommercial waste in the Viability Assessment can still be used	These were the only data available at the time this calculation was performed.
		This assumption is irrelevant to the seepage abstraction because thermal-load information is not used.

ATTACHMENT II**Software Routine T2WEEP v. 1.0**

This attachment contains sample input/output files and the source listing for T2WEEP v. 1.0. A description of the use and verification of this software routine is presented in Section 6.4.3.1. Spot checks were performed on the output files to ensure that the routine was performing correctly for the range of input parameters used. An example of a spot check is provided as follows, for the reported percolation flux and weep spacings for the first repository element, 'fph 2.' (Note: although the repository percolation flux is not used in this AMR, its value may be used in future analyses). To calculate the repository percolation flux in mm/year, we need the mass flow rate between this element and the element above it (kg/s), the connection area between the two elements (m²), and the liquid density (kg/m³).

The mass flow rate between 'fph 2' and the element above it 'foh 2' is given in 'pa_glam1.out' in DTN: LB990801233129.009 as 0.10675E-01 kg/s. The connection area between element 'fph 2' and the element above it is reported in the mesh file (DTN: LB990701233129.001) as 0.4311E+05 m². The water liquid density is equal to 1000 kg/m³ (consistent with the value assumed in the UZ site-scale model to calculate infiltration). The percolation flux can then be calculated as follows: percolation flux = (0.10675E-01 kg/s) ÷ (0.4311E+05 m²) ÷ (1000 kg/m³) = 2.476E-10 m/s. This value can be converted to mm/yr as follows: (2.476E-10 m/s) × (1000 mm/m) × (3.1536E+07 s/yr) = 7.809 mm/yr. This is exactly the number that is reported in the sample output file (see below in bold).

The two weep spacings for element 'fph 2' are calculated using the formulation provided in Eqs. 5-7 of this report. The first weep spacing is calculated using the A^* parameter (DTN: LB990501233129.001) and the residual fracture saturation (DTN: LB997141233129.001, DTN: LB997141233129.002, and DTN: LB997141233129.003), as well as the fracture saturation provided in 'pa_glam1.out' (DTN: LB990801233129.009). The A^* parameter is equal to 12.31 (1/m), and the residual fracture liquid saturation is equal to 0.01. The fracture liquid saturation is equal to 0.15007E-01. Substituting these values into Eqs. 5 and 6 yields the first weep spacing as 32.12 m, which is exactly the value reported in the sample output file below (in bold).

The second weep spacing is given by Eq. 7. For this calculation, the geometric fracture spacing (DTN: LB990501233129.001) and the γ parameter are required (DTN: LB997141233129.001, DTN: LB997141233129.002, and DTN: LB997141233129.003). The geometric fracture spacing and the γ parameter for this test case are equal to 0.25 m and 0.41, respectively. Substituting the required values into Eq. 7 yields a second weep spacing of 2.184 m, which is exactly the value reported in the sample output file below (in bold).

II.1 Sample Input File

```

/home/ckho/tspaSR-LA/base-case_flow_fields/LBNL_grid/SR-repo-nodes
../pa_glam1.out
/home/ckho/tspaSR-LA/base-case_flow_fields/LBNL_grid/lb990701233129.001/mpa_pch1.v1
glam1_weep.out
0.01
1000.
.41,.41,.41,.5
13.54,9.68,12.31,8.6
0.23,0.32,0.25,0.59

```

```

#The gamma values are taken from DTN: LB997141233129.001. The values are
#different for lower, mean, and upper infiltration models, but they are
#the same for perched water models #1 and #2 and for future climates.
#The (Afm/V) parameter and fracture spacings(1/frequency) are taken from
#DTN: LB990501233129.001 (AMR U0090), and they are constant.
-----

```

```

write(*,*)'What is the name of repository element file?'
read(*,*) repo
write(*,*) 'What is the name of the TOUGH2 output file?'
read(*,*) t2out
write(*,*) 'What is the name of the TOUGH2 mesh file?'
read(*,*) t2mesh
write(*,*) 'What would you like to name your output file?'
read(*,*) output
write(*,*)'What is the residual fracture liquid saturation?'
read(*,*) sfr
write(*,*)'What is the liquid density (kg/m^3)?'
read(*,*) rho
write(*,*)'What are the gamma parameters for the units:'
write(*,*)'tswF4, tswF5, tswF6, and tswFf?'
read(*,*) g4,g5,g6,gf
write(*,*)'What are the (Afm/V) parameters for the units:'
write(*,*)'tswF4, tswF5, tswF6, and tswFf?'
read(*,*) afm4,afm5,afm6,afmf
write(*,*)'Geometric fracture spacings (m) for the units:'
write(*,*)'tswF4, tswF5, tswF6, and tswFf?'
read(*,*) d4,d5,d6,df

```

II.2 Sample Output file

Screen Output File:

```

What is the name of repository element file?
What is the name of the TOUGH2 output file?
What is the name of the TOUGH2 mesh file?
What would you like to name your output file?
What is the residual fracture liquid saturation?
What is the liquid density (kg/m^3)?
What are the gamma parameters for the units:
tswF4, tswF5, tswF6, and tswFf?
What are the (Afm/V) parameters for the units:
tswF4, tswF5, tswF6, and tswFf?
Geometric fracture spacings (m) for the units:
tswF4, tswF5, tswF6, and tswFf?
Have read in 97976 elements in ELEME and
275 repository elements in ELEME...
Have read in 396770 number of connections
and 275 number of repository connections...
Have read in 275 repository liquid saturations...
Have read in 275 repository fluxes...

```

Data Output File:

*** Output file from t2weep_v1.f ***

TOUGH2 output file: ../pa_glam1.out

TOUGH2 mesh file: /home/ckho/tspaSR-LA/base-case_flow_fields/LBNL_grid/lb990701233129.001/mpa_pchl.v1

Repository element file: /home/ckho/tspaSR-LA/base-case_flow_fields/LBNL_grid/SR-repo-nodes

Gamma value for tswF4, tswF5, tswF6, and tswFf: 0.41 0.41 0.41 0.50

Afm/V value for tswF4, tswF5, tswF6, and tswFf: 13.54 9.68 12.31 8.60

Fracture spacing for tswF4, tswF5, tswF6, and tswFf: 0.23 0.32 0.25 0.59

The percolation flux is that entering the listed repository element from the element above. The first weep spacing

assumes that the fractures with weeps are saturated

(i.e., weep width in each fracture equals weep spacing).

The second weep spacing assumes that the active fractures

are unsaturated and is taken from eq. 17 of Liu et al.

(1998) WRR, 34(10), 2633-2646.

Note that fault materials (ending in "f") are placed at the end of the file

Element	material	x(m)	y(m)	z(m)	S1	percolation(mm/year)	weep_spacing1(m)	weep_spacing2(m)
Fph 2	tswF6	170424.312	231092.641	1109.641	0.1501E-01	0.7809E+01	0.3212E+02	0.2184E+01
Foh 3	tswF5	170681.094	231009.219	1109.641	0.1484E-01	0.4714E+01	0.4227E+02	0.2835E+01
Fph 4	tswF6	170449.344	231169.672	1108.478	0.1333E-01	0.2641E+01	0.4823E+02	0.2580E+01
Foh 5	tswF6	170474.375	231246.719	1107.315	0.1553E-01	0.1011E+02	0.2911E+02	0.2098E+01
Fph 6	tswF6	170499.391	231323.750	1106.152	0.1548E-01	0.9875E+01	0.2937E+02	0.2106E+01
Fsh 7	tswF6	170267.641	231484.219	1104.990	0.1678E-01	0.1751E+02	0.2372E+02	0.1929E+01
Fph 8	tswF6	170524.422	231400.781	1104.990	0.1592E-01	0.1207E+02	0.2719E+02	0.2040E+01
Fph 9	tswF5	171038.000	231233.922	1104.990	0.1228E-01	0.6374E+00	0.8991E+02	0.3864E+01
Fsh10	tswF6	170292.672	231561.250	1103.827	0.2076E-01	0.5894E+02	0.1494E+02	0.1596E+01
Fqh11	tswF5	170549.453	231477.828	1103.827	0.2066E-01	0.3779E+02	0.1918E+02	0.2051E+01
Fqh12	tswF5	170806.234	231394.391	1103.827	0.1272E-01	0.1041E+01	0.7523E+02	0.3591E+01
Fsh13	tswF6	170317.703	231638.281	1102.664	0.1748E-01	0.2252E+02	0.2149E+02	0.1853E+01
Fph14	tswF5	170574.484	231554.859	1102.664	0.1645E-01	0.1014E+02	0.3170E+02	0.2520E+01
Fqh15	tswF5	170831.266	231471.422	1102.664	0.1276E-01	0.1074E+01	0.7419E+02	0.3571E+01
Foh16	tswF5	171088.062	231388.000	1102.664	0.1440E-01	0.3634E+01	0.4651E+02	0.2949E+01
Frh17	tswF6	170342.734	231715.328	1101.501	0.1440E-01	0.5546E+01	0.3660E+02	0.2304E+01
Fph18	tswF5	170599.516	231631.891	1101.501	0.1865E-01	0.2164E+02	0.2365E+02	0.2235E+01
Fph19	tswF5	170856.297	231548.469	1101.501	0.1454E-01	0.3950E+01	0.4504E+02	0.2910E+01
Foh20	tswF5	171113.094	231465.031	1101.501	0.1437E-01	0.3565E+01	0.4685E+02	0.2958E+01
Frh21	tswF6	170367.750	231792.359	1100.338	0.1715E-01	0.1994E+02	0.2251E+02	0.1888E+01
Fph22	tswF5	170624.547	231708.938	1100.338	0.1628E-01	0.9314E+01	0.3255E+02	0.2547E+01
Fph23	tswF5	170881.328	231625.500	1100.338	0.1308E-01	0.1416E+01	0.6648E+02	0.3414E+01
Fsh24	tswF6	170392.781	231869.391	1099.175	0.1497E-01	0.7639E+01	0.3235E+02	0.2191E+01
Fph25	tswF5	170649.578	231785.969	1099.175	0.1924E-01	0.2595E+02	0.2213E+02	0.2175E+01
Foh26	tswF5	170906.359	231702.531	1099.175	0.1468E-01	0.4310E+01	0.4370E+02	0.2874E+01
Frh27	tswF5	170417.812	231946.438	1098.013	0.1869E-01	0.2192E+02	0.2355E+02	0.2231E+01
Fph28	tswF5	170674.609	231863.000	1098.013	0.1793E-01	0.1732E+02	0.2580E+02	0.2316E+01
Foh29	tswF5	170931.391	231779.578	1098.013	0.1281E-01	0.1108E+01	0.7284E+02	0.3544E+01

Fth30,	tswF6,	170186.062,	232106.906,	1096.850,	0.1879E-01,	0.3462E+02,	0.1830E+02,	0.1734E+01
Fsh31,	tswF5,	170442.844,	232023.469,	1096.850,	0.1587E-01,	0.7710E+01,	0.3483E+02,	0.2619E+01
Fph32,	tswF5,	170699.625,	231940.031,	1096.850,	0.1504E-01,	0.5301E+01,	0.4060E+02,	0.2789E+01
Foh33,	tswF5,	170956.422,	231856.609,	1096.850,	0.1579E-01,	0.7537E+01,	0.3533E+02,	0.2634E+01
Fuh34,	tswF6,	170211.094,	232183.938,	1095.687,	0.1555E-01,	0.1022E+02,	0.2896E+02,	0.2093E+01
Fqh35,	tswF5,	170467.875,	232100.500,	1095.687,	0.1882E-01,	0.2290E+02,	0.2319E+02,	0.2217E+01
Fph36,	tswF5,	170724.656,	232017.078,	1095.687,	0.1806E-01,	0.1803E+02,	0.2536E+02,	0.2300E+01
Foh37,	tswF5,	170981.453,	231933.641,	1095.687,	0.1519E-01,	0.5637E+01,	0.3943E+02,	0.2756E+01
Fth38,	tswF6,	170236.109,	232260.969,	1094.524,	0.2056E-01,	0.5610E+02,	0.1523E+02,	0.1608E+01
Fqh39,	tswF5,	170492.906,	232177.547,	1094.524,	0.1910E-01,	0.2484E+02,	0.2248E+02,	0.2189E+01
Fph40,	tswF5,	170749.688,	232094.109,	1094.524,	0.1665E-01,	0.1086E+02,	0.3074E+02,	0.2488E+01
Foh41,	tswF5,	171006.469,	232010.672,	1094.524,	0.1409E-01,	0.3013E+01,	0.5000E+02,	0.3037E+01
Fth42,	tswF6,	170261.141,	232338.016,	1093.361,	0.1759E-01,	0.2334E+02,	0.2119E+02,	0.1842E+01
Fqh43,	tswF5,	170517.938,	232254.578,	1093.361,	0.1665E-01,	0.1084E+02,	0.3076E+02,	0.2489E+01
Fph44,	tswF5,	170774.719,	232171.141,	1093.361,	0.1876E-01,	0.2248E+02,	0.2335E+02,	0.2223E+01
Foh45,	tswF5,	171031.500,	232087.719,	1093.361,	0.1809E-01,	0.1828E+02,	0.2527E+02,	0.2296E+01
Fqh46,	tswF5,	170542.969,	232331.609,	1092.198,	0.1953E-01,	0.2811E+02,	0.2146E+02,	0.2147E+01
Fph47,	tswF5,	170799.750,	232248.188,	1092.198,	0.1674E-01,	0.1122E+02,	0.3037E+02,	0.2476E+01
Foh48,	tswF5,	171056.531,	232164.750,	1092.198,	0.1601E-01,	0.8266E+01,	0.3405E+02,	0.2595E+01
Fth49,	tswF5,	170311.203,	232492.078,	1091.036,	0.2168E-01,	0.4801E+02,	0.1751E+02,	0.1976E+01
Frh50,	tswF5,	170567.984,	232408.656,	1091.036,	0.1708E-01,	0.1277E+02,	0.2891E+02,	0.2426E+01
Fqh51,	tswF5,	170824.781,	232325.219,	1091.036,	0.1543E-01,	0.6367E+01,	0.3763E+02,	0.2704E+01
Foh52,	tswF5,	171081.562,	232241.781,	1091.036,	0.1773E-01,	0.1613E+02,	0.2646E+02,	0.2340E+01
Fmh53,	tswF6,	170079.453,	232652.547,	1089.873,	0.2044E-01,	0.5479E+02,	0.1540E+02,	0.1616E+01
Fth54,	tswF5,	170336.234,	232569.109,	1089.873,	0.1705E-01,	0.1247E+02,	0.2901E+02,	0.2430E+01
Fqh55,	tswF5,	170593.016,	232485.688,	1089.873,	0.1966E-01,	0.2907E+02,	0.2119E+02,	0.2136E+01
Fph56,	tswF5,	170849.812,	232402.250,	1089.873,	0.1904E-01,	0.2442E+02,	0.2263E+02,	0.2195E+01
Foh57,	tswF5,	171106.594,	232318.828,	1089.873,	0.1676E-01,	0.1130E+02,	0.3026E+02,	0.2472E+01
Frh58,	tswF6,	170104.484,	232729.578,	1088.710,	0.1994E-01,	0.4761E+02,	0.1619E+02,	0.1649E+01
Fth59,	tswF5,	170361.266,	232646.156,	1088.710,	0.2321E-01,	0.6641E+02,	0.1549E+02,	0.1879E+01
Fqh60,	tswF5,	170618.047,	232562.719,	1088.710,	0.1955E-01,	0.2820E+02,	0.2143E+02,	0.2146E+01
Frh61,	tswF5,	170874.844,	232479.297,	1088.710,	0.1602E-01,	0.8358E+01,	0.3395E+02,	0.2592E+01
Foh62,	tswF5,	171131.625,	232395.859,	1088.710,	0.1425E-01,	0.3347E+01,	0.4811E+02,	0.2990E+01
Fph63,	tswF6,	170129.500,	232806.625,	1087.547,	0.2298E-01,	0.9666E+02,	0.1239E+02,	0.1478E+01
Fth64,	tswF5,	170386.297,	232723.188,	1087.547,	0.1921E-01,	0.2560E+02,	0.2221E+02,	0.2178E+01
Fqh65,	tswF5,	170643.078,	232639.750,	1087.547,	0.1643E-01,	0.9905E+01,	0.3182E+02,	0.2524E+01
Fqh66,	tswF5,	170899.859,	232556.328,	1087.547,	0.1926E-01,	0.2608E+02,	0.2208E+02,	0.2172E+01
Foh67,	tswF4,	171156.656,	232472.891,	1087.547,	0.2068E-01,	0.1356E+02,	0.1369E+02,	0.1473E+01
Fmh68,	tswF6,	170154.531,	232883.656,	1086.384,	0.2036E-01,	0.5327E+02,	0.1552E+02,	0.1621E+01
Fth69,	tswF5,	170411.328,	232800.219,	1086.384,	0.2347E-01,	0.7003E+02,	0.1519E+02,	0.1864E+01
Frh70,	tswF5,	170668.109,	232716.797,	1086.384,	0.1884E-01,	0.2300E+02,	0.2315E+02,	0.2215E+01
Fqh71,	tswF5,	170924.891,	232633.359,	1086.384,	0.1668E-01,	0.1100E+02,	0.3061E+02,	0.2484E+01
Foh72,	tswF4,	171181.688,	232549.938,	1086.384,	0.1796E-01,	0.6203E+01,	0.1836E+02,	0.1661E+01
Frh73,	tswF5,	170179.562,	232960.688,	1085.222,	0.2334E-01,	0.6833E+02,	0.1533E+02,	0.1871E+01
Fsh74,	tswF5,	170436.344,	232877.266,	1085.222,	0.2135E-01,	0.4456E+02,	0.1802E+02,	0.1999E+01
Frh75,	tswF5,	170693.141,	232793.828,	1085.222,	0.1657E-01,	0.1048E+02,	0.3115E+02,	0.2502E+01
Frh76,	tswF5,	170949.922,	232710.391,	1085.222,	0.1467E-01,	0.4262E+01,	0.4384E+02,	0.2878E+01
Frh77,	tswF5,	170204.594,	233037.719,	1084.059,	0.1657E-01,	0.1030E+02,	0.3114E+02,	0.2501E+01
Fsh78,	tswF5,	170461.375,	232954.297,	1084.059,	0.1838E-01,	0.1999E+02,	0.2440E+02,	0.2263E+01
Fqh79,	tswF5,	170718.172,	232870.859,	1084.059,	0.1964E-01,	0.2898E+02,	0.2121E+02,	0.2137E+01
Fph80,	tswF5,	170974.953,	232787.438,	1084.059,	0.1757E-01,	0.1531E+02,	0.2701E+02,	0.2360E+01

Fsh81, tswF5, 170229.625, 233114.766, 1082.896, 0.1765E-01, 0.1560E+02, 0.2674E+02, 0.2350E+01
Fsh82, tswF5, 170486.406, 233031.328, 1082.896, 0.2263E-01, 0.5914E+02, 0.1619E+02, 0.1913E+01
Fqh83, tswF5, 170743.203, 232947.906, 1082.896, 0.1864E-01, 0.2166E+02, 0.2367E+02, 0.2236E+01
Foh84, tswF5, 170999.984, 232864.469, 1082.896, 0.1491E-01, 0.4851E+01, 0.4169E+02, 0.2819E+01
Fsh85, tswF5, 170254.656, 233191.797, 1081.733, 0.1614E-01, 0.8736E+01, 0.3329E+02, 0.2571E+01
Fsh86, tswF5, 170511.438, 233108.359, 1081.733, 0.1771E-01, 0.1598E+02, 0.2653E+02, 0.2343E+01
Fqh87, tswF5, 170768.219, 233024.938, 1081.733, 0.1612E-01, 0.8683E+01, 0.3345E+02, 0.2576E+01
Fph88, tswF5, 171025.016, 232941.500, 1081.733, 0.1827E-01, 0.1935E+02, 0.2472E+02, 0.2276E+01
Fsh89, tswF5, 170279.688, 233268.828, 1080.570, 0.1608E-01, 0.8557E+01, 0.3366E+02, 0.2583E+01
Fsh90, tswF5, 170536.469, 233185.406, 1080.570, 0.2214E-01, 0.5331E+02, 0.1684E+02, 0.1944E+01
Fqh91, tswF5, 170793.250, 233101.969, 1080.570, 0.1969E-01, 0.2932E+02, 0.2112E+02, 0.2133E+01
Foh92, tswF5, 171050.047, 233018.547, 1080.570, 0.1675E-01, 0.1131E+02, 0.3029E+02, 0.2473E+01
Fth93, tswF5, 170304.719, 233345.875, 1079.407, 0.2009E-01, 0.3272E+02, 0.2027E+02, 0.2098E+01
Fsh94, tswF5, 170561.500, 233262.438, 1079.407, 0.2007E-01, 0.3246E+02, 0.2031E+02, 0.2099E+01
Fqh95, tswF5, 170818.281, 233179.016, 1079.407, 0.1692E-01, 0.1202E+02, 0.2958E+02, 0.2449E+01
Foh96, tswF5, 171075.062, 233095.578, 1079.407, 0.1433E-01, 0.3496E+01, 0.4727E+02, 0.2968E+01
Fth97, tswF5, 170329.734, 233422.906, 1078.245, 0.1778E-01, 0.1636E+02, 0.2630E+02, 0.2334E+01
Fsh98, tswF5, 170586.531, 233339.469, 1078.245, 0.1707E-01, 0.1272E+02, 0.2894E+02, 0.2428E+01
Fph99, tswF5, 170843.312, 233256.047, 1078.245, 0.1792E-01, 0.1729E+02, 0.2581E+02, 0.2316E+01
Foi 0, tswF4, 171100.094, 233172.609, 1078.245, 0.1864E-01, 0.7284E+01, 0.1693E+02, 0.1607E+01
Fsi 1, tswF5, 170354.766, 233499.938, 1077.082, 0.2254E-01, 0.5801E+02, 0.1631E+02, 0.1919E+01
Fsi 2, tswF5, 170611.562, 233416.516, 1077.082, 0.2148E-01, 0.4595E+02, 0.1782E+02, 0.1990E+01
Fqi 3, tswF5, 170868.344, 233333.078, 1077.082, 0.1623E-01, 0.9139E+01, 0.3285E+02, 0.2557E+01
Foi 4, tswF4, 171125.125, 233249.656, 1077.082, 0.1754E-01, 0.5103E+01, 0.1940E+02, 0.1699E+01
Fsi 5, tswF5, 170379.797, 233576.984, 1075.919, 0.2061E-01, 0.3722E+02, 0.1928E+02, 0.2055E+01
Fsi 6, tswF5, 170636.578, 233493.547, 1075.919, 0.1690E-01, 0.1191E+02, 0.2966E+02, 0.2452E+01
Fsi 7, tswF5, 170893.375, 233410.109, 1075.919, 0.1944E-01, 0.2745E+02, 0.2167E+02, 0.2156E+01
Fsi 8, tswF5, 170404.828, 233654.016, 1074.756, 0.1688E-01, 0.1182E+02, 0.2973E+02, 0.2454E+01
Fsi 9, tswF5, 170661.609, 233570.578, 1074.756, 0.1994E-01, 0.3145E+02, 0.2057E+02, 0.2110E+01
Fqi10, tswF5, 170918.406, 233487.156, 1074.756, 0.1818E-01, 0.1879E+02, 0.2502E+02, 0.2287E+01
Fri11, tswF5, 170173.062, 233814.484, 1073.593, 0.1708E-01, 0.1283E+02, 0.2890E+02, 0.2426E+01
Fsi12, tswF5, 170429.859, 233731.047, 1073.593, 0.2241E-01, 0.5642E+02, 0.1649E+02, 0.1927E+01
Fri13, tswF5, 170686.641, 233647.625, 1073.593, 0.1698E-01, 0.1232E+02, 0.2930E+02, 0.2440E+01
Fri14, tswF5, 170943.438, 233564.188, 1073.593, 0.1559E-01, 0.6935E+01, 0.3660E+02, 0.2673E+01
Fri15, tswF5, 170198.094, 233891.516, 1072.431, 0.1426E-01, 0.3343E+01, 0.4798E+02, 0.2987E+01
Fsi16, tswF5, 170454.891, 233808.078, 1072.431, 0.1671E-01, 0.1106E+02, 0.3048E+02, 0.2480E+01
Fri17, tswF5, 170711.672, 233724.656, 1072.431, 0.1976E-01, 0.2988E+02, 0.2097E+02, 0.2127E+01
Fqi18, tswF5, 170968.453, 233641.219, 1072.431, 0.2019E-01, 0.3357E+02, 0.2007E+02, 0.2089E+01
Fqi19, tswF4, 171225.250, 233557.797, 1072.431, 0.2400E-01, 0.2781E+02, 0.1045E+02, 0.1318E+01
Fsi20, tswF5, 170223.125, 233968.547, 1071.268, 0.1519E-01, 0.5649E+01, 0.3940E+02, 0.2755E+01
Fsi21, tswF5, 170479.922, 233885.125, 1071.268, 0.2158E-01, 0.4703E+02, 0.1766E+02, 0.1983E+01
Fri22, tswF5, 170736.703, 233801.688, 1071.268, 0.1999E-01, 0.3182E+02, 0.2048E+02, 0.2107E+01
Fsi23, tswF5, 170248.156, 234045.594, 1070.105, 0.1352E-01, 0.2027E+01, 0.5809E+02, 0.3230E+01
Fsi24, tswF5, 170504.938, 233962.156, 1070.105, 0.1675E-01, 0.1126E+02, 0.3029E+02, 0.2473E+01
Fsi25, tswF5, 170761.734, 233878.719, 1070.105, 0.1610E-01, 0.8657E+01, 0.3351E+02, 0.2578E+01
Fri26, tswF4, 171018.516, 233795.297, 1070.105, 0.2473E-01, 0.3052E+02, 0.9924E+01, 0.1291E+01
Fsi27, tswF5, 170273.188, 234122.625, 1068.942, 0.1238E-01, 0.6689E+00, 0.8605E+02, 0.3795E+01
Fsi28, tswF5, 170529.969, 234039.188, 1068.942, 0.2247E-01, 0.5714E+02, 0.1641E+02, 0.1923E+01
Fri29, tswF5, 170786.766, 233955.766, 1068.942, 0.1938E-01, 0.2703E+02, 0.2180E+02, 0.2161E+01
Fri30, tswF4, 171043.547, 233872.328, 1068.942, 0.2003E-01, 0.1090E+02, 0.1458E+02, 0.1512E+01
Fsi31, tswF5, 170298.219, 234199.656, 1067.779, 0.1522E-01, 0.5824E+01, 0.3922E+02, 0.2749E+01

Fsi32,	tswF5,	170555.000,	234116.234,	1067.779,	0.2037E-01,	0.3511E+02,	0.1972E+02,	0.2074E+01
Fri33,	tswF5,	170811.797,	234032.797,	1067.779,	0.1614E-01,	0.8783E+01,	0.3330E+02,	0.2571E+01
Fqi34,	tswF4,	171068.578,	233949.359,	1067.779,	0.1637E-01,	0.3281E+01,	0.2294E+02,	0.1820E+01
Fsi35,	tswF5,	170323.250,	234276.703,	1066.616,	0.1420E-01,	0.3234E+01,	0.4867E+02,	0.3004E+01
Fsi36,	tswF5,	170580.031,	234193.266,	1066.616,	0.1660E-01,	0.1063E+02,	0.3097E+02,	0.2496E+01
Fqi37,	tswF5,	170836.812,	234109.828,	1066.616,	0.1834E-01,	0.1980E+02,	0.2453E+02,	0.2268E+01
Fpi38,	tswF4,	171093.609,	234026.406,	1066.616,	0.1821E-01,	0.6709E+01,	0.1781E+02,	0.1641E+01
Fsi39,	tswF5,	170348.281,	234353.734,	1065.454,	0.2016E-01,	0.3333E+02,	0.2013E+02,	0.2092E+01
Fri40,	tswF5,	170605.062,	234270.297,	1065.454,	0.2225E-01,	0.5457E+02,	0.1669E+02,	0.1937E+01
Fqi41,	tswF5,	170861.844,	234186.875,	1065.454,	0.1713E-01,	0.1302E+02,	0.2870E+02,	0.2419E+01
Fpi42,	tswF4,	171118.641,	234103.438,	1065.454,	0.1587E-01,	0.2781E+01,	0.2490E+02,	0.1883E+01
Fsi43,	tswF5,	170373.312,	234430.766,	1064.291,	0.1915E-01,	0.2532E+02,	0.2236E+02,	0.2184E+01
Fsi44,	tswF5,	170630.094,	234347.344,	1064.291,	0.1741E-01,	0.1440E+02,	0.2759E+02,	0.2380E+01
Fqi45,	tswF5,	170886.875,	234263.906,	1064.291,	0.1486E-01,	0.4740E+01,	0.4206E+02,	0.2830E+01
Fpi46,	tswF4,	171143.656,	234180.469,	1064.291,	0.2020E-01,	0.1202E+02,	0.1434E+02,	0.1501E+01
Fsi47,	tswF5,	170398.328,	234507.797,	1063.128,	0.1701E-01,	0.1248E+02,	0.2916E+02,	0.2435E+01
Fri48,	tswF5,	170655.125,	234424.375,	1063.128,	0.2111E-01,	0.4213E+02,	0.1841E+02,	0.2017E+01
Fpi49,	tswF5,	170911.906,	234340.938,	1063.128,	0.1843E-01,	0.2031E+02,	0.2427E+02,	0.2258E+01
Fqi50,	tswF4,	171168.688,	234257.516,	1063.128,	0.1931E-01,	0.9450E+01,	0.1570E+02,	0.1558E+01
Fsi51,	tswF5,	170423.359,	234584.844,	1061.965,	0.2351E-01,	0.7074E+02,	0.1514E+02,	0.1861E+01
Fri52,	tswF5,	170680.156,	234501.406,	1061.965,	0.1948E-01,	0.2767E+02,	0.2158E+02,	0.2152E+01
Fri53,	tswF5,	170936.938,	234417.984,	1061.965,	0.1556E-01,	0.6754E+01,	0.3678E+02,	0.2678E+01
Fri54,	tswF4,	171193.719,	234334.547,	1061.965,	0.1785E-01,	0.5997E+01,	0.1864E+02,	0.1672E+01
Fsi55,	tswF5,	170448.391,	234661.875,	1060.802,	0.1732E-01,	0.1392E+02,	0.2795E+02,	0.2393E+01
Fsi56,	tswF5,	170705.172,	234578.438,	1060.802,	0.1729E-01,	0.1382E+02,	0.2805E+02,	0.2397E+01
Fri57,	tswF5,	170961.969,	234495.016,	1060.802,	0.1947E-01,	0.2767E+02,	0.2159E+02,	0.2153E+01
Fqi58,	tswF4,	171218.750,	234411.578,	1060.802,	0.2151E-01,	0.1658E+02,	0.1271E+02,	0.1429E+01
Fsi59,	tswF5,	170473.422,	234738.906,	1059.640,	0.2375E-01,	0.7442E+02,	0.1487E+02,	0.1848E+01
Fri60,	tswF5,	170730.203,	234655.484,	1059.640,	0.2165E-01,	0.4770E+02,	0.1756E+02,	0.1978E+01
Fpi61,	tswF5,	170987.000,	234572.047,	1059.640,	0.1751E-01,	0.1497E+02,	0.2723E+02,	0.2368E+01
Fpi62,	tswF4,	171243.781,	234488.625,	1059.640,	0.1696E-01,	0.4352E+01,	0.2101E+02,	0.1756E+01
Fsi63,	tswF5,	170498.453,	234815.953,	1058.477,	0.2140E-01,	0.4502E+02,	0.1795E+02,	0.1996E+01
Fri64,	tswF5,	170755.234,	234732.516,	1058.477,	0.1693E-01,	0.1206E+02,	0.2951E+02,	0.2447E+01
Fpi65,	tswF5,	171012.031,	234649.094,	1058.477,	0.1529E-01,	0.5940E+01,	0.3865E+02,	0.2733E+01
Fpi66,	tswF4,	171268.812,	234565.656,	1058.477,	0.2042E-01,	0.1272E+02,	0.1403E+02,	0.1488E+01
Fsi67,	tswF5,	170523.484,	234892.984,	1057.314,	0.1882E-01,	0.2283E+02,	0.2320E+02,	0.2217E+01
Fqi68,	tswF5,	170780.266,	234809.547,	1057.314,	0.1970E-01,	0.2942E+02,	0.2109E+02,	0.2132E+01
Foi69,	tswF5,	171037.047,	234726.125,	1057.314,	0.1932E-01,	0.2648E+02,	0.2195E+02,	0.2167E+01
Fqi70,	tswF5,	170548.516,	234970.016,	1056.151,	0.2076E-01,	0.3874E+02,	0.1900E+02,	0.2043E+01
Fqi71,	tswF5,	170805.297,	234886.594,	1056.151,	0.1895E-01,	0.2378E+02,	0.2286E+02,	0.2204E+01
Fpi72,	tswF5,	171062.078,	234803.156,	1056.151,	0.1546E-01,	0.6499E+01,	0.3748E+02,	0.2699E+01
Fqi73,	tswF5,	170573.531,	235047.062,	1054.988,	0.1584E-01,	0.7666E+01,	0.3500E+02,	0.2624E+01
Fpi74,	tswF5,	170830.328,	234963.625,	1054.988,	0.1648E-01,	0.1017E+02,	0.3157E+02,	0.2515E+01
Foi75,	tswF5,	171087.109,	234880.188,	1054.988,	0.1785E-01,	0.1678E+02,	0.2604E+02,	0.2325E+01
Fqi76,	tswF5,	170598.562,	235124.094,	1053.825,	0.2144E-01,	0.4555E+02,	0.1787E+02,	0.1992E+01
Fpi77,	tswF5,	170855.359,	235040.656,	1053.825,	0.1816E-01,	0.1881E+02,	0.2507E+02,	0.2289E+01
Fqi78,	tswF5,	171112.141,	234957.234,	1053.825,	0.1578E-01,	0.7501E+01,	0.3541E+02,	0.2637E+01
Foi79,	tswF5,	170623.594,	235201.125,	1052.663,	0.2173E-01,	0.4839E+02,	0.1744E+02,	0.1972E+01
Fqi80,	tswF5,	170880.391,	235117.703,	1052.663,	0.1602E-01,	0.8309E+01,	0.3396E+02,	0.2592E+01
Fqi81,	tswF5,	171137.172,	235034.266,	1052.663,	0.1680E-01,	0.1153E+02,	0.3008E+02,	0.2466E+01
Fmi82,	tswF5,	170648.625,	235278.156,	1051.500,	0.1900E-01,	0.2441E+02,	0.2274E+02,	0.2199E+01

Fsi83,	tswF5,	170905.406,	235194.734,	1051.500,	0.2058E-01,	0.3696E+02,	0.1934E+02,	0.2058E+01
Fsi84,	tswF5,	171162.203,	235111.297,	1051.500,	0.1779E-01,	0.1648E+02,	0.2624E+02,	0.2332E+01
Fri85,	tswF5,	170416.875,	235438.625,	1050.337,	0.1998E-01,	0.3177E+02,	0.2049E+02,	0.2107E+01
Fqi86,	tswF5,	170673.656,	235355.203,	1050.337,	0.2026E-01,	0.3411E+02,	0.1994E+02,	0.2084E+01
Fsi87,	tswF5,	170930.438,	235271.766,	1050.337,	0.1604E-01,	0.8425E+01,	0.3388E+02,	0.2589E+01
Fsi88,	tswF5,	171187.234,	235188.344,	1050.337,	0.1726E-01,	0.1375E+02,	0.2816E+02,	0.2400E+01
Fqi89,	tswF5,	170441.906,	235515.672,	1049.174,	0.1625E-01,	0.9277E+01,	0.3271E+02,	0.2552E+01
Fqi90,	tswF5,	170698.688,	235432.234,	1049.174,	0.1627E-01,	0.9268E+01,	0.3262E+02,	0.2549E+01
Fsi91,	tswF5,	170955.469,	235348.797,	1049.174,	0.2075E-01,	0.3861E+02,	0.1903E+02,	0.2044E+01
Fqi92,	tswF5,	171212.266,	235265.375,	1049.174,	0.1738E-01,	0.1429E+02,	0.2771E+02,	0.2385E+01
Fqi93,	tswF5,	170466.922,	235592.703,	1048.011,	0.1865E-01,	0.2178E+02,	0.2365E+02,	0.2235E+01
Fri94,	tswF5,	170723.719,	235509.266,	1048.011,	0.1751E-01,	0.1499E+02,	0.2722E+02,	0.2367E+01
Fri95,	tswF5,	170980.500,	235425.844,	1048.011,	0.1787E-01,	0.1689E+02,	0.2600E+02,	0.2323E+01
Fni96,	tswF5,	171237.281,	235342.406,	1048.011,	0.1585E-01,	0.7722E+01,	0.3497E+02,	0.2623E+01
Foi97,	tswF6,	170491.953,	235669.734,	1046.849,	0.1945E-01,	0.4177E+02,	0.1702E+02,	0.1684E+01
Fsi98,	tswF5,	170748.750,	235586.312,	1046.849,	0.1682E-01,	0.1160E+02,	0.2999E+02,	0.2463E+01
Fqi99,	tswF5,	171005.531,	235502.875,	1046.849,	0.1600E-01,	0.8260E+01,	0.3410E+02,	0.2596E+01
Foj 0,	tswF6,	170516.984,	235746.781,	1045.686,	0.1721E-01,	0.2042E+02,	0.2231E+02,	0.1881E+01
Fsj 1,	tswF5,	170773.766,	235663.344,	1045.686,	0.1964E-01,	0.2897E+02,	0.2122E+02,	0.2137E+01
Fqj 2,	tswF5,	171030.562,	235579.906,	1045.686,	0.1633E-01,	0.9507E+01,	0.3234E+02,	0.2541E+01
Fsj 3,	tswF6,	170542.016,	235823.812,	1044.523,	0.1557E-01,	0.1032E+02,	0.2887E+02,	0.2091E+01
Fsj 4,	tswF5,	170798.797,	235740.375,	1044.523,	0.1649E-01,	0.1014E+02,	0.3154E+02,	0.2514E+01
Frj 5,	tswF5,	171312.375,	235573.516,	1044.523,	0.1595E-01,	0.8139E+01,	0.3435E+02,	0.2604E+01
Foj22,	tswF5,	170734.109,	230966.938,	1109.983,	0.1373E-01,	0.2344E+01,	0.5478E+02,	0.3153E+01
Fnj23,	tswF6,	170794.109,	230967.219,	1109.713,	0.1149E-01,	0.3166E+00,	0.1082E+03,	0.3594E+01
Fnj24,	tswF6,	170793.547,	231057.781,	1108.479,	0.1149E-01,	0.3180E+00,	0.1079E+03,	0.3589E+01
Fnj25,	tswF5,	170733.859,	231051.609,	1108.828,	0.1405E-01,	0.2898E+01,	0.5044E+02,	0.3048E+01
Foj26,	tswF5,	170725.234,	231135.047,	1107.727,	0.1423E-01,	0.3269E+01,	0.4840E+02,	0.2997E+01
Fnj27,	tswF5,	170784.922,	231141.219,	1107.378,	0.1193E-01,	0.4202E+00,	0.1058E+03,	0.4130E+01
Fnj28,	tswF5,	170716.609,	231218.484,	1106.626,	0.1613E-01,	0.8740E+01,	0.3339E+02,	0.2574E+01
Fnj29,	tswF5,	170776.281,	231224.656,	1106.277,	0.1235E-01,	0.7140E+00,	0.8686E+02,	0.3809E+01
Fpj30,	tswF5,	170767.812,	231305.531,	1105.210,	0.1322E-01,	0.1580E+01,	0.6358E+02,	0.3352E+01
Foj31,	tswF5,	170707.828,	231304.500,	1105.491,	0.1586E-01,	0.7767E+01,	0.3489E+02,	0.2621E+01
Fpj32,	tswF5,	170766.797,	231352.031,	1104.580,	0.1528E-01,	0.5821E+01,	0.3876E+02,	0.2736E+01
Foj33,	tswF5,	170707.109,	231358.125,	1104.762,	0.1761E-01,	0.1551E+02,	0.2687E+02,	0.2355E+01
Fqj34,	tswF5,	170716.469,	231449.906,	1103.467,	0.2270E-01,	0.6003E+02,	0.1610E+02,	0.1909E+01
Fqj35,	tswF5,	170776.156,	231443.812,	1103.285,	0.1847E-01,	0.2053E+02,	0.2415E+02,	0.2254E+01
Fqj36,	tswF5,	170725.828,	231541.688,	1102.172,	0.1879E-01,	0.2259E+02,	0.2327E+02,	0.2220E+01
Fpj37,	tswF5,	170785.516,	231535.609,	1101.991,	0.1453E-01,	0.4031E+01,	0.4511E+02,	0.2912E+01
Fpj38,	tswF5,	170735.172,	231633.469,	1100.878,	0.1797E-01,	0.1751E+02,	0.2566E+02,	0.2311E+01
Fpj39,	tswF5,	170794.875,	231627.391,	1100.696,	0.1216E-01,	0.5615E+00,	0.9487E+02,	0.3950E+01
Fpj40,	tswF5,	170744.531,	231725.250,	1099.583,	0.1832E-01,	0.1965E+02,	0.2459E+02,	0.2271E+01
Fpj41,	tswF5,	170804.219,	231719.172,	1099.401,	0.1230E-01,	0.6342E+00,	0.8874E+02,	0.3843E+01
Fqj42,	tswF5,	170753.891,	231817.047,	1098.288,	0.1951E-01,	0.2764E+02,	0.2151E+02,	0.2149E+01
Fpj43,	tswF5,	170813.578,	231810.953,	1098.107,	0.1326E-01,	0.1650E+01,	0.6284E+02,	0.3336E+01
Fqj44,	tswF5,	170998.375,	233694.984,	1071.564,	0.1837E-01,	0.1992E+02,	0.2442E+02,	0.2264E+01
Fqj45,	tswF4,	171052.344,	233721.219,	1070.966,	0.1747E-01,	0.4982E+01,	0.1958E+02,	0.1706E+01
Fpj46,	tswF4,	171091.516,	233640.625,	1071.893,	0.1994E-01,	0.1067E+02,	0.1471E+02,	0.1517E+01
Frj47,	tswF4,	171037.547,	233614.391,	1072.490,	0.2336E-01,	0.2335E+02,	0.1095E+02,	0.1344E+01
Fqj48,	tswF4,	171130.688,	233560.031,	1072.820,	0.1589E-01,	0.2795E+01,	0.2483E+02,	0.1880E+01
Frj49,	tswF4,	171076.734,	233533.797,	1073.417,	0.2550E-01,	0.3611E+02,	0.9433E+01,	0.1264E+01

Fqj50,	tswF4,	171169.859,	233479.438,	1073.746,	0.1801E-01,	0.6348E+01,	0.1826E+02,	0.1658E+01
Fqj51,	tswF4,	171115.906,	233453.203,	1074.344,	0.2264E-01,	0.2030E+02,	0.1157E+02,	0.1375E+01
Foj52,	tswF4,	171156.062,	233370.750,	1075.291,	0.2202E-01,	0.1843E+02,	0.1217E+02,	0.1403E+01
Fpj53,	tswF4,	171208.062,	233400.703,	1074.652,	0.1919E-01,	0.9134E+01,	0.1591E+02,	0.1567E+01
Fpj54,	tswF4,	171209.062,	233285.469,	1076.220,	0.2311E-01,	0.2371E+02,	0.1115E+02,	0.1354E+01
Flj86,	tswF5,	171060.891,	235667.781,	1044.351,	0.1796E-01,	0.1747E+02,	0.2571E+02,	0.2312E+01
Fqj87,	tswF5,	171201.781,	235578.328,	1044.948,	0.1749E-01,	0.1488E+02,	0.2732E+02,	0.2371E+01
Foj88,	tswF5,	171153.562,	235542.625,	1045.649,	0.1918E-01,	0.2567E+02,	0.2229E+02,	0.2181E+01
Fqj89,	tswF5,	171294.438,	235453.156,	1046.246,	0.1398E-01,	0.2768E+01,	0.5138E+02,	0.3072E+01
Fnj90,	tswF5,	171246.219,	235417.469,	1046.947,	0.1582E-01,	0.7515E+01,	0.3515E+02,	0.2629E+01
Fqk23,	tswF5,	170985.000,	234837.000,	1056.031,	0.1675E-01,	0.1126E+02,	0.3031E+02,	0.2474E+01
Fsk26,	tswF5,	170347.000,	233659.000,	1074.945,	0.2612E-01,	0.1126E+03,	0.1269E+02,	0.1731E+01
Fpk31,	tswF5,	171058.000,	231317.000,	1103.766,	0.1227E-01,	0.6355E+00,	0.9027E+02,	0.3870E+01
Ftk32,	tswF6,	170268.000,	232413.000,	1092.307,	0.1612E-01,	0.1320E+02,	0.2628E+02,	0.2012E+01
Fpk33,	tswF4,	171234.000,	234074.000,	1065.344,	0.1558E-01,	0.2413E+01,	0.2623E+02,	0.1923E+01
Fnk34,	tswF5,	170723.000,	235087.000,	1053.780,	0.2051E-01,	0.3636E+02,	0.1947E+02,	0.2063E+01
Fqk45,	tswF4,	171244.422,	233777.672,	1069.344,	0.1985E-01,	0.1099E+02,	0.1484E+02,	0.1523E+01
Fok55,	tswF5,	170752.594,	235159.781,	1052.655,	0.1815E-01,	0.1887E+02,	0.2510E+02,	0.2290E+01
Fpk56,	tswF5,	170708.016,	235024.562,	1054.699,	0.1592E-01,	0.8302E+01,	0.3452E+02,	0.2610E+01
Fok57,	tswF5,	171001.000,	234899.766,	1055.103,	0.1548E-01,	0.6533E+01,	0.3729E+02,	0.2693E+01
Fqk58,	tswF5,	170969.156,	234764.547,	1057.090,	0.2024E-01,	0.3401E+02,	0.1997E+02,	0.2085E+01
Fsk59,	tswF5,	170268.516,	233672.453,	1075.109,	0.1634E-01,	0.9603E+01,	0.3228E+02,	0.2539E+01
Fsk60,	tswF5,	170351.328,	233745.266,	1073.748,	0.2265E-01,	0.5923E+02,	0.1617E+02,	0.1912E+01
Ftk61,	tswF5,	170319.484,	233610.047,	1075.735,	0.1706E-01,	0.1282E+02,	0.2899E+02,	0.2429E+01
FoC10,	tswFf,	170764.109,	230967.078,	1109.848,	0.1065E-01,	0.3439E+00,	0.3526E+03,	0.2297E+02
FnC11,	tswFf,	170763.703,	231054.688,	1108.653,	0.1068E-01,	0.3801E+00,	0.3386E+03,	0.2251E+02
FoC12,	tswFf,	170755.078,	231138.125,	1107.552,	0.1077E-01,	0.5159E+00,	0.2971E+03,	0.2109E+02
FnC13,	tswFf,	170746.453,	231221.578,	1106.452,	0.1095E-01,	0.8259E+00,	0.2423E+03,	0.1905E+02
FpC14,	tswFf,	170737.812,	231305.016,	1105.350,	0.1213E-01,	0.5415E+01,	0.1082E+03,	0.1273E+02
FpC15,	tswFf,	170736.953,	231355.078,	1104.671,	0.1377E-01,	0.2059E+02,	0.6109E+02,	0.9562E+01
FqC16,	tswFf,	170746.312,	231446.859,	1103.376,	0.1426E-01,	0.2744E+02,	0.5398E+02,	0.8989E+01
FqC17,	tswFf,	170755.672,	231538.641,	1102.082,	0.1296E-01,	0.1173E+02,	0.7773E+02,	0.1079E+02
FpC18,	tswFf,	170765.016,	231630.438,	1100.787,	0.1122E-01,	0.1483E+01,	0.1881E+03,	0.1678E+02
FpC19,	tswFf,	170774.375,	231722.219,	1099.492,	0.1271E-01,	0.9582E+01,	0.8483E+02,	0.1127E+02
FpC20,	tswFf,	170783.734,	231814.000,	1098.198,	0.1378E-01,	0.2075E+02,	0.6092E+02,	0.9550E+01
FqC21,	tswFf,	171025.359,	233708.094,	1071.265,	0.1345E-01,	0.1680E+02,	0.6670E+02,	0.9992E+01
FqC22,	tswFf,	171064.531,	233627.500,	1072.192,	0.1365E-01,	0.1921E+02,	0.6301E+02,	0.9711E+01
Frc23,	tswFf,	171103.703,	233546.906,	1073.118,	0.1266E-01,	0.9129E+01,	0.8665E+02,	0.1139E+02
FqC24,	tswFf,	171142.891,	233466.312,	1074.045,	0.1354E-01,	0.1784E+02,	0.6506E+02,	0.9868E+01
FpC25,	tswFf,	171182.062,	233385.719,	1074.972,	0.1290E-01,	0.1125E+02,	0.7931E+02,	0.1090E+02
FnC41,	tswFf,	171085.016,	235685.641,	1044.001,	0.1290E-01,	0.1141E+02,	0.7936E+02,	0.1090E+02
FoC42,	tswFf,	171177.672,	235560.469,	1045.299,	0.1294E-01,	0.1149E+02,	0.7836E+02,	0.1083E+02
FqC43,	tswFf,	171270.328,	235435.312,	1046.596,	0.1187E-01,	0.4004E+01,	0.1232E+03,	0.1358E+02
total area of repository (m^2) = 0.49017E+07								
total kg/s over repository = 0.30314E+01								
average mm/year over repository = 0.19503E+02								

II.3 Source File for T2WEEP v. 1.0

```

c   program t2weep_v1.f
c
c   This program will extract incoming percolation and discrete weep
c   spacings for repository elements that are prescribed by the user.
c   The LBNL 3-D TOUGH2 UZ flow field and mesh are used as input, and a
c   file is created that contains the element, coordinates, percolation
c   flux (mm/year), and weep spacings (using two methods described
c   below).
c
c   1) Read in user-prescribed files and data (Sfr, gamma for repository
c   units, Afm/V parameters, liquid density etc.)
c   2) Read in repository elements from user-prescribed file
c   3) Read in element information (name, material, coordinates) from
c   ELEME and assign parameter values to repository elements based on
c   material type. Record element name directly above repository
c   element to identify appropriate connections.
c   4) Read in connection information from CONNE card for connections
c   identified in step 3. Record connection area for those connections.
c   5) Read TOUGH2 output file prescribed by user. First read in
c   liquid saturations for prescribed repository elements. Then
c   read in mass flow rates for those connections identified in step 3.
c   6) Calculate percolation flux from mass flow using connection area
c   and liquid density.
c   7) Calculate weep spacing using two methods: (a) assume active
c   fractures are saturated and use Xfm=Sfe, and
c   (b) fractures are unsaturated where active weep spacing is
c   calculated from Liu et al. (1998) using da=d/Se^gamma.
c   8) Print results to output file.
c
c   C.X.Ho 11/19/99
c
c23456789012345678901234567890123456789012345678901234567890123456789012
c   implicit double precision (a-h,o-z)
c
c   dimension x(1001),y(1001),z(1001),area(1001),sl(1001),gamma(1001)
c   real ml(1001),a(1001),d(1001)
c   character*100 block,output,t2out,t2mesh,repo
c   character*5 elemr(1001),mat(1001),elemr1(1001),elemr2(1001)
c   character*5 elem1,elem2,elemold
c
c
c   1) Read in user-prescribed files and data (Sfr, gamma for repository
c   units, Afm/V parameters, liquid density etc.)
c
c   write(*,*)'What is the name of repository element file?'
c   read(*,'(a)') repo
c   write(*,*) 'What is the name of the TOUGH2 output file?'
c   read(*,'(a)') t2out
c   write(*,*) 'What is the name of the TOUGH2 mesh file?'
c   read(*,'(a)') t2mesh
c   write(*,*) 'What would you like to name your output file?'
c   read(*,'(a)') output
c   write(*,*)'What is the residual fracture liquid saturation?'
c   read(*,*) sfr
c   write(*,*)'What is the liquid density (kg/m^3)?'
c   read(*,*) rho
c   write(*,*)'What are the gamma parameters for the units:'
c   write(*,*)'tswF4, tswF5, tswF6, and tswFf?'
c   read(*,*) g4,g5,g6,gf
c   write(*,*)'What are the (Afm/V) parameters for the units:'
c   write(*,*)'tswF4, tswF5, tswF6, and tswFf?'
c   read(*,*) afm4,afm5,afm6,afmf
c   write(*,*)'Geometric fracture spacings (m) for the units:'
c   write(*,*)'tswF4, tswF5, tswF6, and tswFf?'
c   read(*,*) d4,d5,d6,df

```

```

open(1,file=t2mesh,status='old')
open(2,file=t2out,status='old')
open(3,file=repo,status='old')
open(4,file=output,status='unknown')

c...Data
  mm_per_m=1000
  sec_per_year=3.1536e7

c...Write header information to output file
  write(4,25) t2out,t2mesh,repo,g4,g5,g6,gf,afm4,afm5,afm6,afmf,
  & d4,d5,d6,df
25  format('*** Output file from t2weep_v1.f ***',/
& 'TOUGH2 output file: ',a,/
& 'TOUGH2 mesh file: ',a,/
& 'Repository element file: ',a,/
& 'Gamma value for tswF4, tswF5, tswF6, and tswFf: ',4f7.2,/
& 'Afm/V value for tswF4, tswF5, tswF6, and tswFf: ',4f7.2,/
& 'Fracture spacing for tswF4, tswF5, tswF6, and tswFf: ',4f7.2,/
& 'The percolation flux is that entering the listed repository '/
& 'element from the element above. The first weep spacing '/
& 'assumes that the fractures with weeps are saturated '/
& '(i.e., weep width in each fracture equals weep spacing).'/
& 'The second weep spacing assumes that the active fractures '/
& 'are unsaturated and is taken from eq. 17 of Liu et al. '/
& '(1998) WRR, 34(10), 2633-2646.'/
& '***Note that fault materials (ending in "f") are placed '
& 'at the end of the file***'//
& 'Element, material, x(m), y(m), z(m), Sl, '
& 'percolation(mm/year), weep_spacing1(m), weep_spacing2(m)')

c
c 2) Read in repository elements from user-prescribed file
c
  read(3,*) nrepo
  read(3,'(a)') (elemr(i),i=1,nrepo)

c
c 3) Read in element information (name, material, coordinates) from
c ELEME and assign parameter values to repository elements based on
c material type. Record element name directly above repository
c element to identify appropriate connections.
c
c...Read in element information from ELEME
c...N is the counter on all elements
c...i is the counter on just repository elements
  N=1
  i=1
  READ(1,1000) BLOCK
1000 FORMAT(A22,28X,3f10.3)
99  READ(1,1000) BLOCK,xx,yy,zz
  IF(BLOCK(1:5).EQ.' ') GO TO 98
  if(block(1:5).ne.elemr(i)) then
c...Remember name of previously read element
    elemold=block(1:5)
    elemold(1:1)='F'
    n=n+1
    go to 99
  end if
c...If a repository element is read, designate element 1 as the
c...repository element and element 2 as the previous element read (which
c...will be the element directly above it). mat(i) is the material type.
  elemr1(i) = elemr(i)
  elemr2(i) = elemold
  mat(i)=block(16:20)
  x(i)=xx
  y(i)=yy
  z(i)=zz
c...Assign gamma value based on material of element.
  if(mat(i).eq.'tswF4') then

```

```

        gamma(i)=g4
        a(i)=afm4
        d(i)=d4
    elseif(mat(i).eq.'tswF5') then
        gamma(i)=g5
        a(i)=afm5
        d(i)=d5
    elseif(mat(i).eq.'tswF6') then
        gamma(i)=g6
        a(i)=afm6
        d(i)=d6
    elseif(mat(i).eq.'tswFF') then
        gamma(i)=gf
        a(i)=afmf
        d(i)=df
    else
        write(*,*) '***Could not match repository materials!***'
    end if
c...If the element is a fracture, subtract 0.5 m from the
c...x-coordinate because LBNL adds 0.5 m for fracture-matrix interactions
    if(elemr1(i)(1:1).eq.'F') x(i)=x(i)-0.5
    i=i+1
    n=n+1
    GO TO 99
98  CONTINUE
    NMAX = N - 1
    nmaxr=i-1

    write(*,50) nmax,nmaxr
50  format('Have read in ',i6,' elements in ELEME and'/
    &      'i6,' repository elements in ELEME...')

c
c 4) Read in connection information from CONNE card for connections
c   identified in step 3. Record connection area for those connections.
c
c...N is the counter on all connections
c...i is the counter on just repository connections
    N=1
    i=1
    areatot=0.
    READ(1,1500) BLOCK
1500 FORMAT(A22,3X,I5,20X,E10.4)
199  READ(1,1500) BLOCK, isot,areax
    IF(BLOCK(1:5).EQ.' '.OR.BLOCK(1:3).EQ.'+++') GO TO 198
    elem1 = BLOCK(1:5)
    elem2 = BLOCK(6:10)
    if(elem1.eq.elemr1(i).and.elem2.eq.elemr2(i)) then
        area(i)=areax
        areatot=areatot+areax
        i=i+1
    end if
    N=N+1
    GO TO 199
198  CONTINUE
    NCMAX = N - 1
4000 CONTINUE

    write(*,197) ncmx,i-1
197  format('Have read in ',i6,' number of connections',/
    &      'and ',i6,' number of repository connections...')

c
c 5) Read TOUGH2 output file prescribed by user. First read in
c   liquid saturations for prescribed repository elements. Then
c   read in mass flow rates for those connections identified in step 4.
c
89  READ(2,1000,END=90) BLOCK
    IF(BLOCK(1:12).NE.' TOTAL TIME') GO TO 89
    READ(2,1001) TIME
1001 FORMAT(E13.4)

```

```

do i=1,6
  READ(2,1000) BLOCK
end do
c...Read in liquid saturations from TOUGH2 output file. If element is
c...a repository element, record liquid saturation.
i=1
N1=1
N2=MIN(NMAX,45)
DO 2000 n=N1,N2
  READ(2,1002) elem1,slx
1002 FORMAT(1x,a5,24x,e12.5)
  if(elem1.eq.elemr(i)) then
    sl(i)=slx
    i=i+1
  end if
2000 CONTINUE
C
2100 CONTINUE
IF(N2.EQ.NMAX) GO TO 91
N1=N2+1
N2=MIN(NMAX,N1+56)
do j=1,3
  READ(2,1000) BLOCK
end do
DO 2010 n=N1,N2
  READ(2,1002) elem1,slx
  if(elem1.eq.elemr(i)) then
    sl(i)=slx
    i=i+1
  end if
2010 CONTINUE
GO TO 2100
C
91 CONTINUE
C
write(*,149)i-1
149 format('Have read in ',i6,' repository liquid saturations...')

c...Read in mass flow rates from TOUGH2 output file
i=1
flotot=0.
289 READ(2,1500,END=190) BLOCK
IF(BLOCK(7:18).NE.'ELEM1 ELEM2') GO TO 289
READ(2,1500) BLOCK
READ(2,1500) BLOCK
C
N1=1
N2=MIN(NCMAX,53)
DO 1600 n=N1,N2
  READ(2,1003) block,flow
1003 FORMAT(a32,E12.5)
  elem1=block(6:10)
  elem2=block(15:19)
  if(elem1.eq.elemr1(i).and.elem2.eq.elemr2(i))then
    ml(i)=flow
    flotot=flotot+flow
    i=i+1
  end if
1600 CONTINUE
C
2150 CONTINUE
IF(N2.EQ.NCMAX) GO TO 191
N1=N2+1
N2=MIN(NCMAX,N1+56)
do j=1,3
  READ(2,1500) BLOCK
end do
DO 2020 n=N1,N2
  READ(2,1003) block,flow
  elem1=block(6:10)
  elem2=block(15:19)

```

```

        if(elem1.eq.elemr1(i).and.elem2.eq.elemr2(i))then
            ml(i)=flow
            fltot=fltot+flow
            i=i+1
        end if
2020 CONTINUE
        GO TO 2150
C
191 CONTINUE
C
190 CONTINUE
        write(*,174)i-1
174 format('Have read in ',i6,' repository fluxes...')

c...Loop through all repository elements and calculate percolation
c...flux (darcy velocity in mm/year) and weep spacing using two methods.
c...Print results to output file

        do i=1,nrepo
c
c 6) Calculate percolation flux (mm/year) from mass flow using
c connection area and liquid density.
c
            perc=ml(i)/area(i)/rho*mm_per_m*sec_per_year

c...Calculate effective saturation, se
            se=(sl(i)-sfr)/(1-sfr)

c
c 7) Calculate weep spacing using two methods: (a) assume active
c fractures are saturated and use Xfm=Sfe, and
c (b) fractures are unsaturated where active weep spacing is
c calculated from Liu et al. (1998) using da=d/Se^gamma.
c
c...Calculate weep_spacing1 (m)
            weep1=2./se/a(i)

c...Calculate weep_spacing2 (m)
            weep2=d(i)/se**gamma(i)

c
c 8) Print results to output file.
c
            if(mat(i)(5:5).ne.'f') then
                write(4,82) elemr(i),mat(i),x(i),y(i),z(i),sl(i),
                & perc,weep1,weep2
82 format(2(a5,' '),3(f11.3,' '),3(e11.4,' '),e11.4)
                end if

            end do

c...Print all fault materials at the end of the file in case the
c...user does not want to include those in the distribution
        do i=1,nrepo
            perc=ml(i)/area(i)/rho*mm_per_m*sec_per_year
            se=(sl(i)-sfr)/(1-sfr)
            weep1=2./se/a(i)
            weep2=d(i)/se**gamma(i)
            if(mat(i)(5:5).eq.'f') then
                write(4,82) elemr(i),mat(i),x(i),y(i),z(i),sl(i),
                & perc,weep1,weep2
            end if
        end do

c...Print out average percolation flux over entire repository area
        percavg=fltot/areatot/rho*mm_per_m*sec_per_year
        write(4,94) areatot,fltot,percavg
94 format('total area of repository (m^2) = ',e12.5/
        & 'total kg/s over repository = ',e12.5/
        & 'average mm/year over repository = ',e12.5)

```

90 CONTINUE
C stop
end

ATTACHMENT III

Repository Elements

Figure III-1 shows the location of the repository elements that are listed in Table III-1. This plot verifies that the elements fall within the boundaries of the repository outline (the segments for the repository outline were obtained from DTN: SN9907T0872799.001). Figure III-2 shows the elevation of the repository elements as a function of the northing direction. Note that they all fall between elevations of 1040 m and 1120 m.

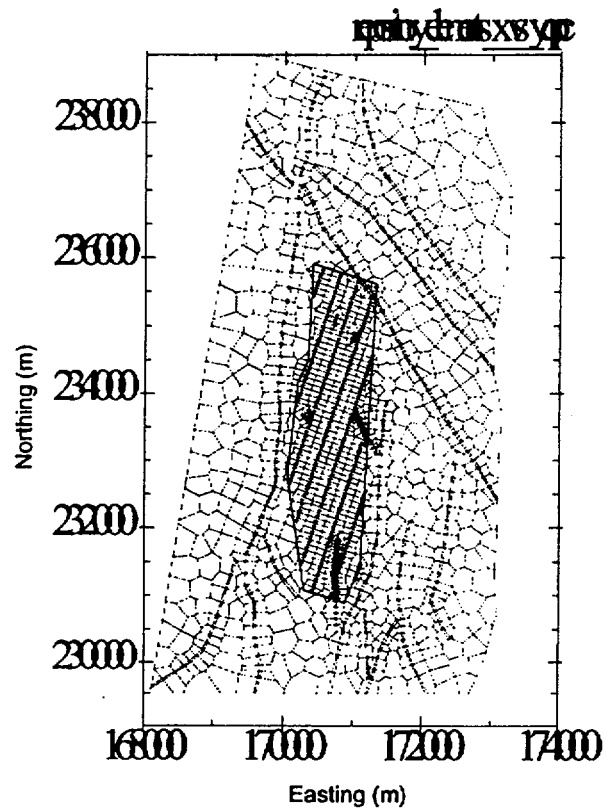


Figure III-1. Prescribed Repository Elements.

Symbols denote location of 275 repository elements (see Table III-1) relative to the outline of the repository (DTN: SN9907T0872799.001).

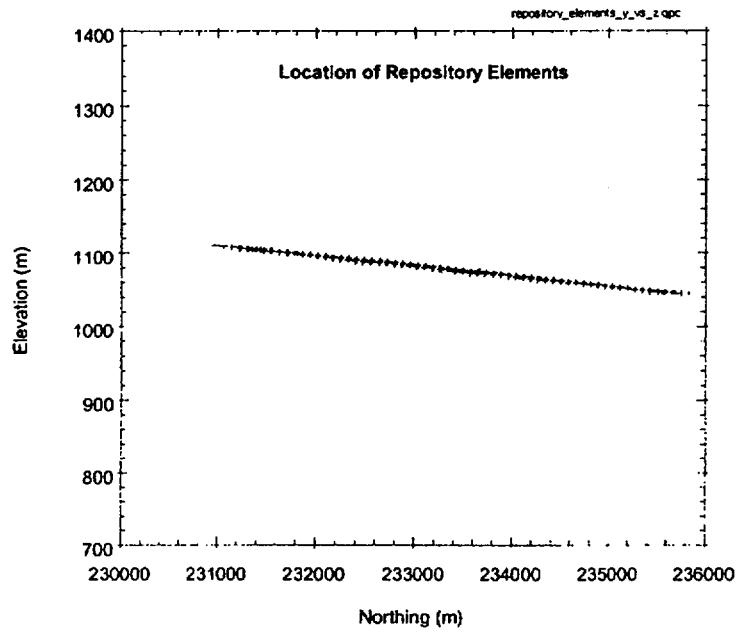


Figure III-2. Elevation of the 275 Repository Elements Along the Northing Coordinate

Table III-1. 275 Fracture Elements Denoted as Repository Elements (taken from 3d2kpa_pc1.mesh; DTN: LB990701233129.001).

Fracture Element	Material	Volume	x (m)	y (m)	z (m)
Fph 2	tswF6	3.23E+03	170424.8	231092.6	1109.641
Foh 3	tswF5	1.00E+03	170681.6	231009.2	1109.641
Fph 4	tswF6	1.64E+03	170449.8	231169.7	1108.478
Foh 5	tswF6	1.53E+03	170474.9	231246.7	1107.315
Fph 6	tswF6	1.50E+03	170499.9	231323.8	1106.152
Fsh 7	tswF6	2.17E+03	170268.1	231484.2	1104.99
Fph 8	tswF6	1.41E+03	170524.9	231400.8	1104.99
Fph 9	tswF5	1.49E+03	171038.5	231233.9	1104.99
Fsh10	tswF6	1.22E+03	170293.2	231561.3	1103.827
Fqh11	tswF5	1.02E+03	170550	231477.8	1103.827
Fqh12	tswF5	7.82E+02	170806.7	231394.4	1103.827
Fsh13	tswF6	1.55E+03	170318.2	231638.3	1102.664
Fph14	tswF5	8.98E+02	170575	231554.9	1102.664
Fqh15	tswF5	6.99E+02	170831.8	231471.4	1102.664
Foh16	tswF5	9.29E+02	171088.6	231388	1102.664
Frh17	tswF6	1.90E+03	170343.2	231715.3	1101.501
Fph18	tswF5	9.08E+02	170600	231631.9	1101.501
Fph19	tswF5	7.65E+02	170856.8	231548.5	1101.501
Foh20	tswF5	1.80E+03	171113.6	231465	1101.501
Frh21	tswF6	1.80E+03	170368.3	231792.4	1100.338
Fph22	tswF5	8.69E+02	170625	231708.9	1100.338
Fph23	tswF5	8.63E+02	170881.8	231625.5	1100.338
Fsh24	tswF6	1.72E+03	170393.3	231869.4	1099.175
Fph25	tswF5	8.36E+02	170650.1	231786	1099.175
Foh26	tswF5	9.12E+02	170906.9	231702.5	1099.175
Frh27	tswF5	1.32E+03	170418.3	231946.4	1098.013
Fph28	tswF5	8.09E+02	170675.1	231863	1098.013
Foh29	tswF5	8.63E+02	170931.9	231779.6	1098.013
Fth30	tswF6	3.06E+03	170186.6	232106.9	1096.85
Fsh31	tswF5	1.21E+03	170443.3	232023.5	1096.85
Fph32	tswF5	1.05E+03	170700.1	231940	1096.85
Foh33	tswF5	1.04E+03	170956.9	231856.6	1096.85
Fuh34	tswF6	1.73E+03	170211.6	232183.9	1095.687
Fqh35	tswF5	1.21E+03	170468.4	232100.5	1095.687
Fph36	tswF5	1.19E+03	170725.2	232017.1	1095.687
Foh37	tswF5	1.40E+03	170981.9	231933.6	1095.687
Fth38	tswF6	1.68E+03	170236.6	232261	1094.524
Fqh39	tswF5	1.21E+03	170493.4	232177.5	1094.524
Fph40	tswF5	1.21E+03	170750.2	232094.1	1094.524
Foh41	tswF5	1.26E+03	171007	232010.7	1094.524
Fth42	tswF6	1.45E+03	170261.6	232338	1093.361
Fqh43	tswF5	1.31E+03	170518.4	232254.6	1093.361
Fph44	tswF5	1.21E+03	170775.2	232171.1	1093.361
Foh45	tswF5	1.29E+03	171032	232087.7	1093.361
Fqh46	tswF5	1.01E+03	170543.5	232331.6	1092.199

Fracture Element	Material	Volume	x (m)	y (m)	z (m)
Fph47	tswF5	1.21E+03	170800.2	232248.2	1092.199
Foh48	tswF5	1.06E+03	171057	232164.8	1092.199
Fth49	tswF5	1.30E+03	170311.7	232492.1	1091.036
Frh50	tswF5	1.32E+03	170568.5	232408.6	1091.036
Fqh51	tswF5	1.21E+03	170825.3	232325.2	1091.036
Foh52	tswF5	8.03E+02	171082.1	232241.8	1091.036
Fmh53	tswF6	2.40E+03	170079.9	232652.5	1089.873
Fth54	tswF5	1.21E+03	170336.7	232569.1	1089.873
Fqh55	tswF5	1.21E+03	170593.5	232485.7	1089.873
Fph56	tswF5	1.21E+03	170850.3	232402.3	1089.873
Foh57	tswF5	8.91E+02	171107.1	232318.8	1089.873
Frh58	tswF6	1.42E+03	170105	232729.6	1088.71
Fth59	tswF5	1.21E+03	170361.8	232646.2	1088.71
Fqh60	tswF5	1.21E+03	170618.5	232562.7	1088.71
Frh61	tswF5	1.21E+03	170875.3	232479.3	1088.71
Foh62	tswF5	1.13E+03	171132.1	232395.9	1088.71
Fph63	tswF6	1.37E+03	170130	232806.6	1087.547
Fth64	tswF5	1.21E+03	170386.8	232723.2	1087.547
Fqh65	tswF5	1.21E+03	170643.6	232639.8	1087.547
Fqh66	tswF5	1.21E+03	170900.4	232556.3	1087.547
Foh67	tswF4	9.56E+02	171157.2	232472.9	1087.547
Fmh68	tswF6	1.75E+03	170155	232883.7	1086.384
Fth69	tswF5	1.21E+03	170411.8	232800.2	1086.384
Frh70	tswF5	1.21E+03	170668.6	232716.8	1086.384
Fqh71	tswF5	1.21E+03	170925.4	232633.4	1086.384
Foh72	tswF4	1.52E+03	171182.2	232549.9	1086.384
Frh73	tswF5	1.07E+03	170180.1	232960.7	1085.222
Fsh74	tswF5	1.21E+03	170436.9	232877.3	1085.222
Frh75	tswF5	1.21E+03	170693.6	232793.8	1085.222
Frh76	tswF5	1.16E+03	170950.4	232710.4	1085.222
Frh77	tswF5	1.16E+03	170205.1	233037.7	1084.059
Fsh78	tswF5	1.21E+03	170461.9	232954.3	1084.059
Fqh79	tswF5	1.21E+03	170718.7	232870.9	1084.059
Fph80	tswF5	1.30E+03	170975.5	232787.4	1084.059
Fsh81	tswF5	1.01E+03	170230.1	233114.8	1082.896
Fsh82	tswF5	1.21E+03	170486.9	233031.3	1082.896
Fqh83	tswF5	1.21E+03	170743.7	232947.9	1082.896
Foh84	tswF5	1.21E+03	171000.5	232864.5	1082.896
Fsh85	tswF5	9.93E+02	170255.2	233191.8	1081.733
Fsh86	tswF5	1.21E+03	170511.9	233108.4	1081.733
Fqh87	tswF5	1.21E+03	170768.7	233024.9	1081.733
Fph88	tswF5	1.30E+03	171025.5	232941.5	1081.733
Fsh89	tswF5	1.21E+03	170280.2	233268.8	1080.57
Fsh90	tswF5	1.21E+03	170537	233185.4	1080.57
Fqh91	tswF5	1.21E+03	170793.8	233102	1080.57
Foh92	tswF5	1.30E+03	171050.5	233018.5	1080.57
Fth93	tswF5	1.13E+03	170305.2	233345.9	1079.408
Fsh94	tswF5	1.21E+03	170562	233262.4	1079.408
Fqh95	tswF5	1.21E+03	170818.8	233179	1079.408
Foh96	tswF5	1.19E+03	171075.6	233095.6	1079.408

Fracture Element	Material	Volume	x (m)	y (m)	z (m)
Fth97	tswF5	1.30E+03	170330.2	233422.9	1078.245
Fsh98	tswF5	1.21E+03	170587	233339.5	1078.245
Fph99	tswF5	1.21E+03	170843.8	233256	1078.245
Foi 0	tswF4	9.33E+02	171100.6	233172.6	1078.245
Fsi 1	tswF5	8.75E+02	170355.3	233499.9	1077.082
Fsi 2	tswF5	1.21E+03	170612.1	233416.5	1077.082
Fqi 3	tswF5	1.33E+03	170868.8	233333.1	1077.082
Foi 4	tswF4	8.81E+02	171125.6	233249.6	1077.082
Fsi 5	tswF5	7.34E+02	170380.3	233577	1075.919
Fsi 6	tswF5	1.21E+03	170637.1	233493.5	1075.919
Fsi 7	tswF5	1.03E+03	170893.9	233410.1	1075.919
Fsi 8	tswF5	7.45E+02	170405.3	233654	1074.756
Fsi 9	tswF5	1.21E+03	170662.1	233570.6	1074.756
Fqi10	tswF5	1.02E+03	170918.9	233487.2	1074.756
Fri11	tswF5	1.57E+03	170173.6	233814.5	1073.593
Fsi12	tswF5	1.01E+03	170430.4	233731	1073.593
Fri13	tswF5	1.21E+03	170687.1	233647.6	1073.593
Fri14	tswF5	8.80E+02	170943.9	233564.2	1073.593
Fri15	tswF5	1.22E+03	170198.6	233891.5	1072.431
Fsi16	tswF5	9.81E+02	170455.4	233808.1	1072.431
Fri17	tswF5	1.27E+03	170712.2	233724.7	1072.431
Fqi18	tswF5	7.21E+02	170969	233641.2	1072.431
Fqi19	tswF4	9.15E+02	171225.7	233557.8	1072.431
Fsi20	tswF5	1.14E+03	170223.6	233968.6	1071.268
Fsi21	tswF5	1.21E+03	170480.4	233885.1	1071.268
Fri22	tswF5	1.06E+03	170737.2	233801.7	1071.268
Fsi23	tswF5	1.46E+03	170248.7	234045.6	1070.105
Fsi24	tswF5	1.21E+03	170505.4	233962.2	1070.105
Fsi25	tswF5	1.31E+03	170762.2	233878.7	1070.105
Fri26	tswF4	8.73E+02	171019	233795.3	1070.105
Fsi27	tswF5	1.26E+03	170273.7	234122.6	1068.942
Fsi28	tswF5	1.21E+03	170530.5	234039.2	1068.942
Fri29	tswF5	1.21E+03	170787.3	233955.8	1068.942
Fri30	tswF4	9.81E+02	171044	233872.3	1068.942
Fsi31	tswF5	1.39E+03	170298.7	234199.7	1067.779
Fsi32	tswF5	1.21E+03	170555.5	234116.2	1067.779
Fri33	tswF5	1.21E+03	170812.3	234032.8	1067.779
Fqi34	tswF4	9.12E+02	171069.1	233949.4	1067.779
Fsi35	tswF5	1.43E+03	170323.7	234276.7	1066.617
Fsi36	tswF5	1.21E+03	170580.5	234193.3	1066.617
Fqi37	tswF5	1.21E+03	170837.3	234109.8	1066.617
Fpi38	tswF4	9.39E+02	171094.1	234026.4	1066.617
Fsi39	tswF5	1.45E+03	170348.8	234353.7	1065.454
Fri40	tswF5	1.21E+03	170605.6	234270.3	1065.454
Fqi41	tswF5	1.21E+03	170862.3	234186.9	1065.454
Fpi42	tswF4	7.90E+02	171119.1	234103.4	1065.454
Fsi43	tswF5	1.46E+03	170373.8	234430.8	1064.291
Fsi44	tswF5	1.21E+03	170630.6	234347.3	1064.291
Fqi45	tswF5	1.21E+03	170887.4	234263.9	1064.291
Fpi46	tswF4	8.00E+02	171144.2	234180.5	1064.291

Fracture Element	Material	Volume	x (m)	y (m)	z (m)
Fsi47	tswF5	1.21E+03	170398.8	234507.8	1063.128
Fri48	tswF5	1.21E+03	170655.6	234424.4	1063.128
Fpi49	tswF5	1.21E+03	170912.4	234340.9	1063.128
Fqi50	tswF4	9.79E+02	171169.2	234257.5	1063.128
Fsi51	tswF5	1.03E+03	170423.9	234584.8	1061.965
Fri52	tswF5	1.21E+03	170680.7	234501.4	1061.965
Fri53	tswF5	1.21E+03	170937.4	234418	1061.965
Fri54	tswF4	9.92E+02	171194.2	234334.5	1061.965
Fsi55	tswF5	1.02E+03	170448.9	234661.9	1060.802
Fsi56	tswF5	1.21E+03	170705.7	234578.4	1060.802
Fri57	tswF5	1.21E+03	170962.5	234495	1060.802
Fqi58	tswF4	1.15E+03	171219.3	234411.6	1060.802
Fsi59	tswF5	1.11E+03	170473.9	234738.9	1059.64
Fri60	tswF5	1.21E+03	170730.7	234655.5	1059.64
Fpi61	tswF5	1.21E+03	170987.5	234572.1	1059.64
Fpi62	tswF4	9.30E+02	171244.3	234488.6	1059.64
Fsi63	tswF5	1.02E+03	170499	234815.9	1058.477
Fri64	tswF5	1.09E+03	170755.7	234732.5	1058.477
Fpi65	tswF5	1.07E+03	171012.5	234649.1	1058.477
Fpi66	tswF4	1.60E+03	171269.3	234565.7	1058.477
Fsi67	tswF5	1.04E+03	170524	234893	1057.314
Fqi68	tswF5	1.24E+03	170780.8	234809.6	1057.314
Foi69	tswF5	1.03E+03	171037.6	234726.1	1057.314
Fqi70	tswF5	9.33E+02	170549	234970	1056.151
Fqi71	tswF5	8.96E+02	170805.8	234886.6	1056.151
Fpi72	tswF5	8.24E+02	171062.6	234803.2	1056.151
Fqi73	tswF5	1.30E+03	170574	235047.1	1054.988
Fpi74	tswF5	1.06E+03	170830.8	234963.6	1054.988
Foi75	tswF5	7.27E+02	171087.6	234880.2	1054.988
Fqi76	tswF5	1.02E+03	170599.1	235124.1	1053.826
Fpi77	tswF5	7.70E+02	170855.9	235040.7	1053.826
Fqi78	tswF5	9.96E+02	171112.6	234957.2	1053.826
Foi79	tswF5	1.07E+03	170624.1	235201.1	1052.663
Fqi80	tswF5	9.12E+02	170880.9	235117.7	1052.663
Fqi81	tswF5	1.05E+03	171137.7	235034.3	1052.663
Fmi82	tswF5	1.14E+03	170649.1	235278.2	1051.5
Fsi83	tswF5	1.06E+03	170905.9	235194.7	1051.5
Fsi84	tswF5	9.90E+02	171162.7	235111.3	1051.5
Fri85	tswF5	1.90E+03	170417.4	235438.6	1050.337
Fqi86	tswF5	1.18E+03	170674.2	235355.2	1050.337
Fsi87	tswF5	1.16E+03	170930.9	235271.8	1050.337
Fsi88	tswF5	1.08E+03	171187.7	235188.3	1050.337
Fqi89	tswF5	1.02E+03	170442.4	235515.7	1049.174
Fqi90	tswF5	1.21E+03	170699.2	235432.2	1049.174
Fsi91	tswF5	1.21E+03	170956	235348.8	1049.174
Fqi92	tswF5	9.19E+02	171212.8	235265.4	1049.174
Fqi93	tswF5	9.19E+02	170467.4	235592.7	1048.011
Fri94	tswF5	1.21E+03	170724.2	235509.3	1048.011
Fri95	tswF5	1.11E+03	170981	235425.8	1048.011
Fni96	tswF5	8.32E+02	171237.8	235342.4	1048.011

Fracture Element	Material	Volume	x (m)	y (m)	z (m)
Foi97	tswF6	1.50E+03	170492.5	235669.7	1046.849
Fsi98	tswF5	1.21E+03	170749.2	235586.3	1046.849
Fqi99	tswF5	1.08E+03	171006	235502.9	1046.849
Foj 0	tswF6	1.67E+03	170517.5	235746.8	1045.686
Fsj 1	tswF5	1.23E+03	170774.3	235663.3	1045.686
Fqj 2	tswF5	9.74E+02	171031.1	235579.9	1045.686
Fsj 3	tswF6	3.56E+03	170542.5	235823.8	1044.523
Fsj 4	tswF5	1.68E+03	170799.3	235740.4	1044.523
Frij 5	tswF5	1.89E+03	171312.9	235573.5	1044.523
FoC10	tswFf	4.73E+02	170764.6	230967.1	1109.848
Foj22	tswF5	2.86E+02	170734.6	230966.9	1109.983
Fnj23	tswF6	9.59E+02	170794.6	230967.2	1109.713
FnC11	tswFf	4.63E+02	170764.2	231054.7	1108.653
Fnj24	tswF6	1.05E+03	170794	231057.8	1108.479
Fnj25	tswF5	2.51E+02	170734.4	231051.6	1108.828
FoC12	tswFf	4.54E+02	170755.6	231138.1	1107.552
Foj26	tswF5	6.53E+02	170725.7	231135	1107.727
Fnj27	tswF5	7.51E+02	170785.4	231141.2	1107.378
FnC13	tswFf	4.53E+02	170746.9	231221.6	1106.452
Fnj28	tswF5	6.38E+02	170717.1	231218.5	1106.626
Fnj29	tswF5	6.72E+02	170776.8	231224.7	1106.277
FpC14	tswFf	3.61E+02	170738.3	231305	1105.351
Fpj30	tswF5	4.45E+02	170768.3	231305.5	1105.21
Foj31	tswF5	5.02E+02	170708.3	231304.5	1105.491
FpC15	tswFf	3.91E+02	170737.5	231355.1	1104.671
Fpj32	tswF5	1.57E+02	170767.3	231352	1104.58
Foj33	tswF5	4.64E+02	170707.6	231358.1	1104.762
FqC16	tswFf	5.07E+02	170746.8	231446.9	1103.376
Fqj34	tswF5	4.85E+02	170717	231449.9	1103.467
Fqj35	tswF5	1.70E+02	170776.7	231443.8	1103.285
FqC17	tswFf	4.99E+02	170756.2	231538.6	1102.082
Fqj36	tswF5	4.76E+02	170726.3	231541.7	1102.172
Fpj37	tswF5	2.29E+02	170786	231535.6	1101.991
FpC18	tswFf	4.99E+02	170765.5	231630.4	1100.787
Fpj38	tswF5	4.02E+02	170735.7	231633.5	1100.878
Fpj39	tswF5	3.02E+02	170795.4	231627.4	1100.696
FpC19	tswFf	4.99E+02	170774.9	231722.2	1099.492
Fpj40	tswF5	3.50E+02	170745	231725.3	1099.583
Fpj41	tswF5	3.18E+02	170804.7	231719.2	1099.401
FpC20	tswFf	7.79E+02	170784.2	231814	1098.198
Fqj42	tswF5	3.63E+02	170754.4	231817	1098.288
Fpj43	tswF5	6.20E+02	170814.1	231811	1098.107
FqC21	tswFf	4.95E+02	171025.9	233708.1	1071.265
Fqj44	tswF5	6.14E+02	170998.9	233695	1071.564
Fqj45	tswF4	4.67E+02	171052.8	233721.2	1070.966
FqC22	tswFf	4.84E+02	171065	233627.5	1072.192
Fpj46	tswF4	4.54E+02	171092	233640.6	1071.893
Frij47	tswF4	2.53E+02	171038.1	233614.4	1072.491
FrC23	tswFf	4.84E+02	171104.2	233546.9	1073.118
Fqj48	tswF4	2.98E+02	171131.2	233560	1072.82

Fracture Element	Material	Volume	x (m)	y (m)	z (m)
Frj49	tswF4	4.19E+02	171077.2	233533.8	1073.417
FqC24	tswFf	4.84E+02	171143.4	233466.3	1074.045
Fqj50	tswF4	3.13E+02	171170.4	233479.4	1073.746
Fqj51	tswF4	6.18E+02	171116.4	233453.2	1074.344
FpC25	tswFf	5.00E+02	171182.6	233385.7	1074.972
Foj52	tswF4	4.83E+02	171156.6	233370.7	1075.291
Fpj53	tswF4	5.10E+02	171208.6	233400.7	1074.652
Fpj54	tswF4	2.49E+02	171209.6	233285.5	1076.221
FnC41	tswFf	9.67E+02	171085.5	235685.6	1044.001
Flj86	tswF5	5.72E+02	171061.4	235667.8	1044.351
FoC42	tswFf	1.13E+03	171178.2	235560.5	1045.299
Fqj87	tswF5	6.83E+02	171202.3	235578.3	1044.948
Foj88	tswF5	7.00E+02	171154.1	235542.6	1045.649
FqC43	tswFf	1.04E+03	171270.8	235435.3	1046.596
Fqj89	tswF5	6.41E+02	171294.9	235453.2	1046.246
Fnj90	tswF5	5.22E+02	171246.7	235417.5	1046.947
Fqk23	tswF5	5.35E+02	170985.5	234837	1056.031
Fsk26	tswF5	2.54E+02	170347.5	233659	1074.945
Fpk31	tswF5	9.90E+02	171058.5	231317	1103.767
Ftk32	tswF6	1.87E+03	170268.5	232413	1092.307
Fpk33	tswF4	8.82E+02	171234.5	234074	1065.344
Fnk34	tswF5	5.74E+02	170723.5	235087	1053.78
Fqk45	tswF4	9.80E+02	171244.9	233777.7	1069.344
Fok55	tswF5	9.14E+02	170753.1	235159.8	1052.655
Fpk56	tswF5	4.06E+02	170708.5	235024.6	1054.699
Fok57	tswF5	8.94E+02	171001.5	234899.8	1055.103
Fqk58	tswF5	4.53E+02	170969.7	234764.5	1057.091
Fsk59	tswF5	9.85E+02	170269	233672.5	1075.109
Fsk60	tswF5	4.64E+02	170351.8	233745.3	1073.748
Ftk61	tswF5	6.04E+02	170320	233610	1075.735

ATTACHMENT IV

Directory of Files Submitted to TDMS

DTN: SN9912T0511599.002

12/15/99 01:55p 340,219 AMR_U0120_data.ZIP
 12/13/99 03:29p 558 README.TXT

ZIP file AMR_U0120_data.ZIP contains the following files:

AMR_U0120_Weep_data.ZIP	11/29/1999 12:24 PM	219,005	Weep-spacing files (Sect. 6.4.3)
README.TXT	12/13/1999 3:29 PM	558	
Readme.weep	11/29/1999 12:24 PM	1,133	
Seep-sr.xls	12/15/1999 1:54 PM	419,328	Abstraction spreadsheet, Rev. 00
Seepage_Abstraction.txt	12/13/1999 3:22 PM	2,736	Abstraction summary, Rev. 00

ZIP file AMR_U0120_Weep_data.ZIP contains the following files, all related to the calculation of weep spacing (Section 6.4.3):

glall_perc.qpc	11/23/1999 11:48 PM	57,430	pa_glall_weep\
glall_weep.out	11/22/1999 3:30 PM	30,223	pa_glall_weep\
glall_weep.QDA	11/23/1999 11:49 PM	33,368	pa_glall_weep\
glall_weep1_log.qpc	11/23/1999 11:43 PM	58,320	pa_glall_weep\
glall_weep2_log.qpc	11/23/1999 11:47 PM	57,790	pa_glall_weep\
glam1_perc.QPC	11/23/1999 11:47 PM	54,392	pa_glam1_weep\
glam1_weep.out	11/22/1999 3:30 PM	30,223	pa_glam1_weep\
glam1_weep.QDA	11/23/1999 11:58 PM	33,368	pa_glam1_weep\
glam1_weep1_log.qpc	11/23/1999 11:59 PM	57,860	pa_glam1_weep\
glam1_weep2_log.qpc	11/24/1999 12:00 AM	57,776	pa_glam1_weep\
glaul_perc.qpc	11/24/1999 12:06 AM	58,004	pa_glaul_weep\
glaul_weep.out	11/22/1999 3:30 PM	30,223	pa_glaul_weep\
glaul_weep.QDA	11/24/1999 12:01 AM	33,368	pa_glaul_weep\
glaul_weep1_log.qpc	11/24/1999 12:02 AM	58,162	pa_glaul_weep\
glaul_weep2_log.qpc	11/24/1999 12:17 AM	58,170	pa_glaul_weep\
Readme	11/23/1999 6:01 PM	556	pa_glall_weep\
Readme	11/23/1999 6:01 PM	556	pa_glam1_weep\
Readme	11/23/1999 6:01 PM	556	pa_glaul_weep\
README.txt	11/29/1999 10:53 AM	1,133	
SR-repo-nodes	11/29/1999 10:55 AM	1,930	repo-nodes\
t2weep_v1.f	11/23/1999 11:32 AM	13,073	SourceFiles\
weep.inp	11/22/1999 3:30 PM	1,607	pa_glall_weep\
weep.inp	11/22/1999 3:30 PM	1,607	pa_glam1_weep\
weep.inp	11/22/1999 3:30 PM	1,607	pa_glaul_weep\
weep.out	11/22/1999 3:30 PM	792	pa_glall_weep\
weep.out	11/22/1999 3:30 PM	792	pa_glam1_weep\
weep.out	11/22/1999 3:30 PM	792	pa_glaul_weep\

DTN: SN0012T0511599.003

01/10/01 03:47p 145,873 AMR_U0120_data1.zip
01/10/01 03:47p 425 README.TXT

ZIP file AMR_U0120_data1.zip contains the following files:

README.TXT	01/10/2001 3:47 PM	425	
Seep-sr1.xls	01/10/2001 3:26 PM	503,808	Abstraction spreadsheet, Rev. 01
Seepage_Abstraction1.txt	01/10/2001 3:40 PM	2,649	Abstraction summary, Rev. 01